12

AFWAL-TR-81-2096

HIGH SPEED PERMANENT MAGNET GENERATOR MATERIAL INVESTIGATIONS--RARE EARTH MAGNETS

Herbert F. Mildrum
George A. Graves, Jr.
University of Dayton
Magnetics Laboratory, School of Engineering
Metals and Ceramics Division, Research Institute
300 College Park Avenue
Dayton, Ohio 45469

12 140

OCTOBER 1981

Final Report for Period 1 June 1979 - 2 April 1981

Approved for public release; distribution unlimited.

Propulsion Laboratory
Air Force Wright Aeronautical Laboratories
Air Force Systems Command
Wright-Patterson Air Force Base, Ohio 45433

105 350 pm

NOTICE

When Government drawings, specifications, or other data are used for any purpose other than in connection with a definitely related Government procurement operation, the United States Government thereby incurs no responsibility nor any obligation whatsoever; and the fact that the government may have formulated, furnished, or in any way supplied the said drawings, specifications, or other data, is not to be regarded by implication or otherwise as in any manner licensing the holder or any other person or corporation, or conveying any rights or permission to manufacture use, or sell any patented invention that may in any way be related thereto.

This report has been reviewed by the Office of Public Affairs (ASD/PA) and is releasable to the National Technical Information Service (NTIS). At NTIS, it will be available to the general public, including foreign nations.

This technical report has been reviewed and is approved for publication.

William W Borger

WILLIAM U. BORGER
Power Systems Branch
Aerospace Power Division
Aero Propulsion Laboratory

Paul R. Bertheaud

PAUL R. BERTHEAUD
Technical Area Manager
Power Systems Branch
Aerospace Power Division
Aero Propulsion Laboratory

FOR THE COMMANDER

James D. Reams

JAMES D. REAMS
Chief, Aerospace Power Division
Aerospace Power Division
Aero Propulsion Laboratory

"If your address has changed, if you wish to be removed from our mailing list, or if the addressee is no longer employed by your organization please notify AFWAL/POOS, *W-PAFB, OH 45433 to help us maintain a current mailing list".*

Copies of this report should not be returned unless return is required by security considerations, contractual obligations, or notice on a specific document.

AIR FORCE/56780/30 November 1981 — 320

Unclassified

SECURITY CLASSIFICATION OF THIS PAGE (When Data Entered)

REPORT DOCUMENTATION PAGE	READ INSTRUCTIONS BEFORE COMPLETING FORM
1. REPORT NUMBER: AFWAL-TR-81-2096	2. GOVT ACCESSION NO.: AD-A108550	3. RECIPIENT'S CATALOG NUMBER:
4. TITLE (and Subtitle): HIGH SPEED PERMANENT MAGNET GENERATOR MATERIAL INVESTIGATIONS--RARE EARTH MAGNETS	5. TYPE OF REPORT & PERIOD COVERED: Final Report 1 June 1979-2 April 1981
	6. PERFORMING ORG. REPORT NUMBER: UDR-TR-81-105
7. AUTHOR(s): Herbert F. Mildrum, George A. Graves, Jr.	8. CONTRACT OR GRANT NUMBER(s): F33615-79-C-2010
9. PERFORMING ORGANIZATION NAME AND ADDRESS: University of Dayton, 300 College Park Avenue, Dayton, Ohio 45469	10. PROGRAM ELEMENT, PROJECT, TASK AREA & WORK UNIT NUMBERS: 2308 S6 02
11. CONTROLLING OFFICE NAME AND ADDRESS: Propulsion Laboratory, AF Wright Aeronautical Laboratories, Air Force Systems Command, Wright-Patterson AFB, Ohio 45433	12. REPORT DATE: October 1981
	13. NUMBER OF PAGES: 124
14. MONITORING AGENCY NAME & ADDRESS (if different from Controlling Office)	15. SECURITY CLASS. (of this report): Unclassified
	15a. DECLASSIFICATION DOWNGRADING SCHEDULE

16. DISTRIBUTION STATEMENT (of this Report)

Approved for public release; distribution unlimited.

17. DISTRIBUTION STATEMENT (of the abstract entered in Block 20, if different from Report)

18. SUPPLEMENTARY NOTES

19. KEY WORDS (Continue on reverse side if necessary and identify by block number)

Sintered $SmCo_5$
Sintered $Sm_2(CoTM)_{17}$
Rare Earth-Cobalt Permanent Magnets
Rare Earth-Transition Metal Magnets
Magnetic Properties
Mechanical Properties
Thermal Properties
Electrical Properties

20. ABSTRACT (Continue on reverse side if necessary and identify by block number)

Permanent magnets with room-temperature energy products of 20-30 MGOe were characterized with a view toward their use in airborne electrical machinery. This report presents the results of an evaluation of commercial sintered rare earth-transition metal magnets potentially suitable for such applications. They include $SmCo_5$, $(SmPr)Co_5$, and modified Sm_2Co_{17}, produced by 11 companies worldwide. Extensive magnetic, physical, mechanical,

(Continued on reverse side)

DD FORM 1 JAN 73 1473 EDITION OF 1 NOV 65 IS OBSOLETE

Unclassified

SECURITY CLASSIFICATION OF THIS PAGE (When Data Entered)

20. Abstract (Concluded)

and electrical property engineering data, based on statistically significant numbers of test magnets for each measurements, are presented. Testing procedures, range of evaluation, and test considerations relevant to the application are also identified.

FOREWORD

The magnet material characterization investigations described in this report were performed by personnel associated with the Magnetics Laboratory, of the Electrical Engineering Department, and the Metals and Ceramics Division of the Research Institute, University of Dayton. The program was sponsored and administered by the Air Force Wright Aeronautical Laboratories (AFWAL/PO) Aero Propulsion Laboratory, Air Force Systems Command, Wright-Patterson Air Force Base, Ohio under Project 2308, Task S6, and Work Unit Number 02. The Contract Number for this report was F33615-79-C-2010. Project Engineer was Dr. William Borger, AFWAL/POOS-2, Tel. (513) 255-6241.

The following personnel participated actively in the investigations during the reporting period: H. F. Mildrum, G. A. Graves, Z. A. Abdelnour, D. L. McCullum, and D. C. Maxwell.

This report covers investigations conducted between 1 June 1979 through 2 April 1981. The report was released by the authors in June 1981 for publication as a technical report.

The authors wish to take this opportunity to formally thank those rare earth permanent magnet manufacturers and representatives who responded and participated in this program.

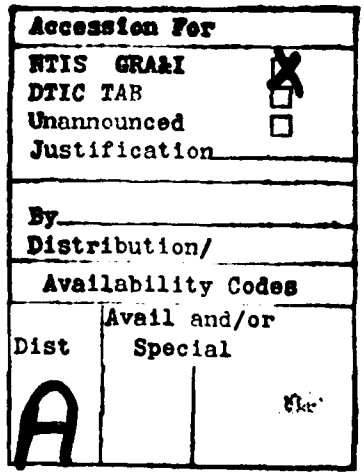

TABLE OF CONTENTS

SECTION		PAGE
1	INTRODUCTION	1
2	PHASE I	4
	A. Test Magnet Selection	4
	B. Magnetic Property Characterization	8
	a) Procedure and Instrumentation	8
	b) Measurements at Room Temperature	13
	c) Measurements at Temperatures of -60°, +100°, and +200°C	22
	C. Mechanical Property Characterization	45
	a) Procedure and Instrumentation	45
3	PHASE II	50
	A. Evaluation of Test Data, Phase I	50
	B. Test Plan and Magnet Procurement for Comprehensive Evaluation	53
	C. Magnetic Characterization at Room Temperature, Phase II	53
	D. Fixture Design, Construction, Modification, and Testing	58
	a) Resistivity Fixture	58
4	PHASE III	62
	A. Comprehensive Property Evaluation of Sintered $SmCo_5$ Permanent Magnets	62
	B. Magnetic Property Characterization, Phase III	62
	a) Measurements at Temperatures of -60°, +100°, and +200°C	62
	b) Magnetization Characteristics of $SmCo_5$ Permanent Magnets	66
	c) Minor Loop Recoil Characteristics	79
	d) Magnetic Property Evaluation on Test Bars	84

TABLE OF CONTENTS (CONTINUED)

SECTION		PAGE
	C. Measuring Techniques and Instruments Used in Task III Thermal and Mechanical Property Determinations	86
	a) Thermal Properties	86
	1. Thermal Diffusivity	86
	2. Heat Capacity (Specific Heat)	86
	3. Thermal Conductivity	88
	4. Coefficient of Thermal Expansion	88
	5. Density Measurements	88
	b) Mechanical Properties	89
	1. Flexural Strength	89
	2. Young's Modulus and Poisson's Ratio	90
	3. Compressive Strength	92
	4. Shock Strength (Impact Strength)	92
	D. Discussion of Experimental Plan and Results of Mechanical and Thermal Property Determinations	92
	a) Mechanical Properties	92
	1. Mechanical Strength and Elasticity, General Comments	92
	2. Statistical Method for Selecting Magnet Tapes for Phase III Testing	95
	3. Mechanical Strength	97
	4. Elastic Modulus and Poisson's Ratio	104
	5. Impact Strength	104
	6. Knoop Hardness	115
	7. Thermal Property Results	115
	E. Electrical Properties	115
	a) Electrical Resistivity	115
5	CONCLUSION AND RECOMMENDATION	121
	REFERENCES	123

LIST OF ILLUSTRATIONS

FIGURE		PAGE
1	High Performance Magnet Characteristics. (Air Force Specification.)	4
2	Phase I Magnetic and Mechanical Characterization of 11 Candidate Brand Type High Performance Sintered RE-TM Permanent Magnets.	7
3	Hysteresigraph Measurement System: Electronic Integrators and Composition Unit, Specimen Coil Probe, and X-Y Plotter.	10
4	Hysteresigraph Coil Probes and Temperature Controlled Fixture.	10
5	Temperature Controlled Probe Fixture Construction.	12
6a,b	Phase I. Range of Demagnetization Curves for Sintered $SmCo_5$ Magnets. Brand Types A-1 and A-2. Produced June 1979, 18 Test Magnets.	15
6c,d	Phase I. Range of Demagnetization Curves for Sintered $SmCo_5$ Magnets. Brand Types B-1 and C-1. Produced June 1979, 18 Test Magnets.	16
6e,f	Phase I. Range of Demagnetization Curves for Sintered $SmCo_5$ Magnets. Brand Type D-1. Produced June 1979, 18 Test Magnets.	17
6g,h	Phase I. Range of Demagnetization Curves for Sintered $SmCo_5$ Magnets. Brand Type E-1. Produced June 1979, 18 Test Magnets.	18
6i,j	Phase I. Range of Demagnetization Curves for Sintered $Sm(Pr)Co_5$ and $Sm(Co,Cu,Fe)_7$. Brand Types B-2 and F-1. Produced June 1979, 18 Test Magnets.	19
6k,l	Phase I. Range of Demagnetization Curves for Sintered $Sm_2(CoTM)_{17}$ Magnets. Brand Types B-3 and C-2. Produced June 1979, 18 Test Magnets.	20

LIST OF ILLUSTRATIONS (CONTINUED)

FIGURE		PAGE
6m	Phase I. Range of Demagnetization Curves for Sintered $Sm_2(CoTM)_{17}$ Magnets. Brand Type C-3. Produced June 1979, 18 Test Magnets.	21
7a,b	Phase I. Typical Demagnetization Curves for Sintered $SmCo_5$ Magnets Evaluated at Four Temperatures from -60° to +200°C. Brand Types A-1 and A-2.	23
7c,d	Phase I. Typical Demagnetization Curves for Sintered $SmCo_5$ Magnets Evaluated at Four Temperatures from -60° to +200°C. Brand Types B-1 and C-1.	24
7e,f	Phase I. Typical Demagnetization Curves for Sintered $SmCo_5$ Magnets Evaluated at Four Temperatures from -60° to +200°C. Brand Types D-1 and E-1.	25
7g,h	Phase I. Typical Demagnetization Curves for Sintered $(SmPr)Co_5$ and $Sm(Co,Cu,Fe)_7$ Magnets Evaluated at Four Temperatures from -60° to +200°C. Brand Types B-2 and F-1.	26
7i,j	Phase I. Typical Demagnetization Curves for Sintered $Sm_2(CoTM)_{17}$ Magnets Evaluated at Four Temperatures from -60° to +200°C. Brand Types B-3 and C-2.	27
7k	Phase I. Typical Demagnetization Curves for Sintered $Sm_2(CoTM)_{17}$ Magnets Evaluated at Four Temperatures from -60° to +200°C. Brand Type C-3.	28
8a,b	Phase I. Temperature Dependence of Selected Second-Quadrant Magnetic Properties of Sintered $SmCo_5$ Magnets, Over a Temperature Range of -60° to +200°C. Brand Types A-1 and A-2.	36
8c,d	Phase I. Temperature Dependence of Selected Second-Quadrant Magnetic Properties of Sintered $SmCo_5$ Magnets, Over a Temperature Range of -60° to +200°C. Brand Types B-1 and C-1.	37

LIST OF ILLUSTRATIONS (CONTINUED)

FIGURE		PAGE
8e,f	Phase I. Temperature Dependence of Selected Second-Quadrant Magnetic Properties of Sintered $SmCo_5$ Magnets, Over a Temperature Range of -60° to +200°C. Brand Types D-1 and E-1.	38
8g,h	Phase I. Temperature Dependence of Selected Second-Quadrant Magnetic Properties of Sintered $(SmPr)Co_5$ and $Sm(Co,Cu,Fe)_7$ Magnets, Over a Temperature Range of -60° to +200°C. Brand Types B-2 and F-1.	39
8i,j	Phase I. Temperature Dependence of Selected Second-Quadrant Magnetic Properties of Sintered $Sm_2(CoTM)_{17}$ Magnets, Over a Temperature Range of -60° to +200°C. Brand Types B-3 and C-2.	40
8k	Phase I. Temperature Dependence of Selected Second-Quadrant Magnetic Properties of Sintered $Sm_2(CoTM)_{17}$ Magnets, Over a Temperature Range of -60° to +200°C. Brand Type C-3.	41
9	Illustration of Specific Coefficient Data Reference Points and Spans Calculated for Thermally Dependent Magnetic Properties.	42
10	Compression Test Equipment.	46
11	Compression Test Orientation with Respect to Magnetization Direction.	46
12	Phase I. Average Compressive Strength and Standard Deviation. F||M Only.	49
13	Phase II. Initial Characterization and Test Specimen Allocation of $SmCo_5$ Magnet Specimens for Phase III.	54
14	Phase II. Range of Demagnetization Curves for Sintered $SmCo_5$ Magnets. Brand Type B-1. Produced February 1980, 108 Test Magnets Measured As-Received.	56

LIST OF ILLUSTRATIONS (CONTINUED)

FIGURE		PAGE
15a,b	Phase II. Range of Demagnetization Curves for Sintered $SmCo_5$ Magnets. Brand Type E-1. Produced February 1980, 18 Test Magnets Measured As-Received.	57
16	Sectional View, Four Wire Point Contact Resistance Fixture.	60
17	Instrumentation for Electrical Resistivity Measurements.	60
18	Phase III. Test Specimen Allocation of Two Brand Type Sintered $SmCo_5$ Magnets, B-1, E-1.	63
19a,b	Phase III. Typical Demagnetization Curves for Sintered $SmCo_5$ Magnets Evaluated at Four Temperatures from -60° to +200°C. Brand Types B-1 and E-1.	64
20a,b	Phase III. Temperature Dependence of Selected Second-Quadrant Magnetic Properties of Sintered $SmCo_5$ Magnets, Over a Temperature Range of -60° to +200°C. Brand Types B-1 and E-1.	69
21a,b	Characteristic Virgin State d.c. Magnetization and Demagnetization Hysteresis Curves of Sintered $SmCo_5$ Permanent Magnets. Brand Types B-1 and E-1.	72
22a,b	Characteristic d.c. Magnetization and Demangetization Hysteresis Curves of Sintered $SmCo_5$ Permanent Magnets from a Zero Remanence d.c. Knock Down State. Brand Types B-1 and E-1.	75
23a,b	Characteristic Demagnetization Hysteresis Curves of Sintered $SmCo_5$ Permanent Magnets Pulse Magnetized from a Zero Remanence d.c. Knock Down State. Brand Types B-1 and E-1.	78
24	Typical Minor Loop Recoil Characteristics of Sintered $SmCo_5$ Permanent Magnets from Low Permeance Intercepts on the Intrinsic Demagnetization Curve. Brand Types B-1 and E-1.	80

LIST OF ILLUSTRATIONS (CONTINUED)

FIGURE		PAGE
25	Average Minor Loop Recoil Lines from the Normal Induction Curve (B vs. H) at Four Permeance Intercepts from -1/2 to -4 and Temperatures of -60° to +200°C. Brand Type B-1.	81
26	Average Minor Loop Recoil Lines from the Normal Induction Curve (B vs. H) at Four Permeance Intercepts from -1/2 to -4 and Temperatures of -60° to +200°C. Brand Type E-1.	82
27	Thermal Diffusivity Measuring Apparatus.	87
28	Thermal Expansion Measuring Apparatus.	89
29	NATO Four-Point Bend Fixture.	91
30	Instron Universal Testing Machine.	91
31	Confidence Limits for Various Sample Sizes.	96
32	Representative Photomicrographs of the Microstructure of B-1 Type Magnets at Three Flexural Strength Levels (300X).	102
33	Representative Photomicrographs of the Microstructure of E-1 Type Magnets at Three Flexural Strength Levels (300X).	103
34	Resistivity Versus Temperature for Brand Types B-1 and E-1.	120

LIST OF TABLES

TABLE		PAGE
1	TEST MAGNET IDENTIFICATION, COMPOSITION, AND FABRICATION METHOD	6
2	COMPARISON OF AVERAGE AND STANDARD DEVIATION OF MAGNETIC PROPERTIES FOR EACH BRAND TYPE MEASURED AT ROOM TEMPERATURE, 25°C	14
3	TEMPERATURE DEPENDENCE OF REMANENCE, B_r(kG)	30
4	TEMPERATURE DEPENDENCE OF INDUCTION COERCIVE FORCE, $_BH_c$(kOe)	31
5	TEMPERATURE DEPENDENCE OF INTRINSIC COERCIVE FORCE, $_MHc$(kOe)	32
6	TEMPERATURE DEPENDENCE OF ENERGY PRODUCT, $(BH)_{max}$ (MGOe)	33
7	TEMPERATURE DEPENDENCE OF LOOP SQUARENESS, H_K(kOe)	34
8	TEMPERATURE DEPENDENCE OF MAGNETIC PROPERTIES PERCENT CHANGE FROM VALUES AT 25°C	35
9	AVERAGE TEMPERATURE COEFFICIENT OF REMANENCE, COERCIVITY, AND ENERGY PRODUCT OF SINTERED MAGNETS MEASURED	43
10	SUMMARY OF COMPRESSION TESTS ON SAMARIUM-COBALT PERMANENT MAGNETS	48
11	PERCENTAGE OF MAGNET SPECIMENS EQUAL TO OR GREATER THAN MINIMUM MAGNETIC PROPERTY SPECIFICATIONS	51
12	MAGNETIC PROPERTIES OF SINTERED $SmCo_5$ TEST MAGNETS AT 25°C	65
13	TEMPERATURE DEPENDENCE OF SINTERED $SmCo_5$ MAGNETIC PROPERTIES	67
14	TEMPERATURE DEPENDENCE OF SINTERED $SmCo_5$ MAGNET PROPERTIES (PERCENT CHANGE FROM VALUES AT 25°C)	68
15	AVERAGE TEMPERATURE COEFFICIENTS OF REMANENCE, COERCIVITY, AND ENERGY PRODUCT OF SINTERED $SmCo_5$ MAGNETS MEASURED	70

LIST OF TABLES (CONTINUED)

TABLE		PAGE
16	PERCENTAGE OF MAXIMUM MAGNETIC PROPERTIES OF VIRGIN SINTERED $SmCo_5$ MAGNETS AT SPECIFIC D.C. MAGNETIZATION FIELD LEVELS	73
17	PERCENTAGE OF MAXIMUM MAGNETIC PROPERTIES OF SINTERED $SmCo_5$ MAGNETS AT SPECIFIC D.C. MAGNETIZATION FIELD LEVELS	76
18	PERCENTAGE OF MAXIMUM MAGNETIC PROPERTIES OF SINTERED $SmCo_5$ MAGNETS AT SPECIFIC PULSE MAGNETIZATION FIELD LEVELS	77
19	AVERAGE RECOIL PERMEABILITY OF SINTERED $SmCo_5$ PERMANENT MAGNETS	83
20	MAGNETIC PROPERTIES OF SPECIMEN BARS USED IN MECHANICAL TEST EVALUATIONS	85
21	AVERAGE FLEXURAL STRENGTH VERSUS TEMPERATURE	98
22	PHASE III FLEXURE TEST RESULTS FOR BRAND TYPE B-1 MAGNETS	99
23	PHASE III FLEXURE TEST RESULTS FOR BRAND TYPE E-1 MAGNETS	100
24	RANGE OF FLEXURE STRENGTH VALUES FOR PHASE III MAGNETS	101
25	PHASE III - AVERAGE COMPRESSIVE STRENGTH AND STANDARD DEVIATION	105
26	PHASE III - COMPRESSIVE STRENGTH OF BRAND TYPE B-1 AND E-1 MAGNETS	106
27	YOUNG'S MODULUS AND POISSON'S RATIO VERSUS TEMPERATURE	114
28	HARDNESS VALUES OBTAINED FROM B-1 AND E-1 FLEXURAL TEST SPECIMENS	116
29	THERMAL PROPERTIES OF SINTERED $SmCo_5$	117
30	AVERAGE ELECTRICAL RESISTIVITY AND TEMPERATURE COEFFICIENT (-60° to +200°C)	119

SUMMARY

The objective of this program was to characterize basic electrical, mechanical, and thermal properties of "high performance" rare-earth transition metal (RE-TM) permenant magnets, as a part of an overall Air Force effort to develop lightweight, high performance motors and generators for advanced aerospace applications. The magnetic properties of these "high performance" (greater than 20 MGOe energy product, 200°C operational stability, and nearly square intrinsic hysteresis loop) RE-TM permanent magnets permit rotating machinery such as motors and generators to be designed which offer tremendous advantages over Alnico containing or conventional wire wound machinery, not only with respect to size and weight, but in electrical performance and efficiency.

Serious limitations in exploiting the total capabilities and potential of the high performance RE-TM permanent magnets in rotating machinery are the lack of reliable physical and mechanical property data which force engineers to take a conservative approach in the design of such machinery. Specific engineering data required are tensile and compressive strengths, elastic modulus, Poisson's ratio, hardness, mechanical shock resistance, heat capacity, thermal conductivity, coefficient of thermal expansion, and electrical resistivity.

In view of the number and complexity of the tests required to obtain these engineering data, it is absolutely essential that the measurements be performed on truly "high performance" permanent magnets, as defined above, and that these magnetic characteristics be verified prior to initiation of physical property testing. Furthermore, the RE-TM magnets meeting the "high performance" criteria should be typical of the vendor's current production, or at least typical of what could be produced in quantity.

With these criteria in mind the program was defined and executed in three phases:

- The first phase was essentially a magnetic and mechanical test screening exercise to choose two RE-TM brand type magnet materials, from 11 candidate types in commercial production circa 1979-1980, for more extensive characterization.

- In the second phase a technical review of the Phase I results culminated in the selection and purchase of two candidate sintered $SmCo_5$ magnet types which proved to be more satisfactory for the intended applications than the other magnet types evaluated. Fixture design, laboratory testing, and test plan procedures for the final phase were submitted for approval at this point.

- In the final phase extensive and comprehensive test evaluations were performed to examine the thermal dependency and directional variation of specific engineering data on a statistically meaningful number of test specimens.

At the completion of this program it was concluded that even under the best of commercial production conditions certain properties, particularly the magnetic and physical strength, of sintered RE-TM permanent magnets will invariably be dependent on small changes in alloy composition, heat treatments, quenching rates, and microstructural inhomogeneities in the finished magnet. As our data indicates, safe optimum or lower limit property values and characteristic behavior above or below room temperature can be assumed for specific application requirements.

SECTION 1
INTRODUCTION

In recent years there has been a significant improvement in the overall magnetic quality of high performance rare earth-transition metal (RE-TM) permanent magnet materials available to the magnetic circuit design engineer.[1,2,3] Today, for near room temperature applications he can readily choose from several sources an alloy composition to meet his magnetic requirements.[4,5] For more demanding advanced aerospace applications and environments such as that encountered by light weight high-speed airborne motors and generators, there has been a serious lack of information pertaining to comprehensive engineering property data.[6,7,8] This situation particularly exists with regard to the thermal dependency of various engineering parameters, the method of magnet fabrication, magnetic orientation, and method of powder compaction prior to sintering.

In particular, the uncertainty of available physical and mechanical property data poses a serious limitation in exploiting the total capability and potential of high performance RE-TM permanent magnets in a given design. As a consequence, once the magnetic property requirements were satisfied, a conservative or "worst case" approach was often taken when considering physical or mechanical design limits imposed by the magnets in the application. As a result optimum size and weight reductions and electrical performance or efficiencies afforded by these materials were often compromised.

To alleviate this problem in future aerospace machine design considerations, an Air Force program was defined to characterize the basic electrical, mechanical, and thermal properties of high performance RE-TM permanent magnets.

The specific engineering data requirements cited were:

- Compressive strength
- Tensile strength
- Elastic modulus
- Poisson's ratio

- Hardness
- Impact resistance
- Heat capacity
- Thermal conductivity
- Coefficient of thermal expansion
- Electrical resistivity.

In view of the number and complexity of the tests required to obtain these engineering data, it became absolutely essential that the measurements be performed on truly "high performance" permanent magnets, which were defined as having energy products equal to or greater than 20 MGOe, 200°C operational stability, and nearly square intrinsic hysteresis loops. Furthermore, the RE-TM magnets meeting this high performance criteria should be typical of the manufacturer's current production, or at least typical of what could be produced in quantity. Therefore, it also became essential to verify the magnetic characteristics prior to the initiation of physical property testing.

To meet the Air Force objectives, the general technical effort of the program was divided into three phases. The phase objectives included and addressed the following.

- Phase I

Selection and purchase of several brand type sintered RE-TM permanent magnets for preliminary screening evaluation tests. These evaluations addressed two important aspects to be considered in selecting candidate brand types for extensive characterization in Phases II and III. They were the magnetic and compressive strength properties at room temperature and magnetic properties at -60°, +100°, and 200°C. Sufficient numbers of brand types, test specimens, and comprehensive test data accomplished the primary objective of this phase.

- Phase II

Evaluation of test data results from Phase I. Selection and purchase of two candidate brand types in sufficient quantities and shape configuration was completed in preparation for comprehensive testing in Phase III. It was envisioned that

one of the candidate brand types would be $SmCo_5$ and the other a Sm_2Co_{17} based material. Test fixture maintenance, calibration, design, and fabrication was completed as required. Initial room temperature magnetic characterization of magnet specimens was performed prior to test distribution in Phase III.

- Phase III

Perform the comprehensive physical property tests previously described as a function of temperature and magnetization orientation using a sufficient number of test specimens to yield statistically meaningful data. In a similar manner the thermal dependency of key magnetic properties was also evaluated to complete the overall objective of the program.

SECTION 2

PHASE I

A. Test Magnet Selection

Preliminary efforts in this phase of the program included the selection of manufacturers deemed capable of producing the quality magnet necessary to meet the Air Forces' requirements. These requirements specifically called for production magnets having:

- Energy products $\geq$ 20 MGOe
- 200°C operational stability
- Nearly square intrinsic demagnetization curves
- Magnet production size capability - up to ∿25 mm cubes
- Minimum B vs. H specifications as shown in Figure 1.

Prospective brand types must possess second-quadrant characteristics to the left of the solid line at ambient temperature (∿25°C).

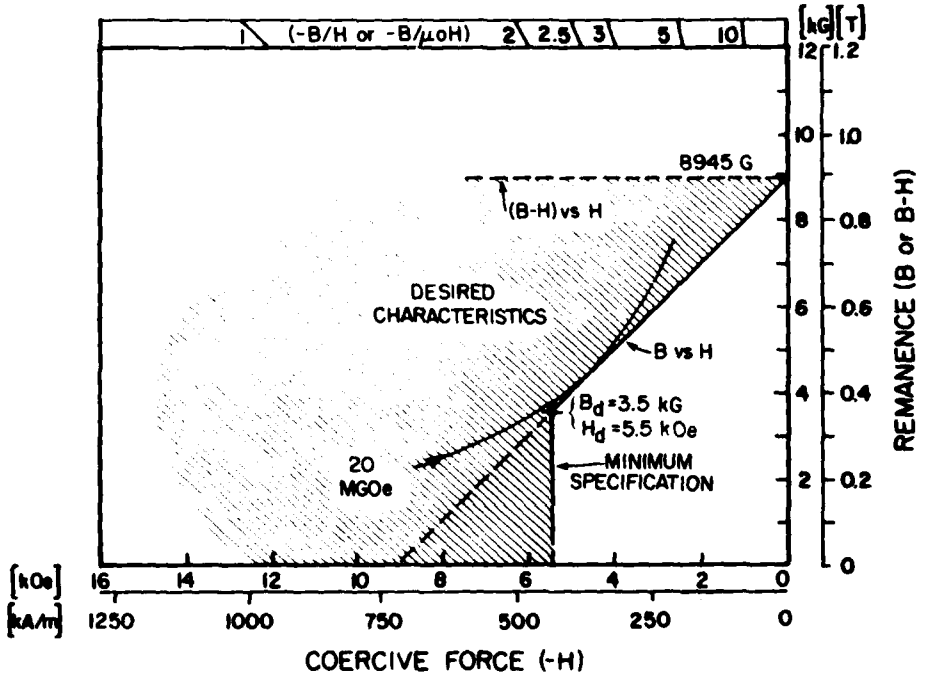

Figure 1. High Performance Magnet Characteristics. (Air Force Specification.)

Initial contacts were made directly with representatives of both domestic and foreign RE-TM magnet producers, to inform them of the scope and intent of the Air Force program, test specimen requirements, and to solicit their present applicable product capability and interest in participating in the program.

From the number of positive responses received from manufacturers who expressed interest in participating in the program, a prospective list of candidate brand type magnets was prepared and submitted to the Air Force Project Engineer for approval. Candidate RE-TM magnet materials selected for evaluation in the initial phase were of $SmCo_5$ and Sm_2Co_{17} based compositions, and composition variations modified on either the rare earth or transition metal side. Candidate materials selected also encompassed the range of production compaction and field alignment techniques presently used in industry to produce sintered RE-TM permanent magnets. Those magnet materials selected are identified in Table 1 by an arbitrary brand type code designation. The only correlation between the brand types listed is the occasional common letter code prefix signifying a common production source and composition - but different fabrication method (i.e., see A-1 and A-2), or a common source but different alloy composition (i.e., see B-1, B-2, and B-3).

As indicated in Table 1, 11 brand types of production magnets were selected and purchased from six domestic or foreign sources. For the tests envisioned in this phase, as indicated in the diagram shown in Figure 2, production lot quantities of 18 test magnet specimens were obtained from the manufacturers of each brand type. These specimens were procurred with the additional stipulation that the specimens delivered have:

- Dimensions and tolerance: 8.17 x 8.17 x 8.17 + 0.00/-0.05 mm
- Opposing specimen surface parallel
- Surface finish $\leq$ 16μ inches
- Virgin magnetization condition
- Original direction of magnetization identified

TABLE 1

TEST MAGNET IDENTIFICATION, COMPOSITION, AND FABRICATION METHOD

Brand Type	Alloy Composition	Fabrication Method[a)]
A-1	$SmCo_5$	P||M
A-2	$SmCo_5$	I
B-1	$SmCo_5$	I
C-1	$SmCo_5$	P⊥M
D-1	$SmCo_5$	P⊥M
E-1	$SmCo_5$	P||M
B-2	$(SmPr)Co_5$	P⊥M
F-1	$Sm(CoCuFe)_7$	P⊥M
B-3	$Sm_2(CoTM)_{17}$[b)]	P⊥M
C-2	$Sm_2(CoTM)_{17}$	P||M
C-3	$Sm_2(CoTM)_{17}$	P⊥M

a) Fabrication Method: (P⊥M) Die pressed with force perpendicular to magnetic aligning field. (P||M) Die pressed with force and field parallel. (I) Isostatically pressed.

b) TM is one or more transition metals (Fe, Cu, Zr, Hf).

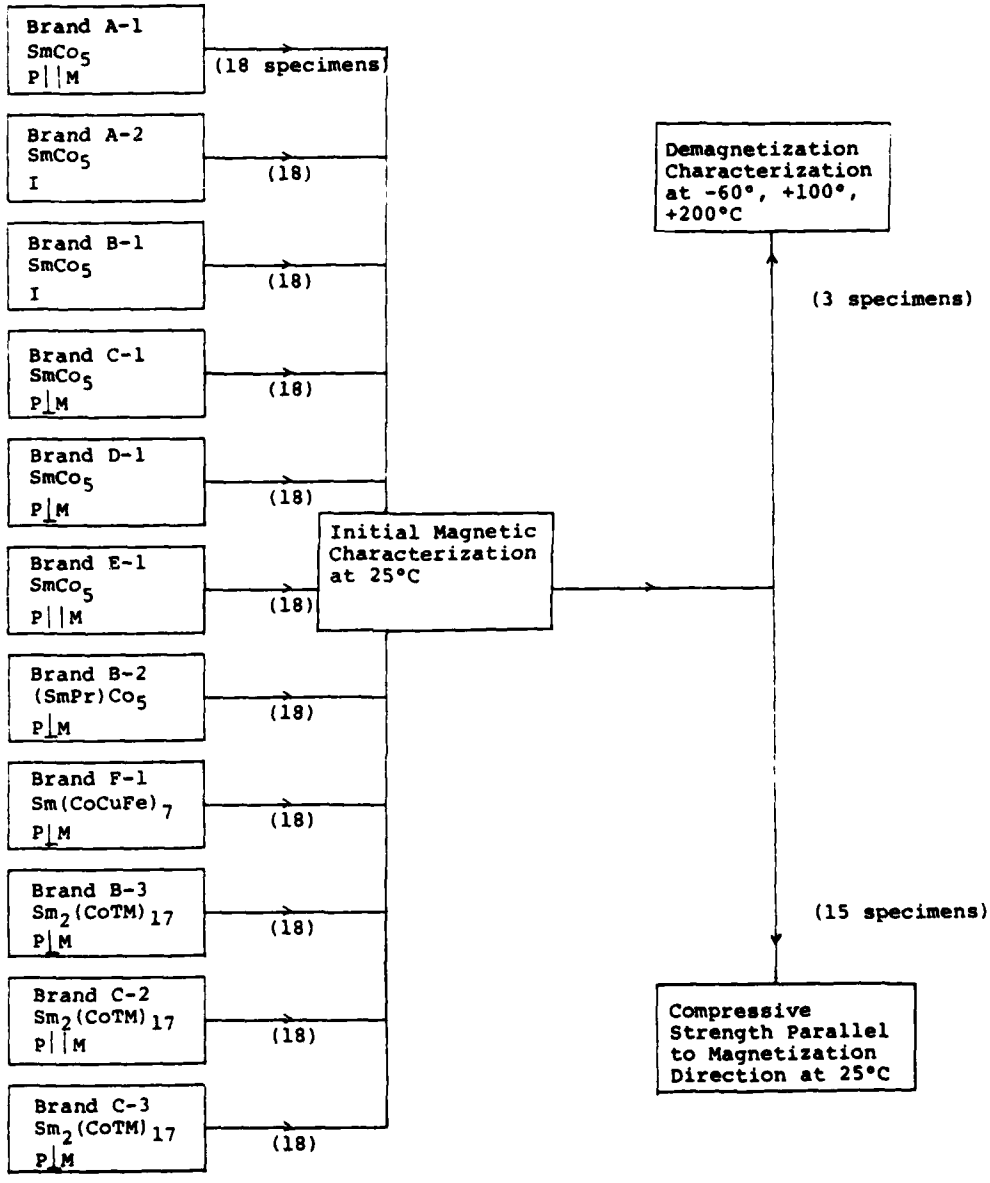

Figure 2. Phase I Magnetic and Mechanical Characterization of 11 Candidate Brand-Type High Performance Sintered RE-TM Permanent Magnets.

- Magnet brand-type identification and general composition noted
- Compaction direction with respect to magnetic alignment orientation noted.

The choice of ∿8 mm cubic-sized test magnet specimens specified stems from several factors considered applicable for all phases of the program:

- The specimen configuration is of the same shape and permeance as in the intended aerospace applications.
- The size and shape is compatible to all measurements proposed ... except for determining flexural strength, elastic modulus, and Poisson's ratio in Phase III.
- The specimen size and weight would minimize the cost incurred in magnet procurement.

From the approach outlined thus far, and the scope and numbers of magnet material types investigated, it was anticipated that a comparative evaluation of meaningful magnetic and mechanical property data, measured under identical conditions would yield average and standard deviation numbers for each of the brand types tested. These results would then be used to select two types for further evaluation in Phases II and III.

B. Magnetic Property Characterization

a) Procedure and Instrumentation

Prior to initiating the magnetic evaluations individual magnet test specimens were identified, inventoried, inspected for surface defects and measurements of physical dimensions recorded for each brand type as received. Cross-sectional areas for each specimen were also calculated for future reference.

There are five general magnetic property values considered when characterizing and comparing one magnet material against another. These are the room temperature values of remanence (B_r), the induction ($_BH_c$) and intrinsic coercivities ($_MH_c$), energy product

$BH_{(max)}$ and "loop squareness," of the intrinsic demagnetization curve as indicated by the reverse field (H_K) required to decrease the remanence 10 percent of its value measured at H=0. All these data (and measurements of magnetization, demagnetization, and recoil loop effects required in Phase III) can be effectively and efficiently accomplished with a properly designed laboratory hysteresigraph system. The hysteresigraph system used in the measurements which follow was developed at the University of Dayton under contract for the Air Force Materials Laboratory. The first instrument of this type was used in the rare earth-cobalt magnet research program at AFML.[9] New and improved versions of this instrument and sensing probes have been developed and are now in use at the University of Dayton Magnetics Laboratory.[10,11] See Figures 3 and 4.

This instrument employs induction coils for the detection of both the B-flux and the H-field. The probe coils are designed and constructed to conform closely to the surface of the magnet specimen. Upon inserting a specimen, the coil windings are physically located symmetrically about the geometric center plane of the magnet (lengthwise), and have a winding length relatively short in comparison to magnet length (∿33% of specimen length). Such a coil is capable of measuring a field value approximately equal to the true internal field inside the magnet; that is, it automatically takes into account the demagnetizing field and thus avoids the problems encountered in making mathematical corrections using doubtful values of the demagnetizing factor.

Two highly stable operational amplifier Miller integrators are used for electronic time integration of the signals. The air-flux compensation, to form the intrinsic induction (B-H) is done by electronically subtracting a portion of the H-coil output from the B signal after integration. The same annular H-coil is used to generate the compensation voltage and the H signal for the horizontal recorder deflection. Direct compensation for individual magnet cross-sectional area is provided; therefore, the data plotted is representative of the specimen and needs no further correction.

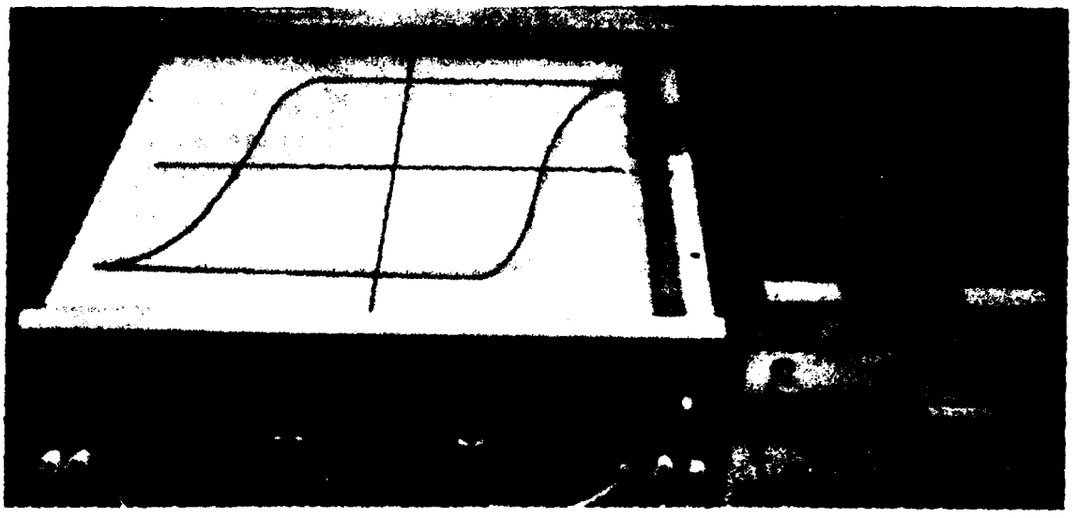

Figure 3. Hysteresigraph Measurement System: Electronic Integrators and Composition Unit, Specimen Coil Probe, and X-Y Plotter.

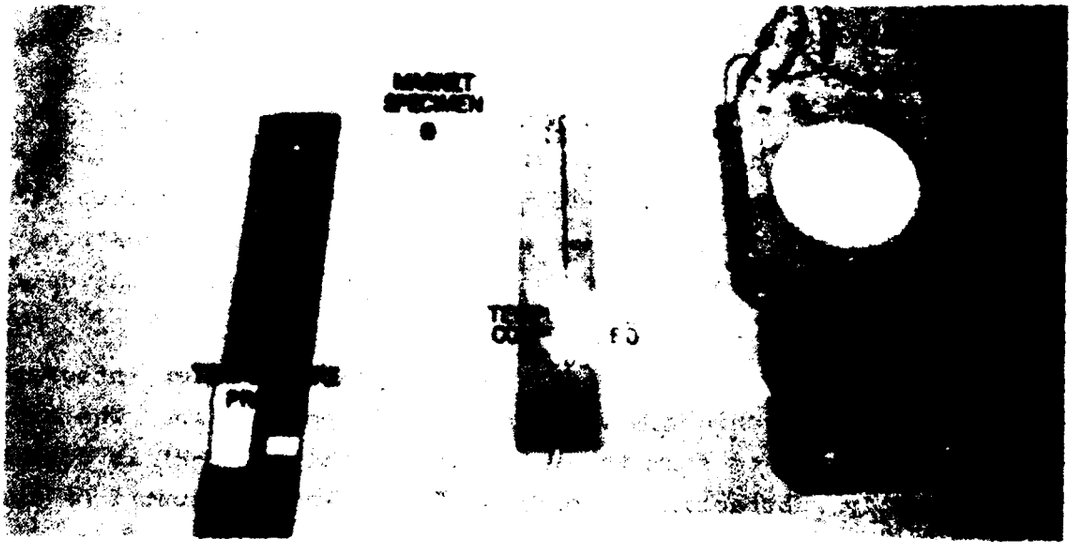

Figure 4. Hysteresigraph Coil Probes and Temperature Controlled Fixture.

In these measurements a standard coil was used (for 8.17 mm square specimens). A pure nickel standard of the same dimensions as the test magnets was used for calibration purposes. In calculating the calibration factor for (B-H), we reference the saturation induction of the Ni to be 6,200 Gauss, with an applied field of 10 kOe at 25°C. The H calibration of the coil was checked with the empty coil placed in a homogeneous DC field, referenced to a Rawson-Lush rotating coil gaussmeter (0.1% accuracy).

The magnetizing device used in the demagnetization curve measurements was a 9 inch iron-core electromagnet. Typically, the magnet specimens were pulse magnetized open circuit in a coil with 100 kOe peak field. Then they were transferred to the gap of the electromagnet and remagnetized in the closed circuit with a maximum DC field of 32 kOe, and a first and second quadrant intrinsic demagnetization curve directly plotted. The B vs. H curves, data for energy product and loop squareness, were mathematically constructed and derived from the intrinsic curves.

For hysteresis measurements at temperatures above or below room temperature, intrinsic demagnetization curves were measured with a special temperature and (B-H) compensated hysteresigraph probe fixture, built to accommodate the cubic specimens purchased. The probe and fixture are shown in Figure 4, and pictorially illustrated in the sectional view in Figure 5. In this probe two coplanar coils nearly identical in area-turns were used to detect the B-flux through the specimen and the H-field in a symmetric location near the specimen. Coil winding length with respect to specimen length was also short (~33%) by comparison The measurement is still performed closed circuit in the air gap of an iron-core laboratory electromagnet.

The special temperature-compensated fixture provides a controlled temperature environment for specimen, coils, and electromagnet pole piece extensions. The fixture is preheated or cooled to the desired temperature. The empty coils were then compensated electronically for (B-H) = 0 while the field is swept.

Then the magnet specimen was placed in the fixture and allowed to stabilize at the measuring temperature before the integrators were turned on and the specimen was transferred to the coil. The full field was applied in the forward direction, and while H was slowly swept from +32 to -32 kOe, the first- and second-quadrant curves were obtained. The specimen temperature was measured with a 0.08 mm copper-constantan thermocouple placed in the probe 0.3 mm from the test magnet. The specimen remained stable within ±1°C of the nominal value. The B vs. H curves, energy product and H_K, were derived from the intrinsic curves in the same manner as would be derived from curves measured at room temperature.

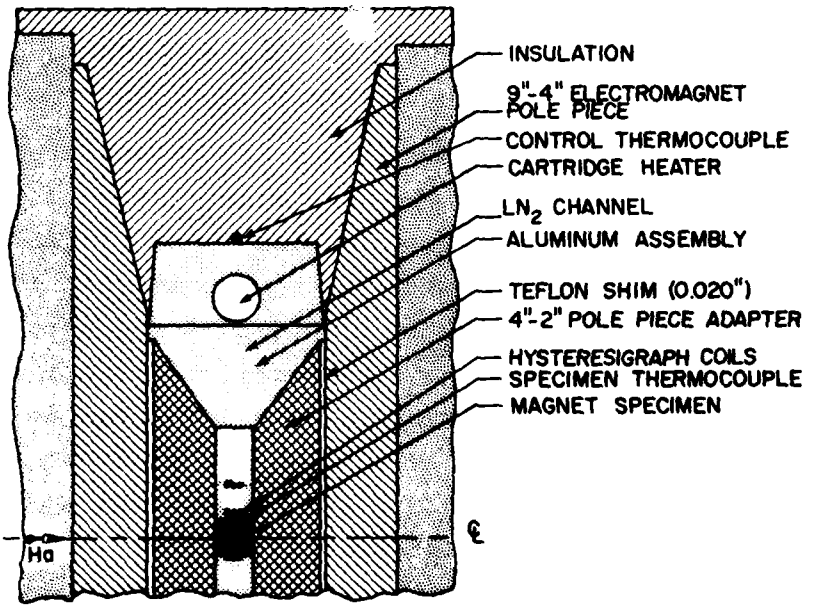

Figure 5. Temperature Controlled Probe Fixture Construction.

b) Measurements at Room Temperature

Using the integrating hysteresigraph system described, first- and second-quadrant intrinsic demagnetization curves were measured and recorded at room temperature for all brand type specimens purchased. Prior to these measurements, each specimen was pulse magnetized with a 100 kOe field in the original direction of magnetization indicated by the manufacturer.[a]

The salient second-quadrant magnetic properties B_r, $_BH_c$, $_MH_c$, H_K, and $(BH)_{max}$ for each magnet specimen were derived from the recorder plots. Numerical average values and the standard deviation based on all 18 test specimens measured for each brand type were calculated and are listed in Table 2.

Figures 6a-m graphically illustrate the range of magnetic properties measured at room temperature for each alloy composition and fabrication method employed by the respective manufacturers. Recall that the specifications, as previously noted in Figure 1, require second-quadrant magnetic characteristics to the left of the boundary line identified as "minimum specifications." This specification is also illustrated in the figures, and all subsequent graphs, illustrating this type data as a dotted boundary. In addition, the lowest remanent induction value which could yield an energy product of 20 MGOe, provided the intrinsic demagnetization curve was also ideal, would be 8945 Gauss, as indicated by the horizontal dotted line in each figure.

A precursory examination of the graphical illustrations reveals quite a variation in the inherent intrinsic demagnetization curves for the respective brand types of $SmCo_5$ alloy composition. In one case, type B-1, this is understandable since the manufacturer classifies the magnet material as having 22 MGOe energy product. The variations for the other types can be attributed in part to

---

[a]Initial magnetization curves were measured on selected virgin specimens. Data pertaining to typical magnetization properties from the virgin state will be discussed in Section 4, Phase III.

TABLE 2

COMPARISON OF AVERAGE AND STANDARD DEVIATION OF MAGNETIC PROPERTIES FOR EACH BRAND TYPE MEASURED AT ROOM TEMPERATURE, 25°C

Brand Type	Alloy Composition	Fabrication[a] Method	Numerical[b]	B_r (kG)	$_BH_c$ (kOe)	$_MH_c$ (kOe)	H_K (kOe)	$(BH)_{max}$ (MGOe)
A-1	$SmCo_5$	P||M	Average	8.58	8.26	>31.60	11.82	18.0
			St. Dev.	0.127	0.114	0.098	0.254	0.49
A-2	$SmCo_5$	I	Average	8.75	8.28	30.26	11.14	18.6
			St. Dev.	0.077	0.079	1.100	1.079	0.38
B-1	$SmCo_5$	I	Average	10.02	9.22	16.80	10.68	23.5
			St. Dev.	0.074	0.201	0.070	1.405	0.49
C-1	$SmCo_5$	P⊥M	Average	8.88	7.56	12.58	6.99	19.2
			St. Dev.	0.087	0.111	0.412	0.232	0.36
D-1	$SmCo_5$	P⊥M	Average	8.88	8.02	26.21	8.56	18.6
			St. Dev.	0.143	0.133	5.255	1.205	0.54
E-1	$SmCo_5$	P||M	Average	8.90	8.69	23.75	13.20	19.7
			St. Dev.	0.106	0.149	5.386	1.916	0.48
B-2	$(SmPr)Co_5$	P⊥M	Average	9.67	8.82	11.55	9.48	21.8
			St. Dev.	0.028	0.377	1.702	1.326	0.18
F-1	$Sm(CoCuFe)_7$	P⊥M	Average	9.45	7.44	8.13	6.73	21.9
			St. Dev.	0.048	0.119	0.107	0.205	0.29
B-3	$Sm_2(CoTM)_{17}$[c]	P⊥M	Average	10.94	4.85	5.08	4.25	25.7
			St. Dev.	0.086	0.112	0.114	0.122	0.66
C-2	$Sm_2(CoTM)_{17}$	P||M	Average	9.99	6.05	7.12	4.71	22.0
			St. Dev.	0.054	0.065	0.093	0.079	0.23
C-3	$Sm_2(CoTM)_{17}$	P⊥M	Average	10.82	6.04	6.55	5.20	27.2
			St. Dev.	0.042	0.110	0.116	0.130	0.40

[a] Fabrication Methods: [P⊥M] Die pressed with force perpendicular to magnet aligning field, [I] Isostatically pressed, [P||M] Die pressed with force and field parallel.

[b] Average values based on 18 test specimens.

[c] TM is one or more transition metals (Fe, Cu, Zr, Hf).

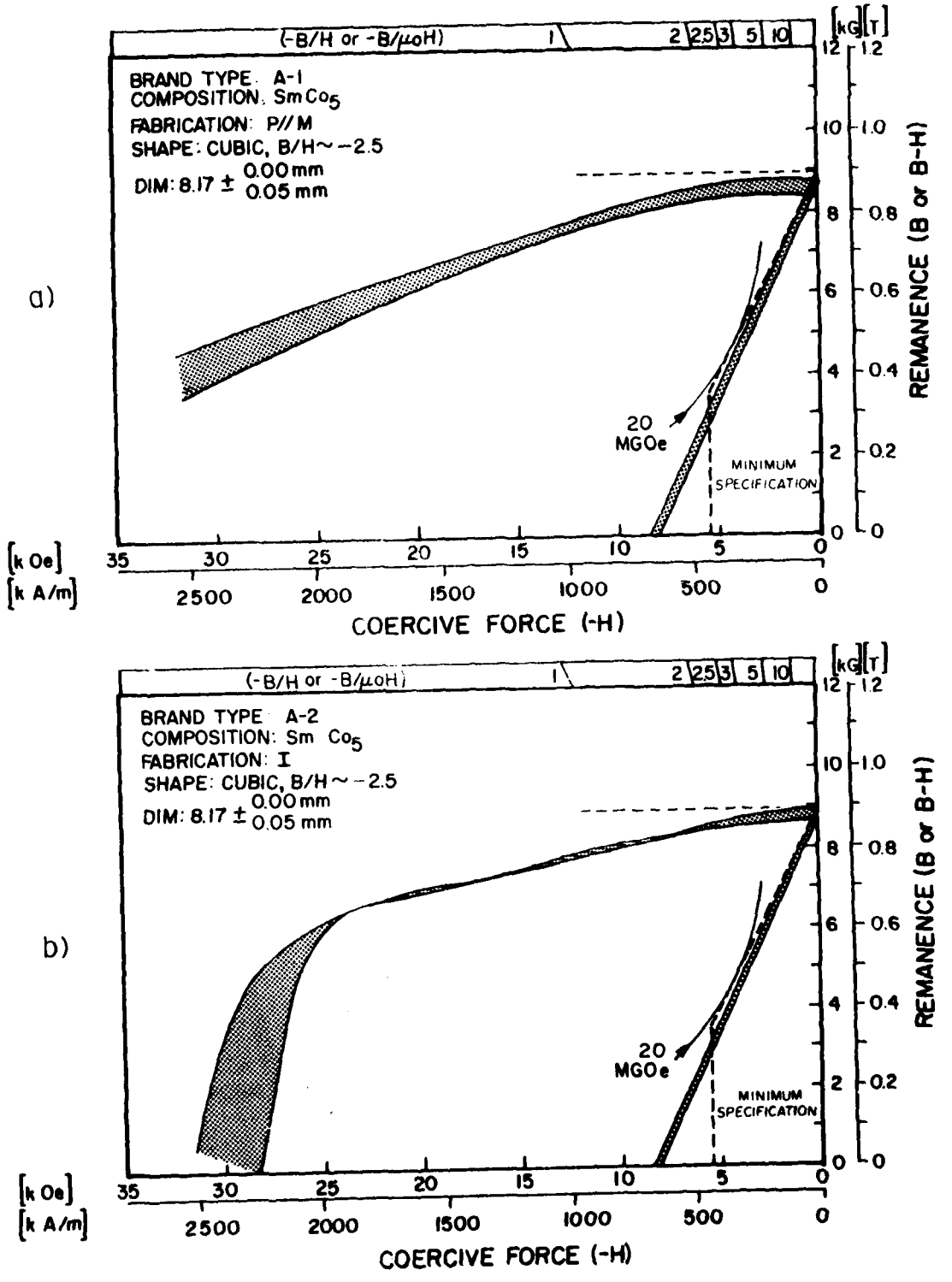

Figure 6a,b Phase I. Range of Demagnetization Curves for Sintered $SmCo_5$ Magnets. Brand Types A-1 and A-2. Produced June 1979, 18 Test Magnets.

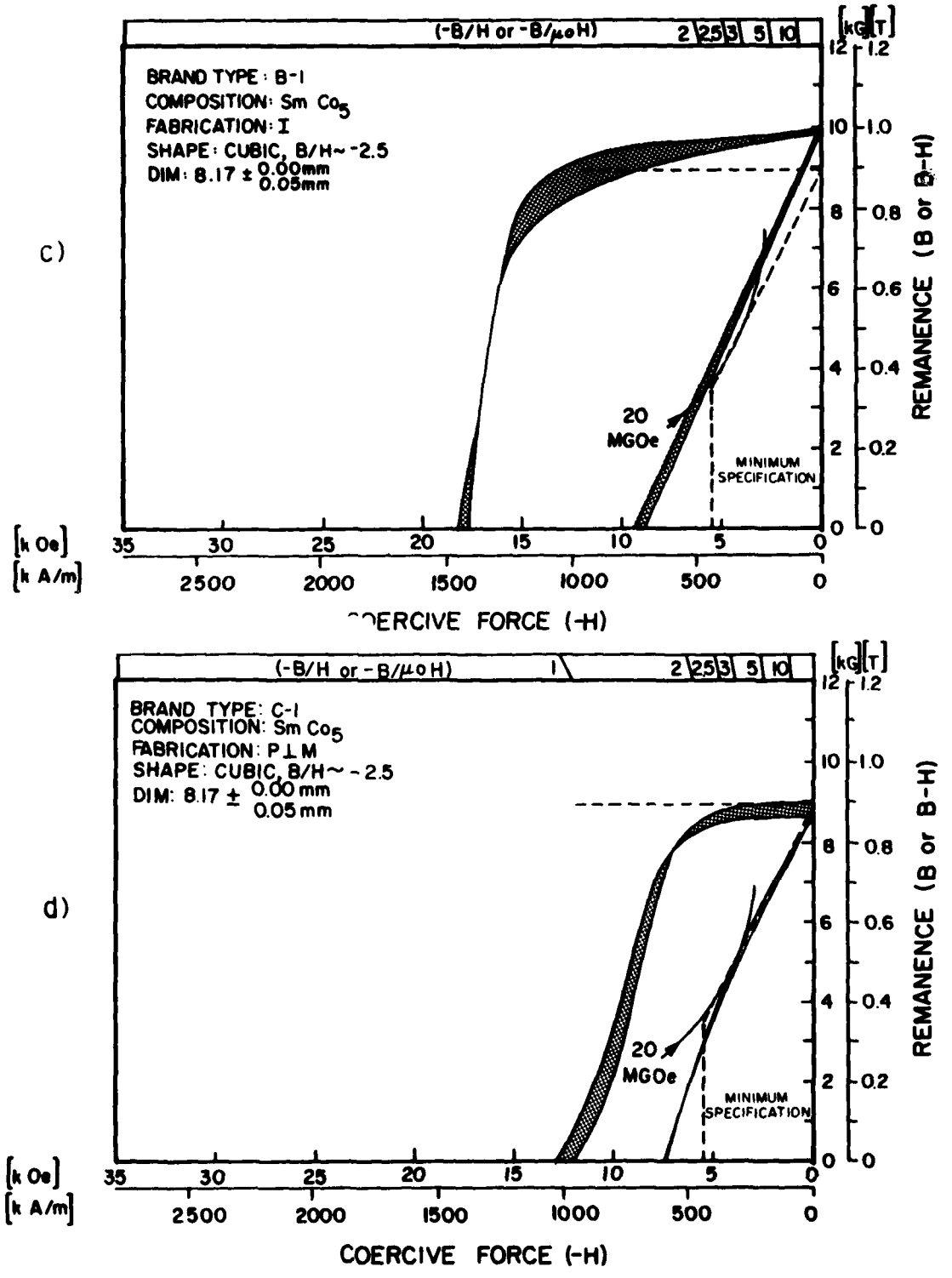

Figure 6c,d Phase I. Range of Demagnetization Curves for Sintered $SmCo_5$ Magnets. Brand Types B-1 and C-1. Produced June 1979, 18 Test Magnets.

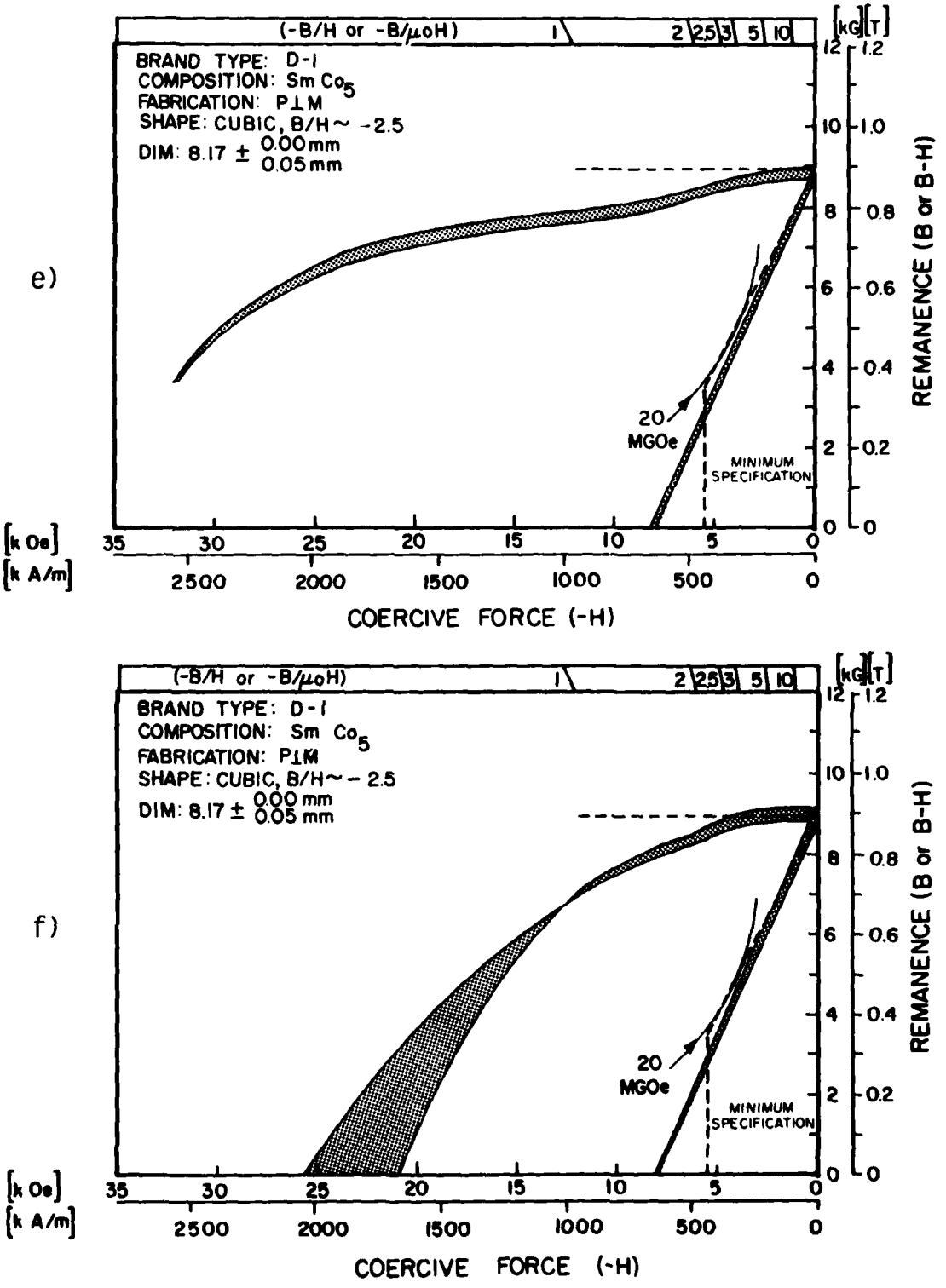

Figure 6e,f Phase I. Range of Demagnetization Curves for Sintered $SmCo_5$ Magnets. Brand Type D-1. Produced June 1979, 18 Test Magnets.

g)

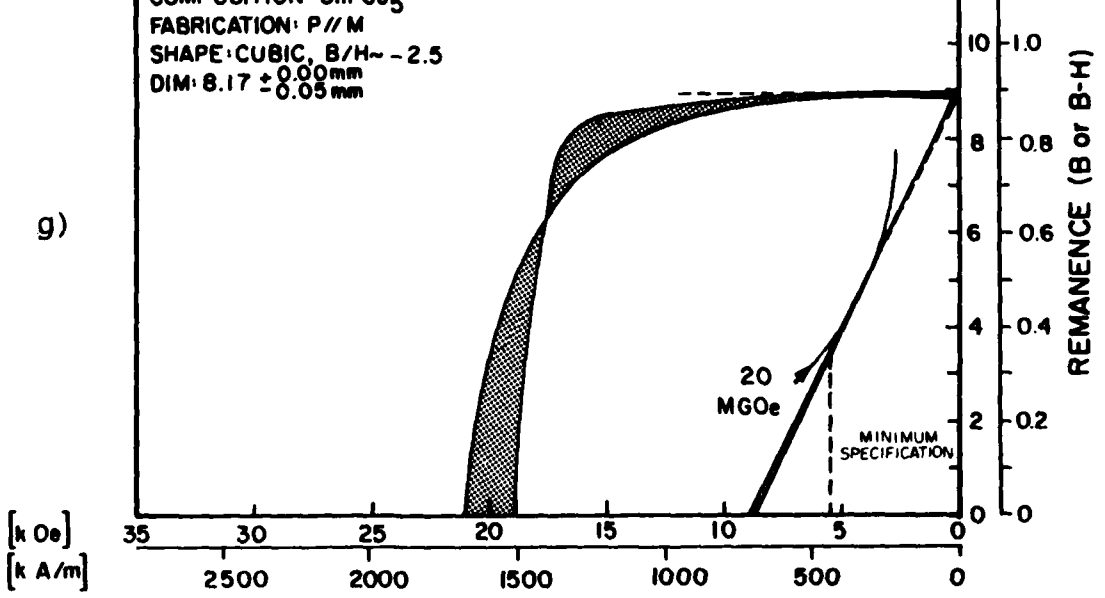

h)

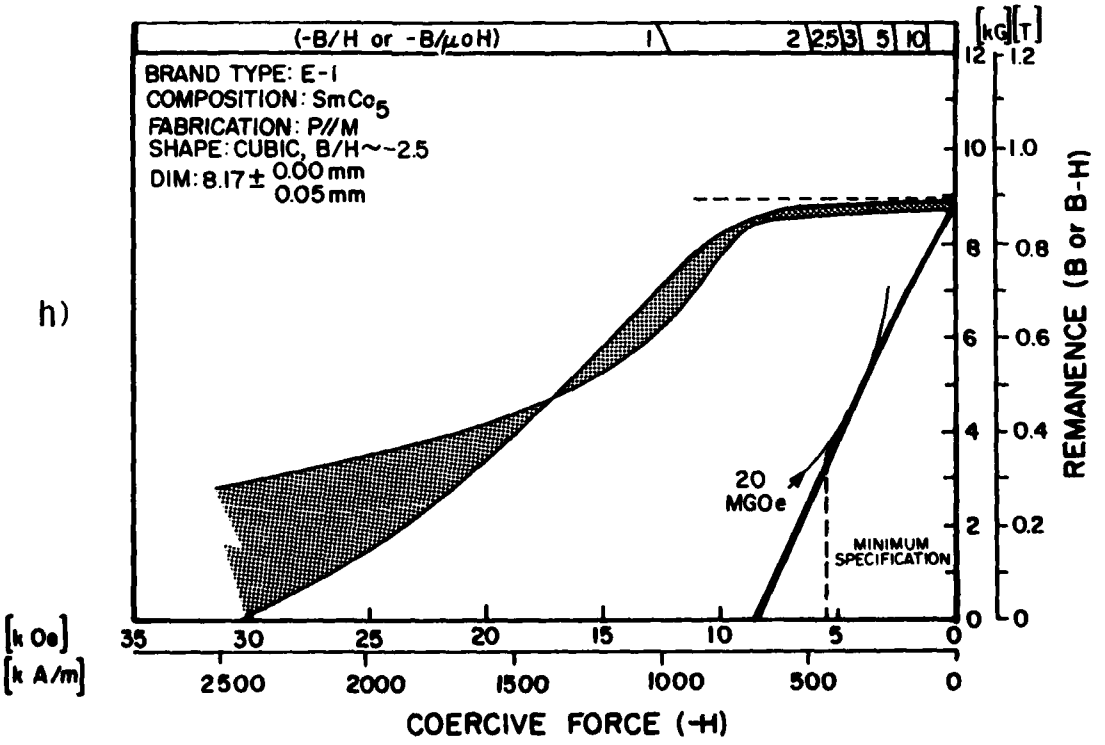

Figure 6g,h Phase I. Range of Demagnetization Curves for Sintered $SmCo_5$ Magnets. Brand Type E-1. Produced June 1979, 18 Test Magnets.

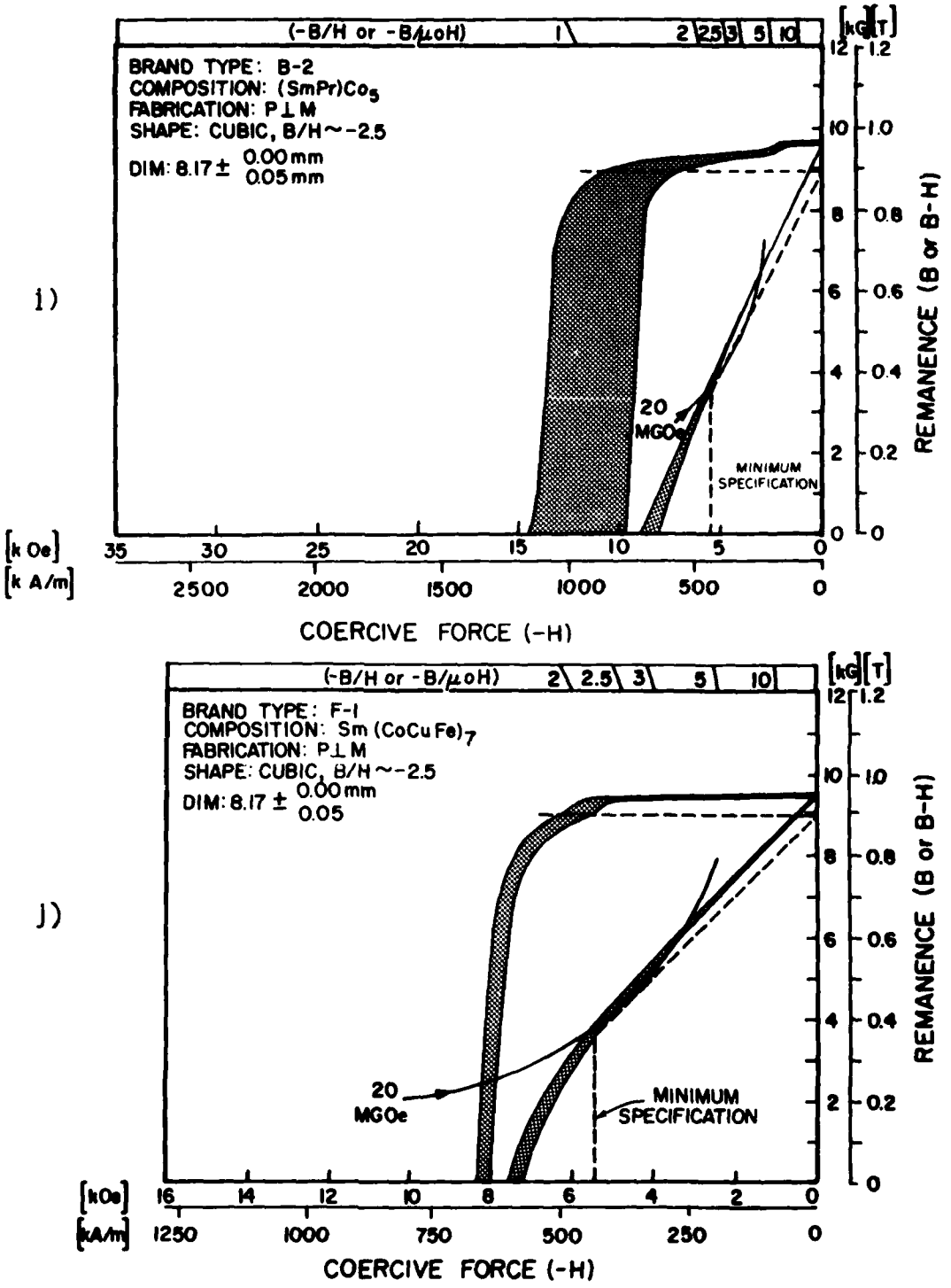

Figure 6i,j Phase I. Range of Demagnetization Curves for Sintered $Sm(Pr)Co_5$ and $Sm(Co,Cu,Fe)_7$. Brand Types B-2 and F-1. Produced June 1979, 18 Test Magnets.

k)

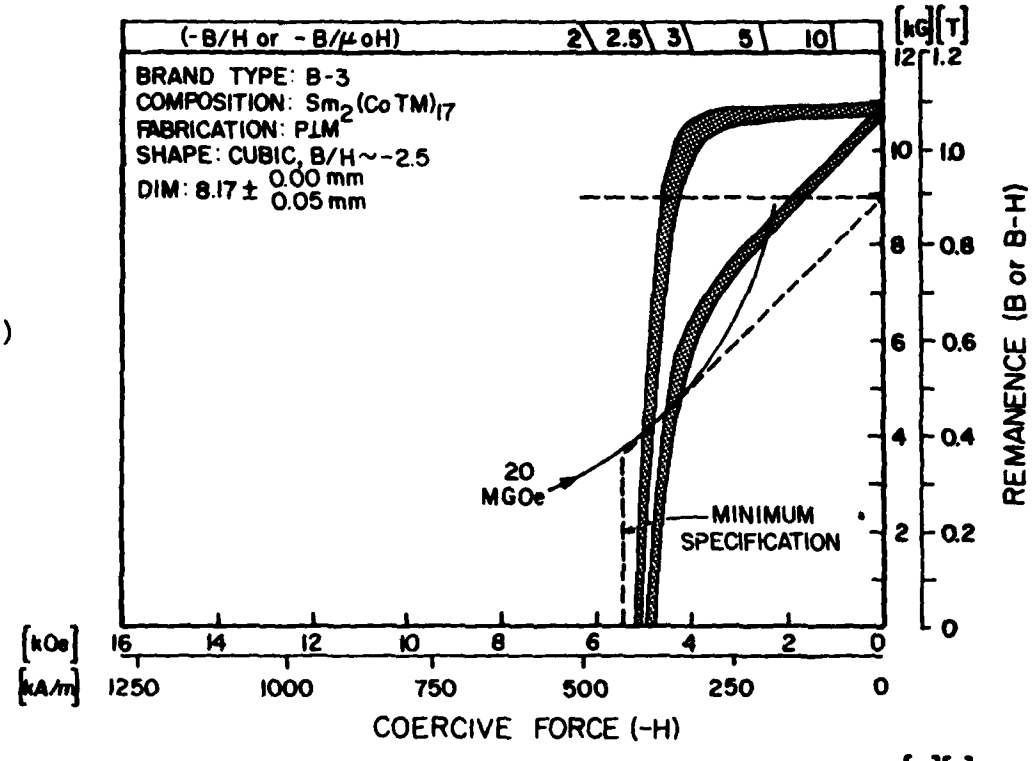

l)

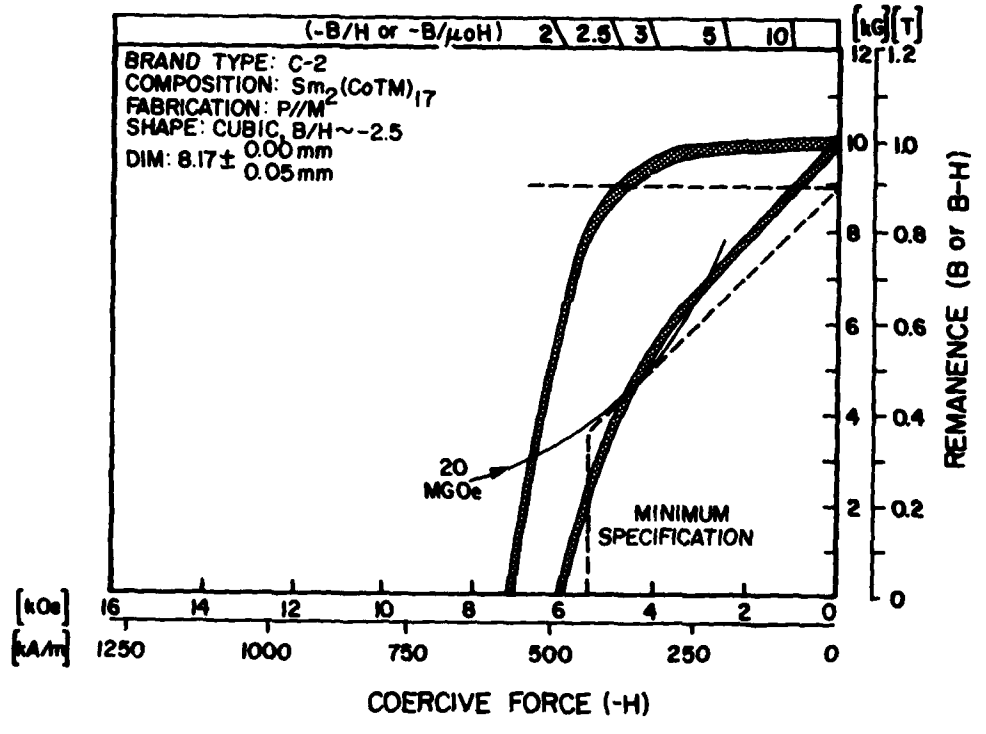

Figure 6k,l Phase I. Range of Demagnetization Curves for Sintered $Sm_2(CoTM)_{17}$ Magnets. Brand Types B-3 and C-2. Produced June 1979, 18 Test Magnets.

m)

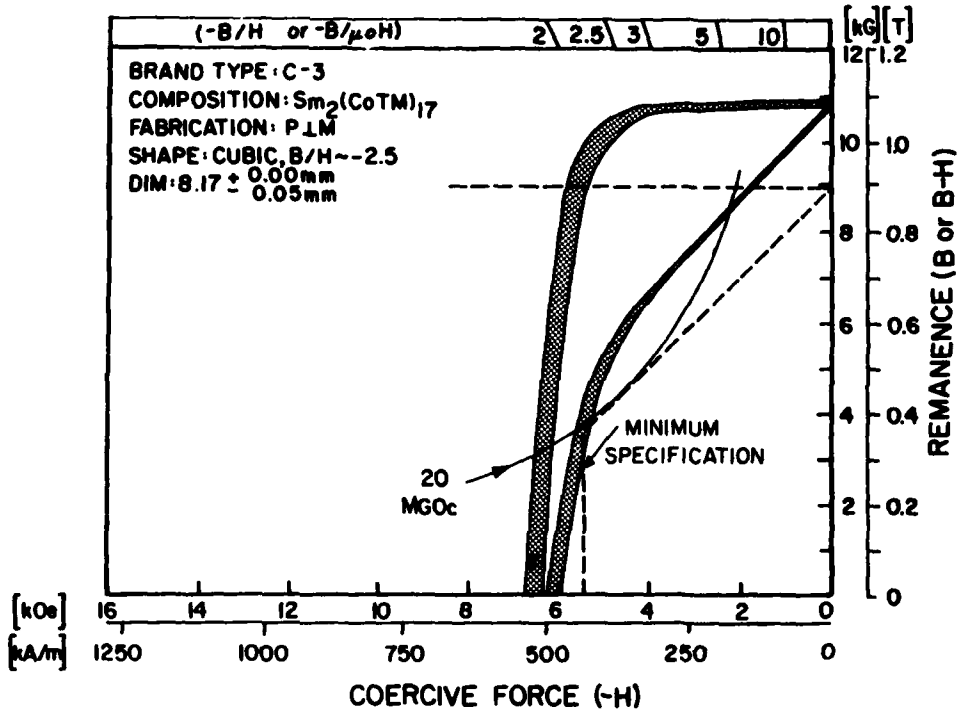

Figure 6m Phase I. Range of Demagnetization Curves for Sintered $Sm_2(CoTM)_{17}$ Magnets. Brand Type C-3. Produced June 1979, 18 Test Magnets.

various compactions and magnetic alignment methods, and sintering heat treatment and quenching rates used in production. For two of the brand type lots measured (D-1 and E-1), we observe distinctly different sets of characteristic intrinsic demagnetization curves. For brand type D-1, 8 of 18 test specimens (∿44%) appear as shown in Figure 6f. For brand type E-1, 3 of 18 test specimens (∿84%) appear as shown in Figure 6g, the remaining as shown in Figure 6h. These distinctly different intrinsic characteristics with a given specimen lot will greatly affect the numerical average and standard deviation values calculated for intrinsic coercive force and loop squareness of both brand types.

For the other alloys, the characteristic demagnetization curves are directly related to the compositions on either the rare earth side or transition metal side of the alloy, or as in the case of brand types C-2 and C-3, the same alloy, but different fabrication method.

Further comments summarizing the room temperature characterizations will be presented in Section 3, Phase II, as a basis for selecting two brand types for comprehensive testing.

c) Measurements at Temperatures of -60°, +100°, and +200°C

To investigate the thermal dependency of the magnetic properties of all 11 brand types, three magnets were selected for further characterization at temperatures above (100°, 200°C) and below (-60°C) room temperature. Using the temperature controlled fixture and hysteresigraph probe, second-quadrant intrinsic demagnetization curves were measured and plotted at each specific temperature starting at -60°C. Each magnet specimen was pulse magnetized at 100 kOe field in the original direction prior to remeasurement at another temperature. Figures 7a-k illustrate typical intrinsic and normal composite demagnetization curves for each of the brand types measured relative to the characteristic curves at 25°C.

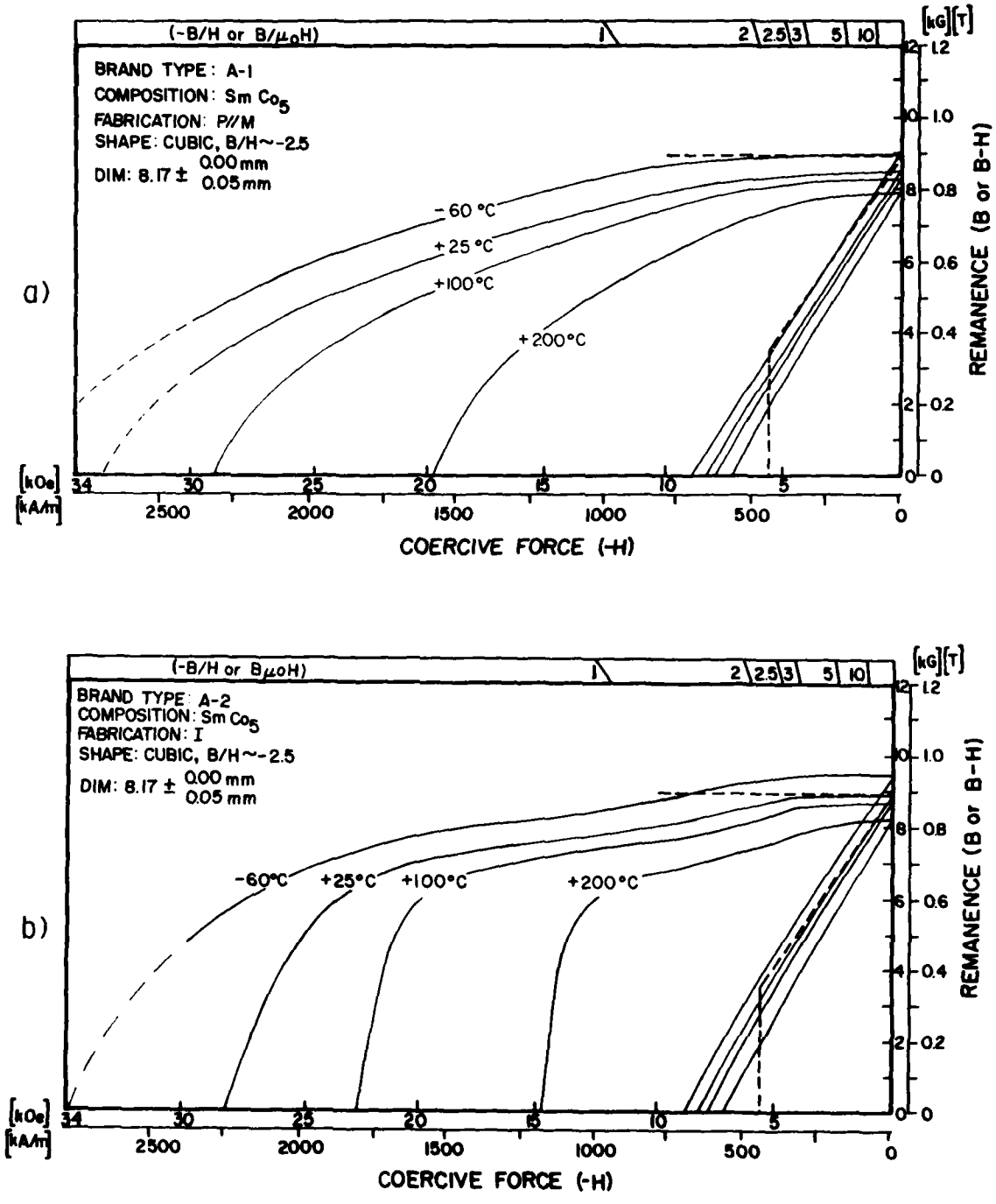

Figure 7a,b Phase I. Typical Demagnetization Curves for Sintered $SmCo_5$ Magnets Evaluated at Four Temperatures from -60° to +200°C. Brand Types A-1 and A-2.

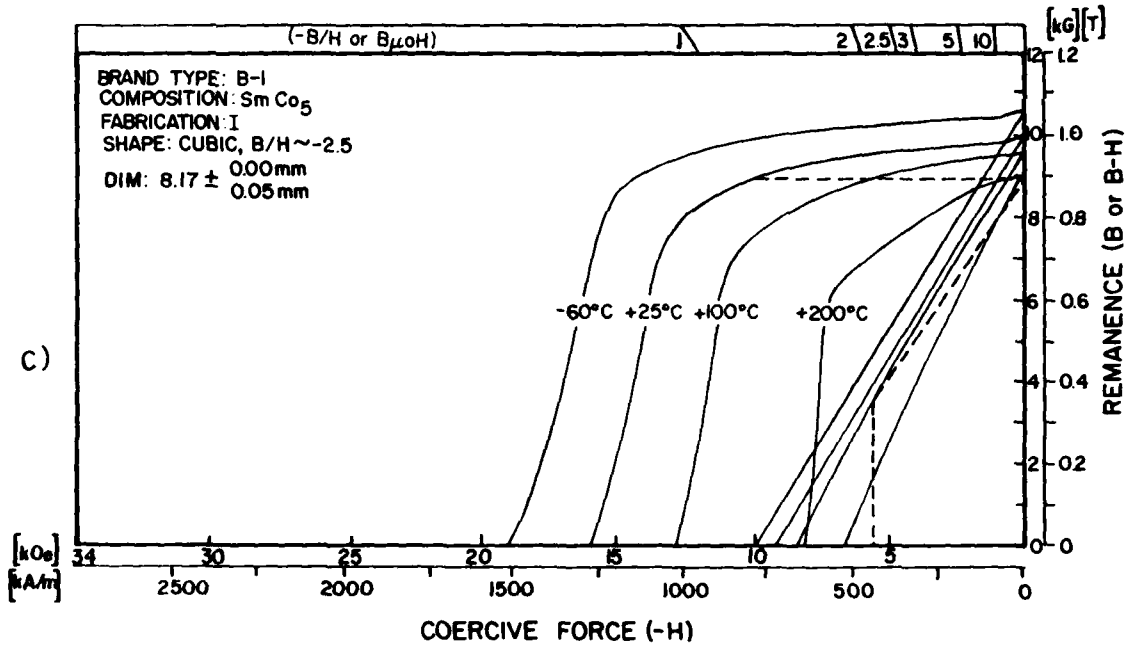

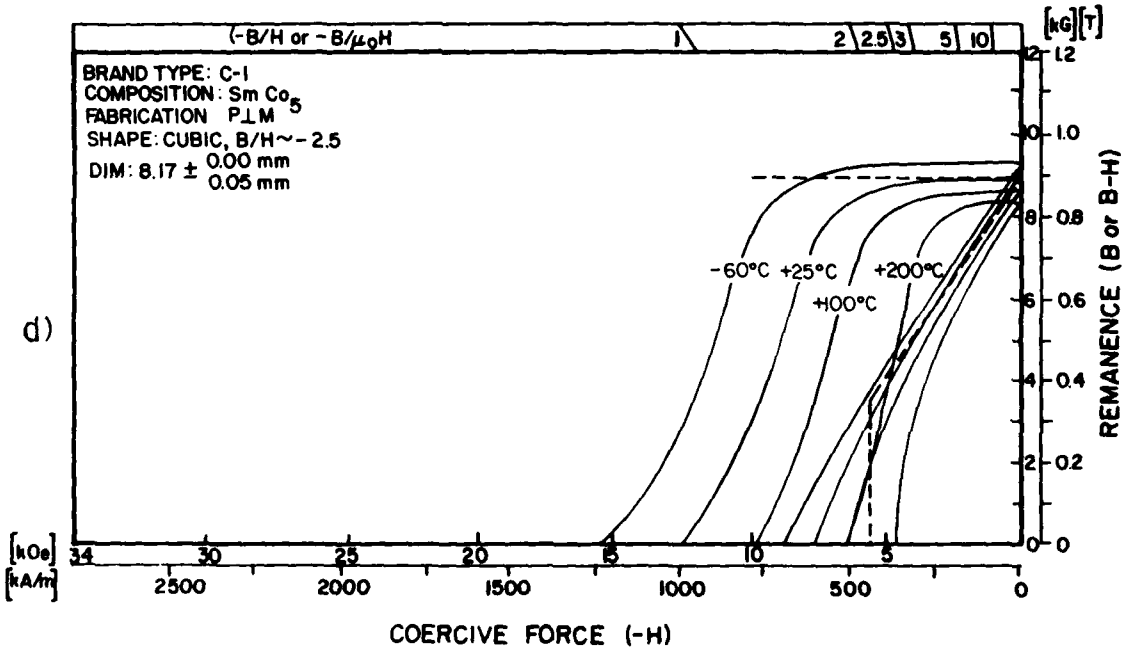

Figure 7c,d Phase I. Typical Demagnetization Curves for Sintered $SmCo_5$ Magnets Evaluated at Four Temperatures from -60° to +200°C. Brand Types B-1 and C-1.

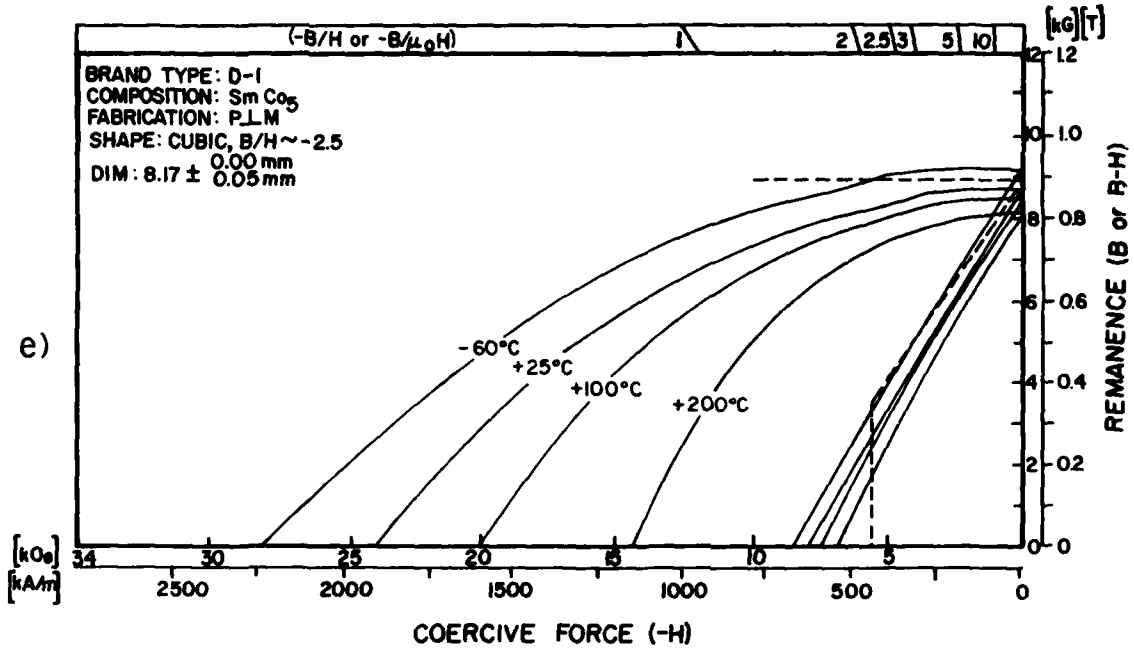

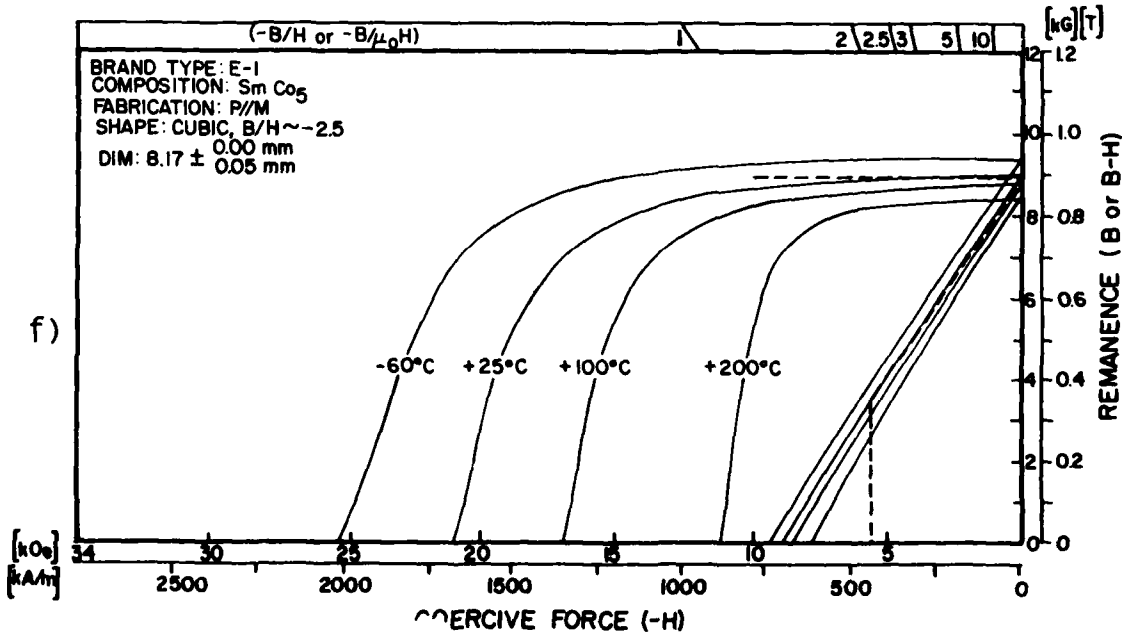

Figure 7e,f Phase I. Typical Demagnetization Curves for Sintered SmCo Magnets Evaluated at Four Temperatures from -60° to +200°C. Brand Types D-1 and E-1.

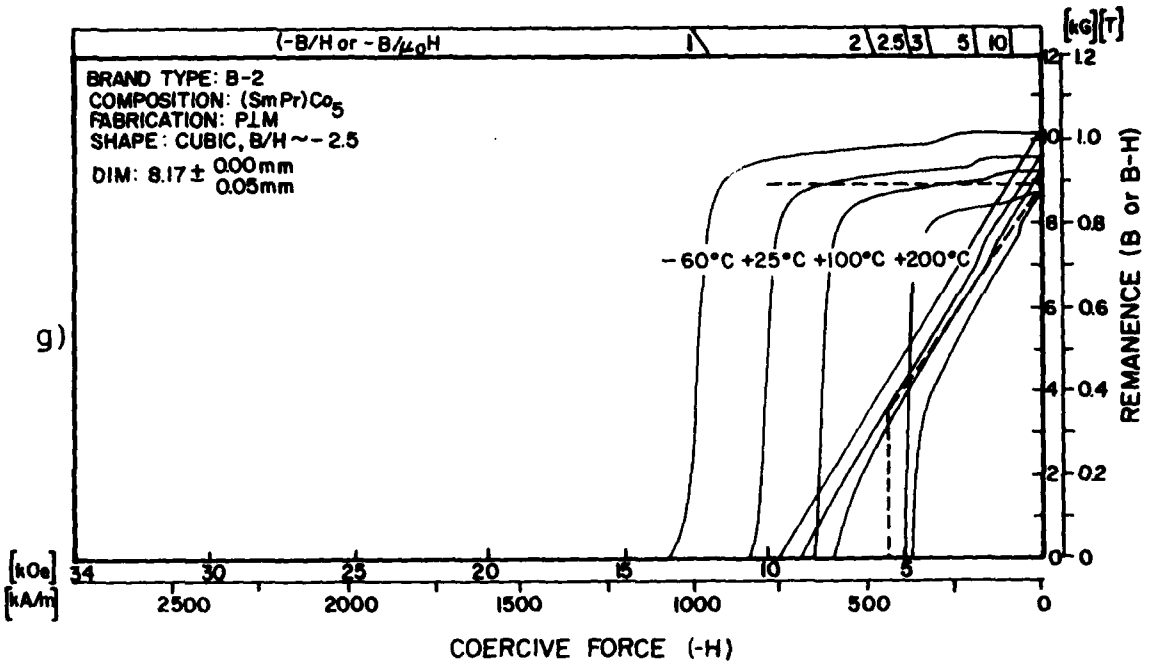

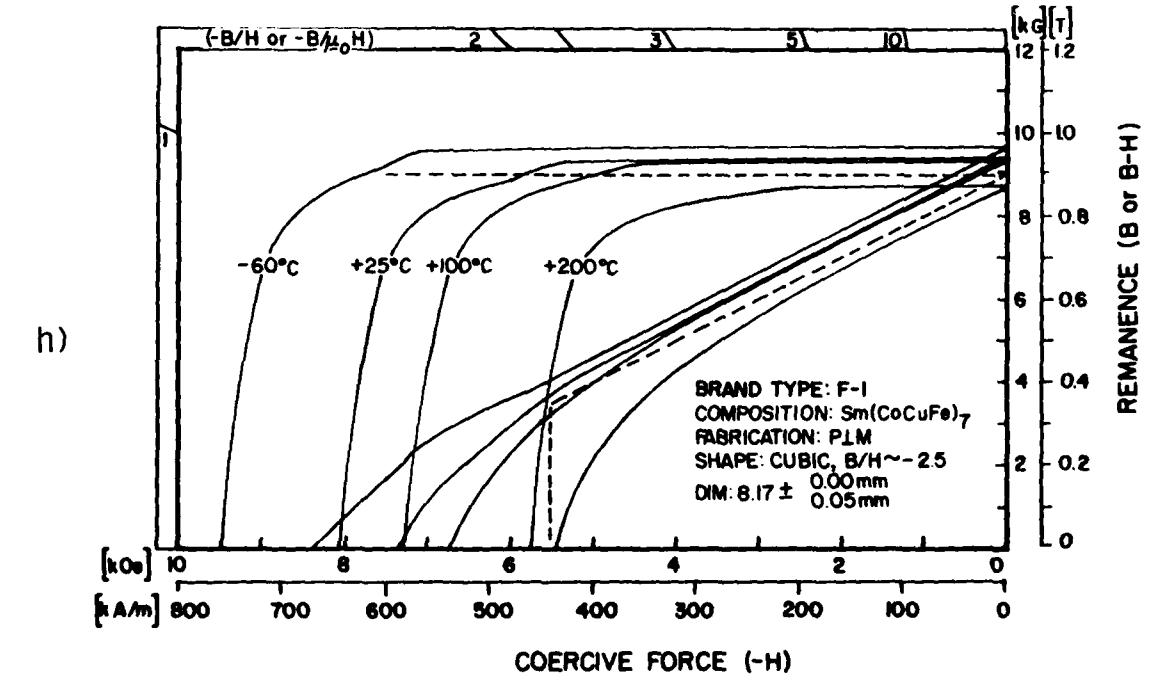

Figure 7g,h Phase I. Typical Demagnetization Curves for Sintered $(SmPr)Co_5$ and $Sm(Co,Cu,Fe)_7$ Magnets Evaluated at Four Temperatures from -60° to +200°C. Brand Types B-2 and F-1.

i)

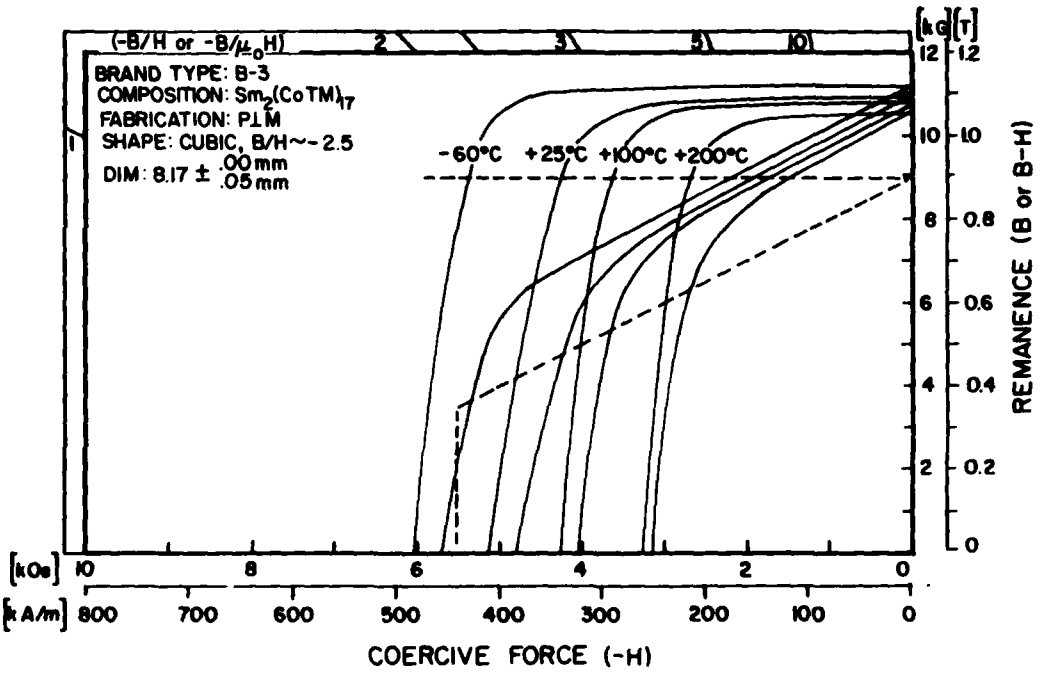

j)

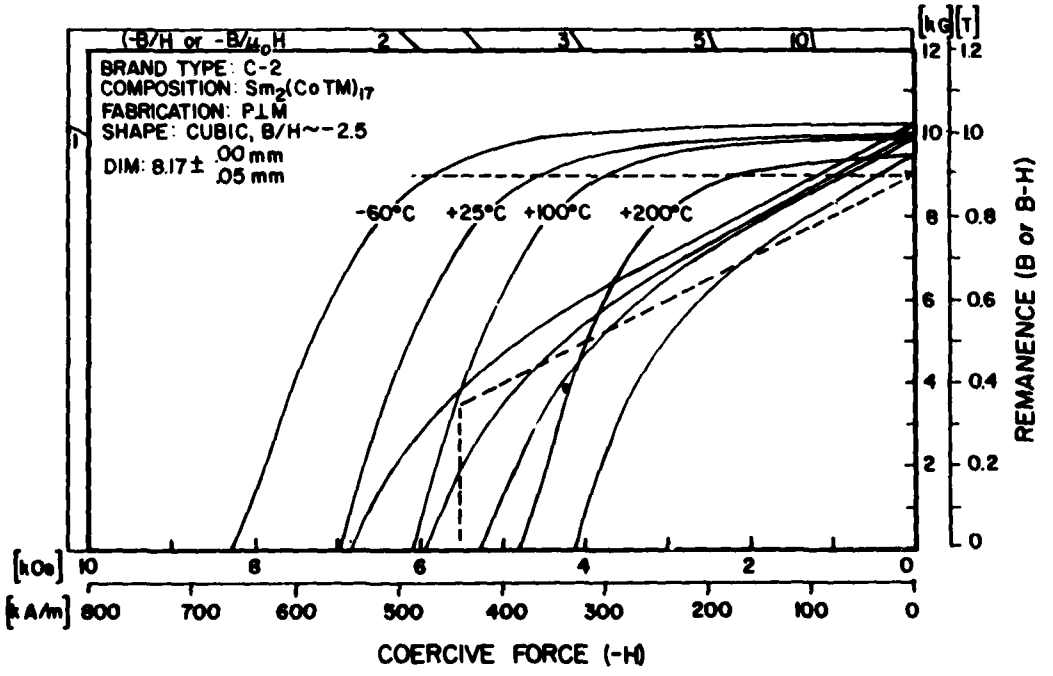

Figure 7i,j Phase I. Typical Demagnetization Curves for Sintered $Sm_2(CoTM)_{17}$ Magnets Evaluated at Four Temperatures from -60° to +200°C. Brand Types B-3 and C-2.

k)

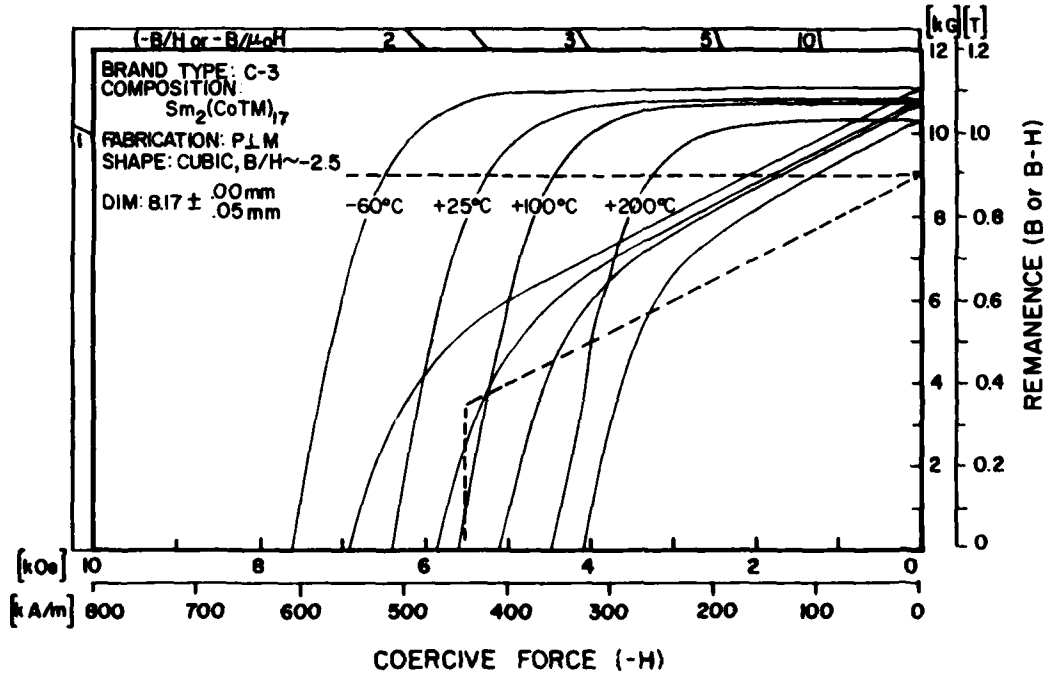

Figure 7k Phase I. Typical Demagnetization Curves for Sintered $Sm_2(CoTM)_{17}$ Magnets Evaluated at Four Temperatures from -60° to +200°C. Brand Type C-3.

The average numerical values of the salient magnetic properties as a function of temperature are given in Tables 3 through 7. The percent change in property values relative to room temperature values are summarized in Table 8 for comparison.

These data were also used to plot three of the primary salient magnetic properties [Br, $_{B}H_{c}$, and $(BH)_{max}$] as a function of temperature as shown in Figures 8a-k. Each point represents the average of measurements on three similar specimens. Using these curves, temperature coefficients for remanence, induction coercive force, and energy product were calculated. As shown in Figure 9, coefficients were determined from the slope of the curves taken at -60°, +25°, +100°, and +200°C, using Equation (1). Average coefficients for the temperature range or span of -60° to +100°C, 0° to 100°C, and 0° to +200°C referred to the room temperature property value were determined using Equation (2). Where K represents the respective quantity B_r, $_{B}H_{c}$, or $(BH)_{max}$.

$$C_r(atT) = \lim_{\Delta T \to 0} - \frac{K(T) - K(T+\Delta T)}{K(T) \cdot \Delta T} \times 100 \ (\% \text{ per } °C) \qquad (1)$$

$$C_r(T_1 \to T_2) = - \frac{K(T_2) - K(T_1)}{K(25°C) \cdot (T_2 - T_1)} \times 100 \ (\% \text{ per } °C) \qquad (2)$$

Table 9 summarizes the thermal coefficients of interest at specific temperature levels and practical operating spans.

Analyzing the thermal dependency of the properties, we note that B_r decreases much more rapidly (∿16%) on heating for the isostatically compacted $SmCo_5$ brand types than it does for $SmCo_5$ pressed parallel (P||M) or transverse (P⊥M) to an alignment

TABLE 3

TEMPERATURE DEPENDENCE OF REMANENCE, B_r(kG)[a]

Brand Type	Alloy Composition	Fabrication Method[b]	At Temperature Level (°C) -60	+25	+100	+200
A-1	$SmCo_5$	P||M	8.83	8.45	8.18	7.81
A-2	$SmCo_5$	I	9.21	8.82	8.52	8.09
B-1	$SmCo_5$	I	10.41	10.00	9.64	9.09
C-1	$SmCo_5$	P⊥M	9.25	8.92	8.61	8.20
D-1	$SmCo_5$	P⊥M	9.10	8.73	8.50	8.12
E-1	$SmCo_5$	P||M	9.36	8.95	8.71	8.31
B-2	$(SmPr)Co_5$	P⊥M	10.13	9.65	9.32	8.80
F-1	$Sm(CoCuFe)_7$	P⊥M	9.66	9.44	9.25	8.82
B-3	$Sm_2(CoTM)_{17}$[c]	P⊥M	11.15	10.99	10.74	10.50
C-2	$Sm_2(CoTM)_{17}$	P||M	10.21	10.00	9.87	9.45
C-3	$Sm_2(CoTM)_{17}$	P⊥M	11.11	10.85	10.73	10.34

[a]Average values based on three test specimens.

[b]Fabrication Methods: [P⊥M] Die pressed with force perpendicular to magnet aligning field, [I] Isostatically pressed, [P||M] Die pressed with force and field parallel.

[c]TM is one or more transition metals (Fe, Cu, Zr, Hf).

TABLE 4

TEMPERATURE DEPENDENCE OF INDUCTION COERCIVE FORCE, $_BH_c$(kOe)[a]

Brand Type	Alloy Composition	Fabrication Method[b]	At Temperature Level (°C) -60	+25	+100	+200
A-1	$SmCo_5$	P||M	8.59	8.12	7.73	6.97
A-2	$SmCo_5$	I	8.73	8.27	7.85	7.08
B-1	$SmCo_5$	I	9.92	9.24	8.42	6.69
C-1	$SmCo_5$	P⊥M	8.56	7.53	6.39	4.70
D-1	$SmCo_5$	P⊥M	8.45	7.89	7.60	7.02
E-1	$SmCo_5$	P||M	9.24	8.66	8.30	7.42
B-2	$(SmPr)Co_5$	P⊥M	9.54	8.85	7.86	5.03
F-1	$Sm(CoCuFe)_7$	P⊥M	8.31	7.45	6.58	5.44
B-3	$Sm_2(CoTM)_{17}$[c]	P⊥M	5.73	5.01	4.31	3.00
C-2	$Sm_2(CoTM)_{17}$	P||M	6.79	6.12	5.32	4.10
C-3	$Sm_2(CoTM)_{17}$	P⊥M	6.94	6.14	5.30	4.13

[a]Average values based on three test specimens.

[b]Fabrication Methods: [P⊥M] Die pressed with force perpendicular to magnet aligning field, [I] Isostatically pressed, [P||M] Die pressed with force and field parallel.

[c]TM is one or more transition metals (Fe, Cu, Zr, Hf).

TABLE 5

TEMPERATURE DEPENDENCE OF INTRINSIC COERCIVE FORCE, $_{M}H_{c}$ (kOe)[a]

Brand Type	Alloy Composition	Fabrication Method[b]	At Temperature Level (°C) -60	+25	+100	+200
A-1	$SmCo_5$	P||M	36.3[d]	33.0[d]	28.79	19.47
A-2	$SmCo_5$	I	34.8[d]	29.7[d]	23.66	15.76
B-1	$SmCo_5$	I	19.80	16.92	13.43	8.48
C-1	$SmCo_5$	P⊥M	15.59	12.65	9.91	6.53
D-1	$SmCo_5$	P⊥M	30.38[d]	27.35[d]	23.12	16.66
E-1	$SmCo_5$	P||M	27.30	24.47	19.52	13.24
B-2	$SmPr)Co_5$	P⊥M	14.14	11.41	8.77	5.23
F-1	$Sm(CoCuFe)_7$	P⊥M	9.38	8.15	7.14	5.76
B-3	$Sm_2(CoTM)_{17}$[c]	P⊥M	6.09	5.20	4.29	3.32
C-2	$Sm_2(CoTM)_{17}$	P||M	8.19	7.21	6.05	4.73
C-3	$Sm_2(CoTM)_{17}$	P⊥M	7.37	6.66	5.64	4.49

[a]Average values based on three test specimens.

[b]Fabrication Methods: [P⊥M] Die pressed with force perpendicular to magnet aligning field, [I] Isostatically pressed, [P||M] Die pressed with force and field parallel.

[c]TM is one or more transition metals (Fe, Cu, Zr, Hf).

[d]Estimated average, one or more of specimens $_{M}H_{c}$ > 32 kOe.

TABLE 6

TEMPERATURE DEPENDENCE OF ENERGY PRODUCT, $(BH)_{max}$ (MGOe)[a]

Brand Type	Alloy Composition	Fabrication Method[b]	At Temperature Level (°C) -60	+25	+100	+200
A-1	$SmCo_5$	P||M	19.2	17.5	16.2	14.3
A-2	$SmCo_5$	I	21.0	19.0	17.5	15.0
B-1	$SmCo_5$	I	26.2	23.3	21.3	16.8
C-1	$SmCo_5$	P⊥M	21.3	19.3	17.5	14.4
D-1	$SmCo_5$	P⊥M	19.9	18.2	16.8	14.8
E-1	$SmCo_5$	P||M	21.8	20.0	18.6	16.7
B-2	$(SmPr)Co_5$	P⊥M	24.2	21.6	20.1	16.7
F-1	$Sm(CoCuFe)_7$	P⊥M	23.1	21.8	20.4	17.6
B-3	$Sm_2(CoTM)_{17}$[c]	P⊥M	29.0	26.4	22.9	17.8
C-2	$Sm_2(CoTM)_{17}$	P||M	24.2	22.0	19.6	15.5
C-3	$Sm_2(CoTM)_{17}$	P⊥M	29.8	27.6	24.8	19.9

[a]Average values based on three test specimens.

[b]Fabrication Methods: [P⊥M] Die pressed with force perpendicular to magnet aligning field, [I] Isostatically pressed, [P||M] Die pressed with force and field parallel.

[c]TM is one or more transition metals (Fe, Cu, Zr, Hf).

TABLE 7

TEMPERATURE DEPENDENCE OF LOOP SQUARENESS,[a] H_K(kOe)[b]

Brand Type	Alloy Composition	Fabrication Method[c]	At Temperature Level (°C) -60	+25	+100	+200
A-1	$SmCo_5$	P||M	13.83	11.77	9.55	6.74
A-2	$SmCo_5$	I	11.81	10.30	8.57	6.11
B-1	$SmCo_5$	I	13.30	10.48	7.56	3.81
C-1	$SmCo_5$	P⊥M	8.89	6.86	5.29	3.41
D-1	$SmCo_5$	P⊥M	10.17	8.58	7.61	5.85
E-1	$SmCo_5$	P||M	16.30	13.49	10.65	7.39
B-2	$(SmPr)Co_5$	P⊥M	11.83	9.45	7.36	4.35
F-1	$Sm(CoCuFe)_7$	P⊥M	8.04	6.75	5.74	4.53
B-3	$Sm_2(CoTM)_{17}$[d]	P⊥M	5.14	4.42	3.45	2.58
C-2	$Sm_2(CoTM)_{17}$	P||M	5.56	4.50	3.71	2.61
C-3	$Sm_2(CoTM)_{17}$	P⊥M	6.17	5.33	4.28	3.21

[a] Value of the "knee field" H_K, at $B = 0.9B_r$.

[b] Average values based on three test specimens.

[c] Fabrication Methods: [P⊥M] Die pressed with force perpendicular to magnet aligning field, [I] Isostatically pressed, [P||M] Die pressed with force and field parallel.

[d] TM is one or more transition metals (Fe, Cu, Zr, Hf).

TABLE 8

TEMPERATURE DEPENDENCE OF MAGNETIC PROPERTIES
PERCENT CHANGE FROM VALUES AT 25°C[a]

Brand Type	Alloy Composition	Fabrication Method[b]	Temp. °C	B_r Δ%	$_BH_c$ Δ%	$_MH_c$ Δ%	H_k Δ%	$(BH)_{max}$ Δ%
A-1	$SmCo_5$	P||M	-60	+4.5	+5.8	+10.0	+17.5	+9.2
			+100	-3.2	-4.8	-12.7	-18.9	-6.8
			+200	-7.6	-14.2	-41.0	-42.7	-18.3
A-2	$SmCo_5$	I	-60	+4.4	+5.5	+17.2	+14.7	+10.5
			+100	-3.4	-5.1	-20.3	-16.8	-8.7
			+200	-8.3	-14.4	-46.9	-40.7	-21.0
B-1	$SmCo_5$	I	-60	+4.1	+7.3	+17.0	+26.8	+12.4
			+100	-3.6	-8.9	-20.6	-27.9	-8.6
			+200	-9.1	-27.6	-49.8	-63.6	-27.9
C-1	$SmCo_5$	P⊥M	-60	+3.7	+13.7	+23.2	+29.6	+10.3
			+100	-3.5	-15.1	-21.6	-22.9	-9.3
			+200	-8.1	-37.6	-48.4	-50.3	-25.4
D-1	$SmCo_5$	P⊥M	-60	+4.2	+7.1	+11.0	+18.5	+9.3
			+100	-2.6	-3.7	-15.5	-11.3	-7.7
			+200	-7.0	-11.0	-39.0	-31.8	-18.7
E-1	$SmCo_5$	P||M	-60	+4.7	+6.6	+11.5	+20.9	+9.0
			+100	-2.7	-4.2	-20.2	-20.7	-7.0
			+200	-7.1	-14.3	-45.9	-45.2	-16.5
B-2	$(SmPr)Co_5$	P⊥M	-60	+5.0	+7.8	+23.9	+25.2	+12.0
			+100	-3.4	-11.1	-23.2	-22.2	-7.3
			+200	-8.8	-43.1	-54.1	-54.0	-22.8
F-1	$Sm(CoCuFe)_7$	P⊥M	-60	+2.3	+11.5	+13.6	+19.1	+6.0
			+100	-2.0	-11.6	-16.1	-14.9	-6.4
			+200	-6.5	-27.0	-34.4	-32.8	-19.3
B-3	$Sm_2(CoTM)_{17}$[c]	P⊥M	-60	+1.4	+14.4	+17.1	+16.3	+9.8
			+100	-2.3	-20.0	-17.5	-21.9	-13.2
			+200	-4.5	-36.1	-36.1	-41.6	-32.6
C-2	$Sm_2(CoTM)_{17}$	P||M	-60	+2.1	+10.9	+13.6	+16.0	+9.8
			+100	-1.3	-13.1	-16.1	-22.7	-10.9
			+200	-5.5	-32.9	-34.4	-45.5	-29.5
C-3	$Sm_2(CoTM)_{17}$	P⊥M	-60	+2.4	+13.0	+14.6	+15.7	+8.0
			+100	-1.0	-13.7	-15.3	-19.6	-10.1
			+200	-4.7	-32.7	-32.6	-39.6	-27.9

[a] Average percent change based on three test specimens.

[b] Fabrication Methods: [P⊥M] Die pressed with force perpendicular to magnet aligning field, [I] Isostatically pressed, [P||M] Die pressed with force and field parallel.

[c] TM is one or more transition metals (Fe, Cu, Zr, Hf).

a)

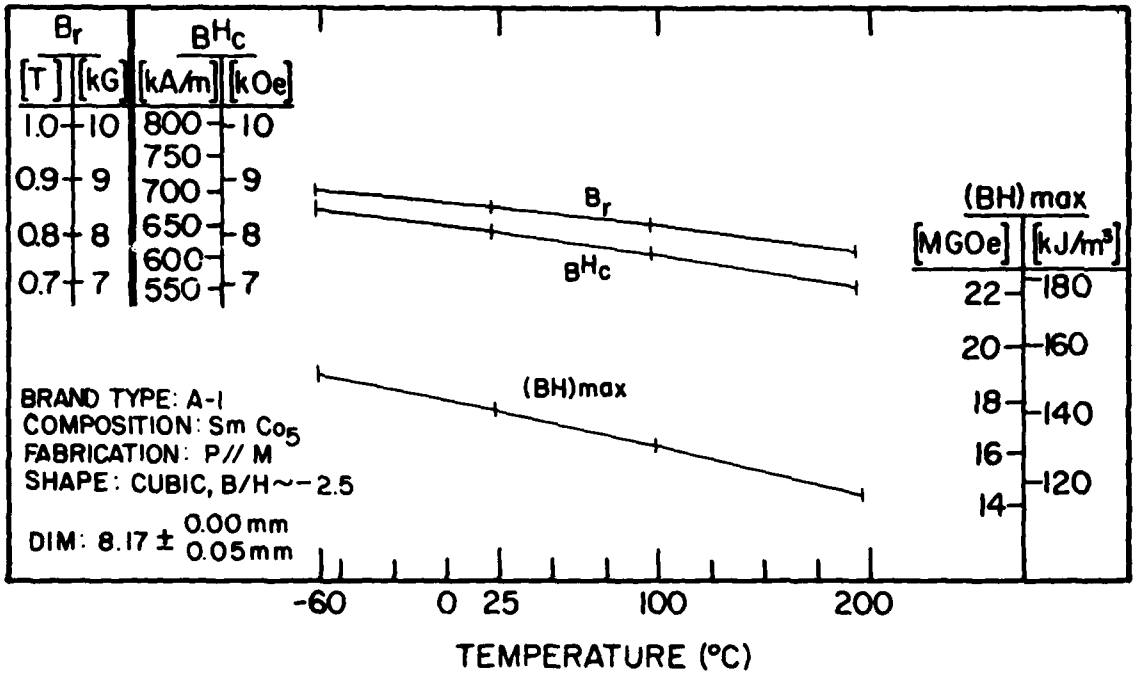

b)

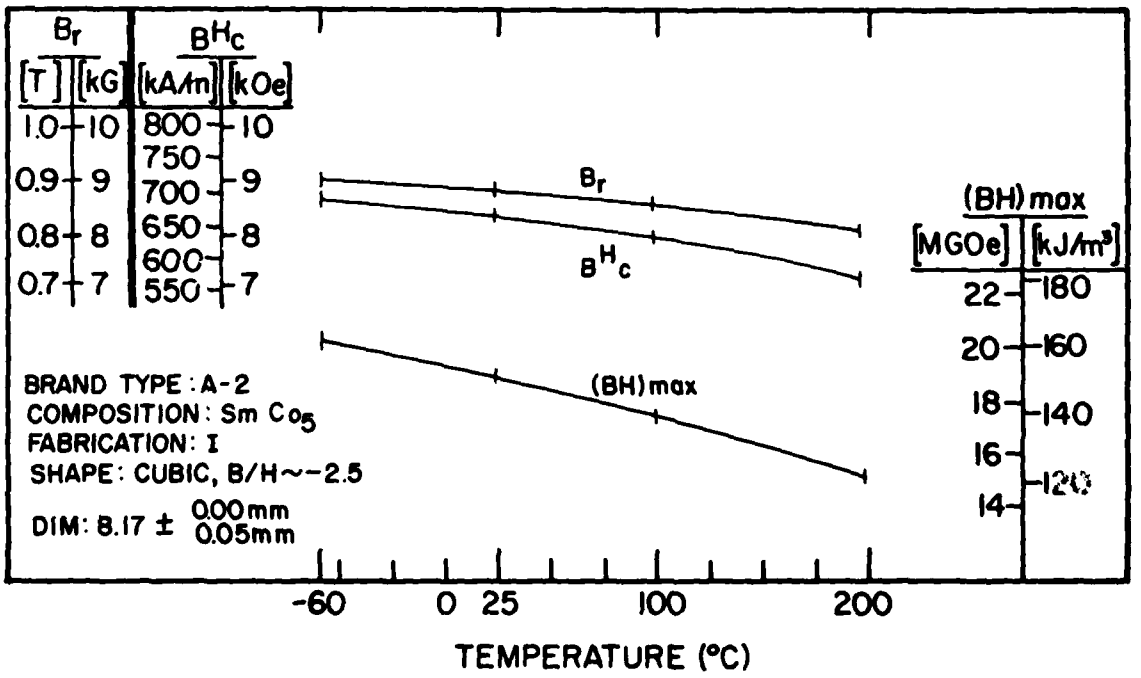

Figure 8a,b Phase I. Temperature Dependence of Selected Second-Quadrant Magnetic Properties of Sintered $SmCo_5$ Magnets, Over a Temperature Range of -60° to +200°C. Brand Types A-1 and A-2.

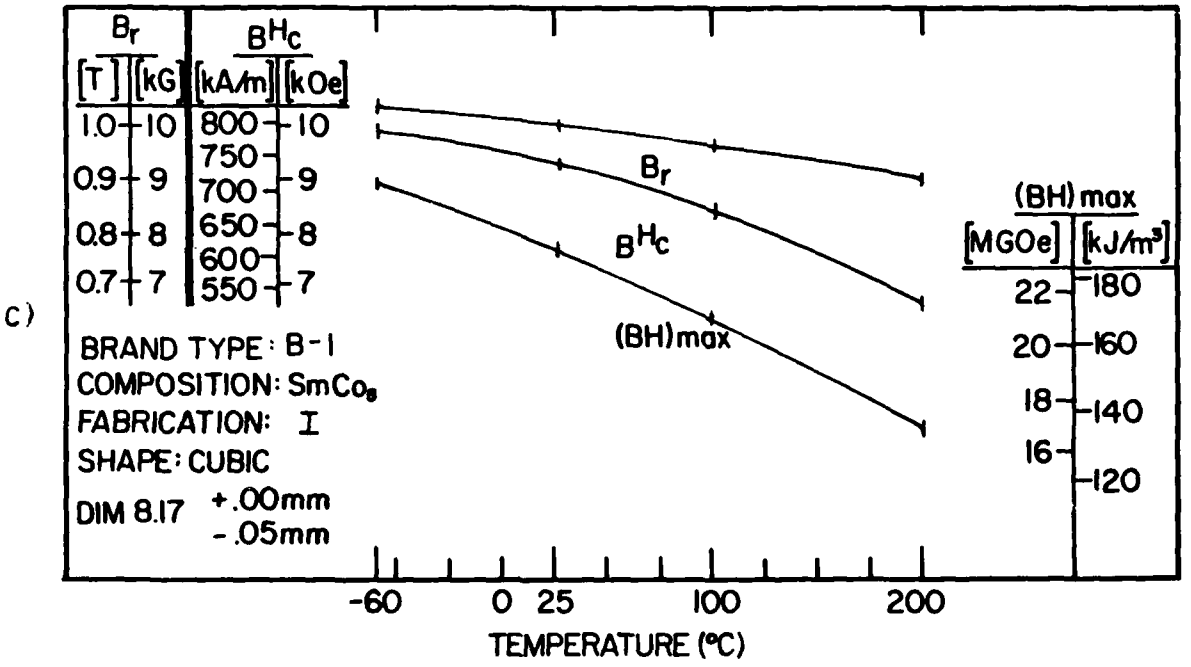

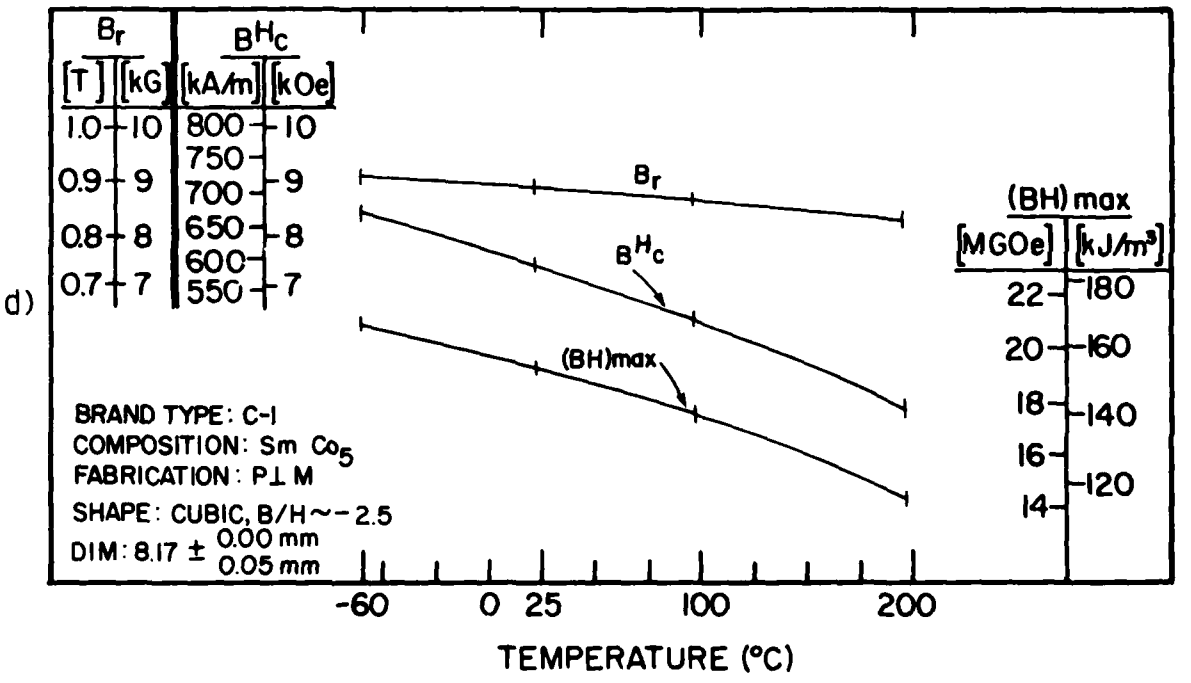

Figure 8c,d Phase I. Temperature Dependence of Selected Second-Quadrant Magnetic Properties of Sintered $SmCo_5$ Magnets, Over a Temperature Range of -60° to +200°C. Brand Types B-1 and C-1.

e)

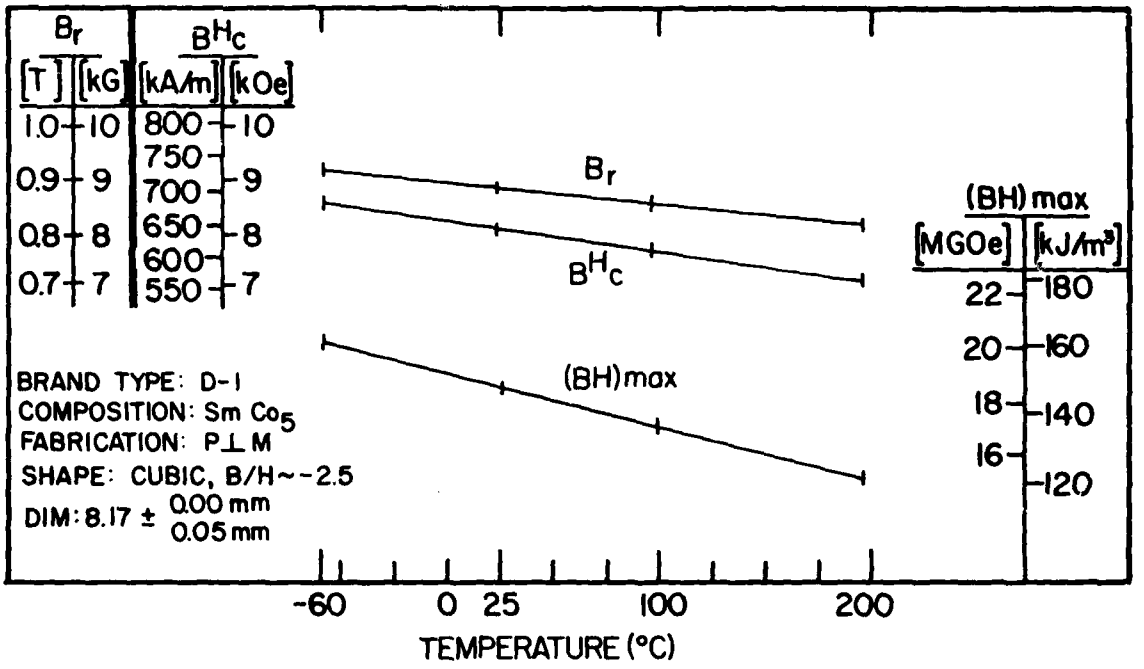

f)

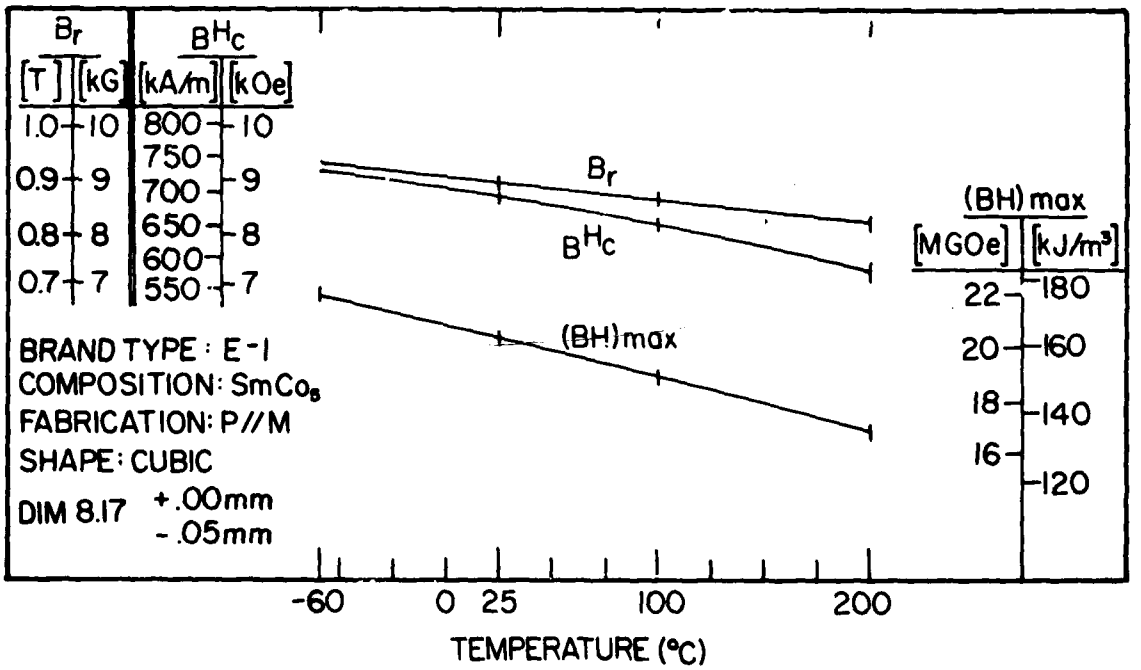

Figure 8e,f Phase I. Temperature Dependence of Selected Second-Quadrant Magnetic Properties of Sintered $SmCo_5$ Magnets, Over a Temperature Range of -60° to +200°C. Brand Types D-1 and E-1.

g)

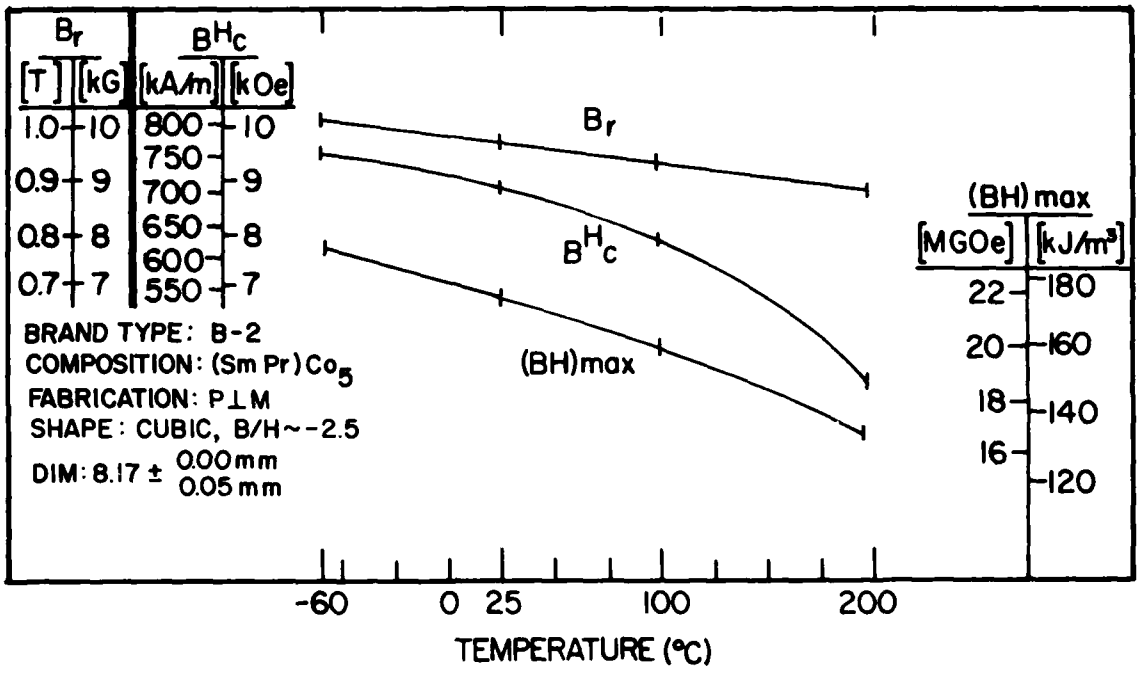

h)

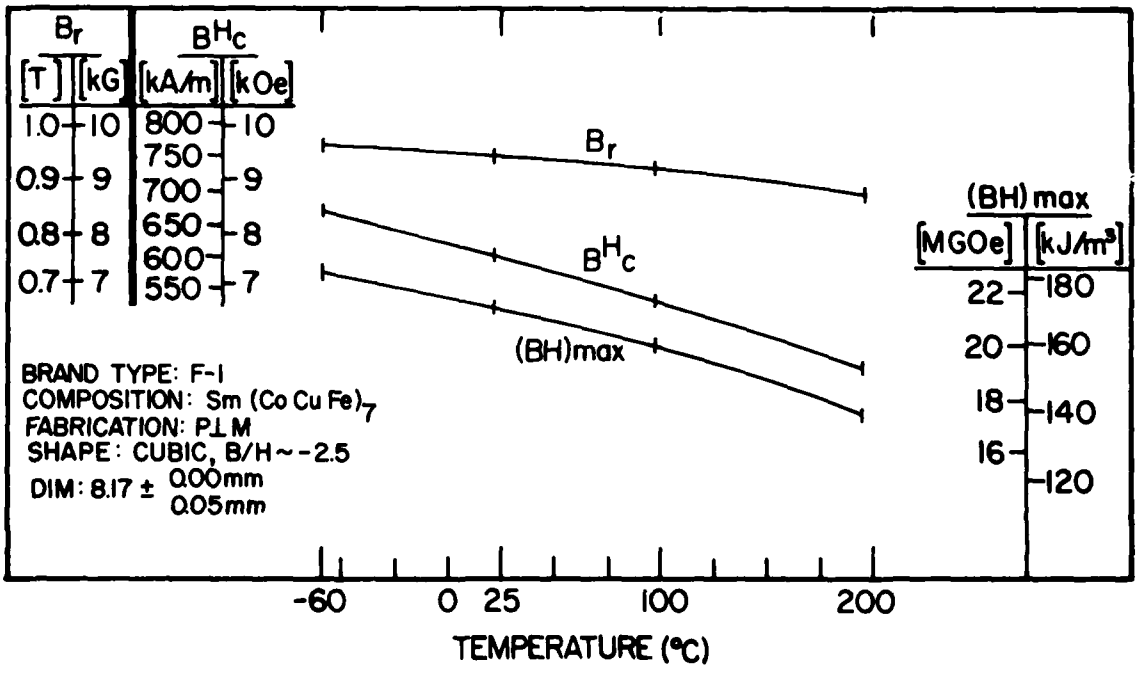

Figure 8g,h Phase I. Temperature Dependence of Selected Second-Quadrant Magnetic Properties of Sintered $(SmPr)Co_5$ and $Sm(Co,Cu,Fe)_7$ Magnets, Over a Temperature Range of -60° to +200°C. Brand Types B-2 and F-1.

i)

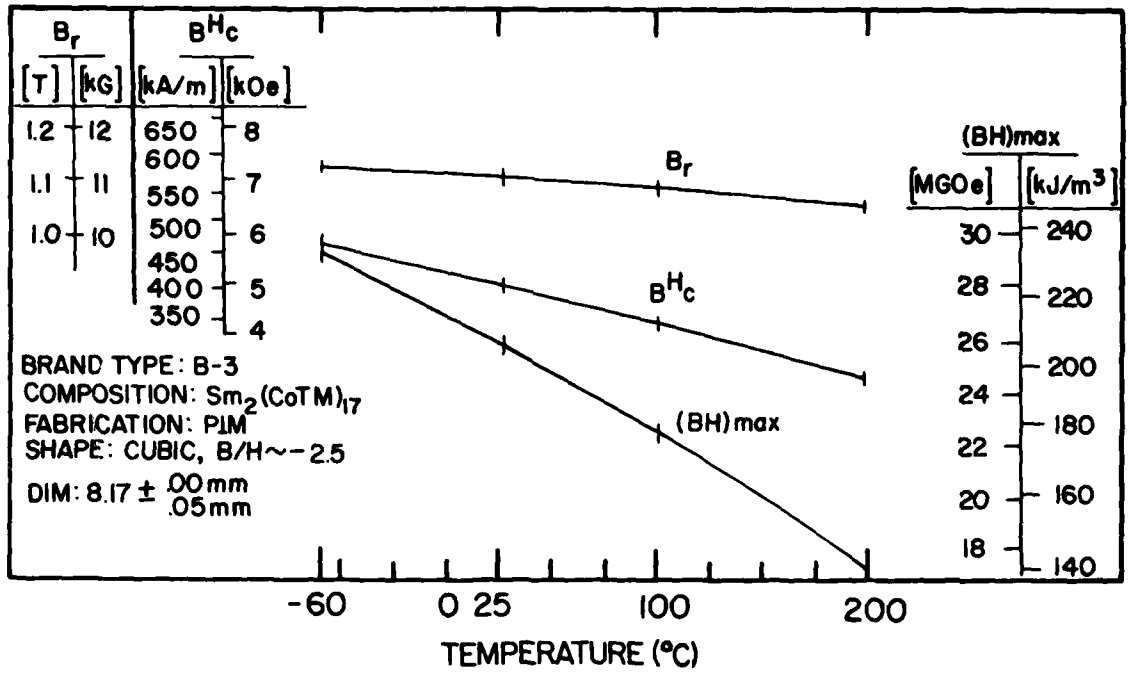

j)

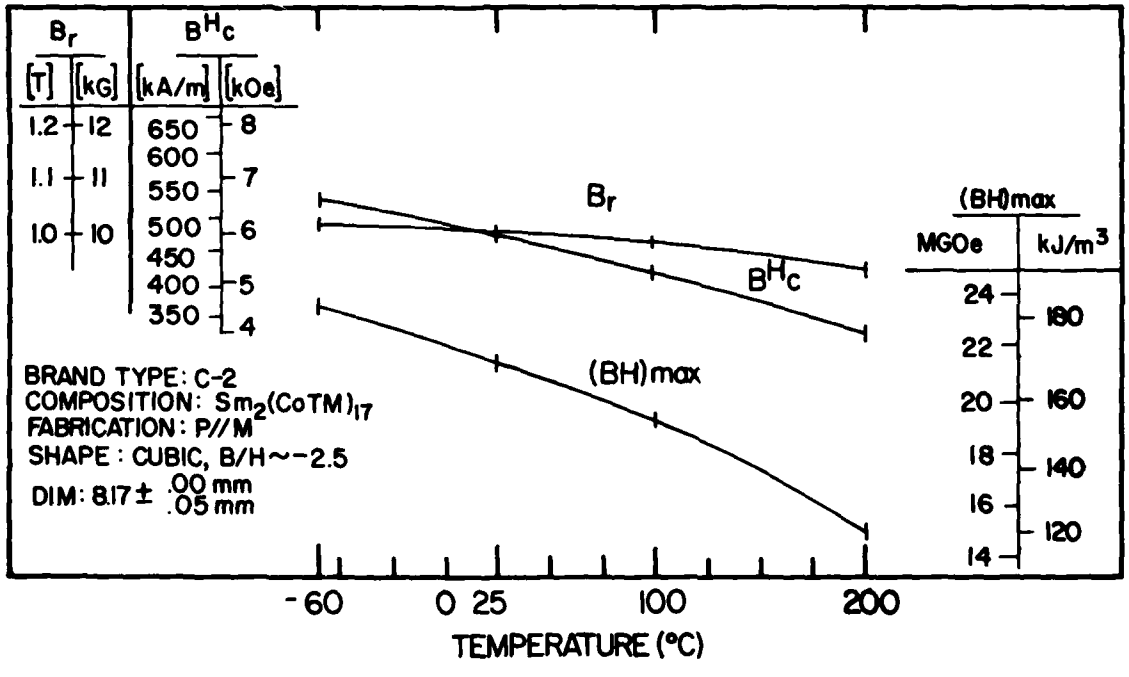

Figure 8i,j Phase I. Temperature Dependence of Selected Second-Quadrant Magnetic Properties of Sintered $Sm_2(CoTM)_{17}$ Magnets, Over a Temperature Range of -60° to +200°C. Brand Types B-3 and C-2.

k)

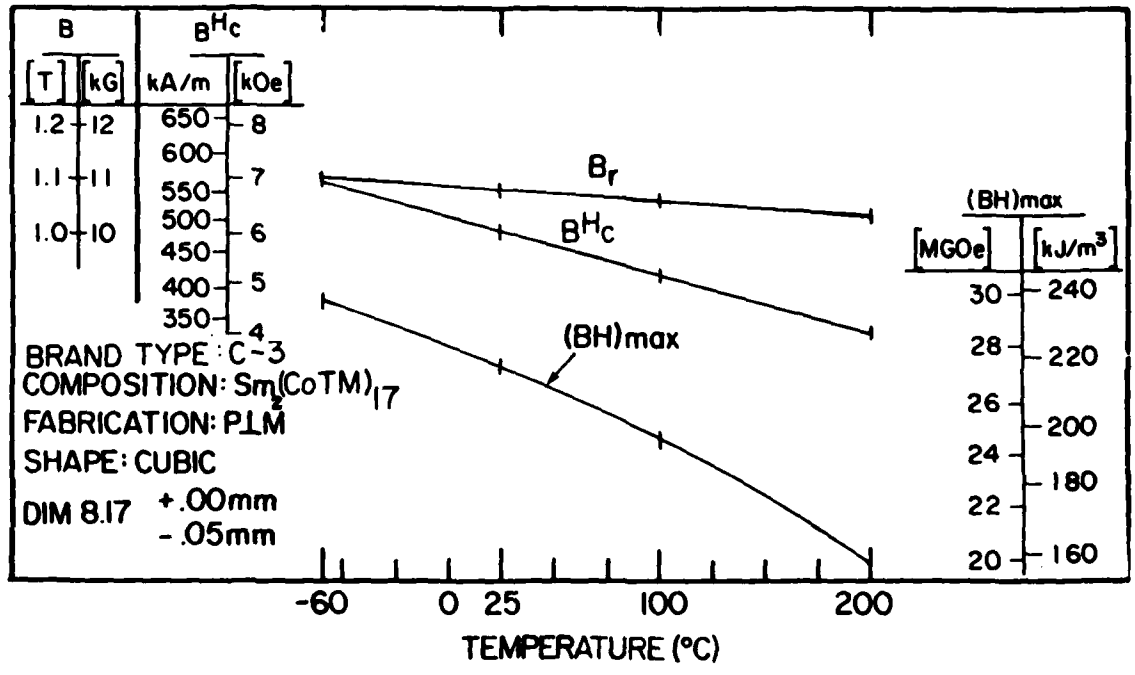

Figure 8k Phase I. Temperature Dependence of Selected Second-Quadrant Magnetic Properties of Sintered $Sm_2(CoTM)_{17}$ Magnets, Over a Temperature Range of -60° to +200°C. Brand Type C-3.

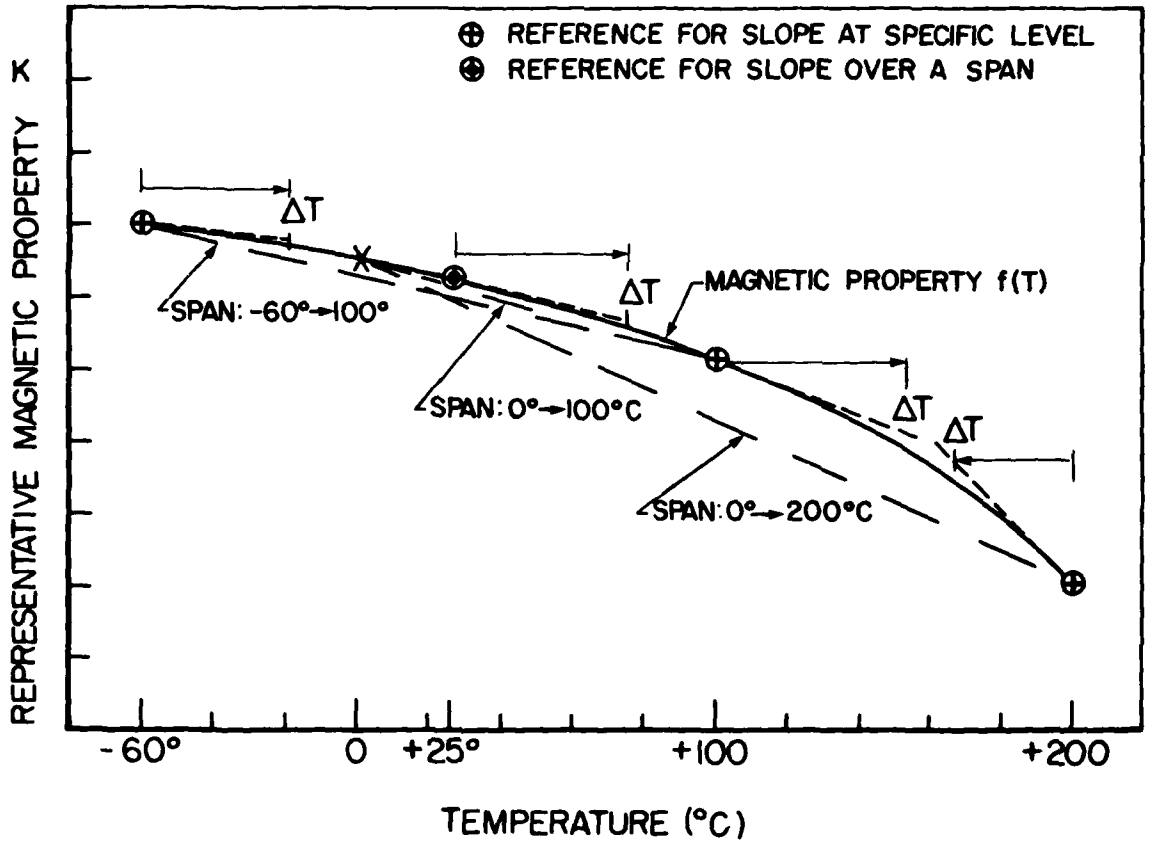

Figure 9. Illustration of Specific Coefficient Data Reference Points and Spans Calculated for Thermally Dependent Magnetic Properties.

TABLE 9

AVERAGE TEMPERATURE COEFFICIENT OF REMANENCE, COERCIVITY, AND ENERGY PRODUCT OF SINTERED MAGNETS MEASURED[a]

Brand Type	Composition and Fabrication[b]	Magnetic Property	Temperature Coefficient (-% per °C)						
			At Temperature Level				Over Temperature Span[d]		
			-60°	+25°	+100°	+200°	-60°—+100°	0°—100°	0°—200°
A-1	$SmCo_5$ (P⊥M)	B_r	0.041	0.043	0.046	0.048	0.048	0.048	0.048
		$_BH_c$	0.058	0.061	0.089	0.125	0.066	0.070	0.082
		$(BH)_{max}$	0.091	0.106	0.108	0.120	0.107	0.109	0.109
A-2	$SmCo_5$ (I)	B_r	0.042	0.042	0.048	0.050	0.048	0.048	0.049
		$_BH_c$	0.057	0.062	0.092	0.114	0.067	0.068	0.080
		$(BH)_{max}$	0.113	0.115	0.130	0.150	0.115	0.116	0.123
B-1	$SmCo_5$ (I)	B_r	0.040	0.044	0.054	0.068	0.048	0.050	0.052
		$_BH_c$	0.071	0.100	0.164	0.308	0.102	0.114	0.151
		$(BH)_{max}$	0.118	0.120	0.184	0.292	0.133	0.134	0.161
C-1	$SmCo_5$ (P⊥M)	B_r	0.037	0.040	0.048	0.060	0.045	0.045	0.047
		$_BH_c$	0.131	0.180	0.234	0.395	0.180	0.198	0.211
		$(BH)_{max}$	0.105	0.120	0.155	0.261	0.123	0.129	0.145
D-1	$SmCo_5$ (P⊥M)	B_r	0.039	0.043	0.050	0.061	0.043	0.046	0.047
		$_BH_c$	0.060	0.064	0.080	0.088	0.067	0.068	0.071
		$(BH)_{max}$	0.092	0.100	0.110	0.130	0.106	0.110	0.110
E-1	$SmCo_5$ (P∥M)	B_r	0.038	0.040	0.048	0.060	0.045	0.047	0.047
		$_BH_c$	0.058	0.066	0.084	0.143	0.067	0.068	0.084
		$(BH)_{max}$	0.091	0.099	0.106	0.126	0.100	0.100	0.102
B-2	$(SmPr)Co_5$ (P⊥M)	B_r	0.049	0.053	0.054	0.061	0.052	0.052	0.053
		$_BH_c$	0.071	0.124	0.239	0.843	0.119	0.140	0.229
		$(BH)_{max}$	0.103	0.117	0.144	0.249	0.119	0.120	0.139
F-1	$Sm(CoCuFe)_7$ (P⊥M)	B_r	0.023	0.023	0.041	0.070	0.027	0.029	0.037
		$_BH_c$	0.123	0.153	0.161	0.232	0.145	0.150	0.152
		$(BH)_{max}$	0.065	0.073	0.112	0.195	0.077	0.084	0.107
B-3	$Sm_2(CoTM)_{17}$[c] (P⊥M)	B_r	0.017	0.020	0.024	0.025	0.023	0.024	0.024
		$_BH_c$	0.150	0.155	0.260	0.490	0.177	0.197	0.230
		$(BH)_{max}$	0.091	0.156	0.211	0.309	0.144	0.163	0.178
C-2	$Sm_2(CoTM)_{17}$ (P∥M)	B_r	0.016	0.022	0.026	0.051	0.021	0.023	0.032
		$_BH_c$	0.094	0.147	0.196	0.317	0.150	0.171	0.184
		$(BH)_{max}$	0.084	0.127	0.194	0.284	0.130	0.145	0.163
C-3	$Sm_2(CoTM)_{17}$ (P⊥M)	B_r	0.017	0.023	0.028	0.046	0.022	0.023	0.029
		$_BH_c$	0.135	0.164	0.188	0.329	0.167	0.172	0.182
		$(BH)_{max}$	0.074	0.116	0.184	0.264	0.113	0.130	0.154

[a] Average values based on three test specimens.

[b] Fabrication Methods: [P⊥M] Die pressed with force perpendicular to magnet aligning field, [I] Isostatically pressed, [P∥M] Die pressed with force and field parallel.

[c] TM is one or more transition metals (Fe, Cu, Zr, Hf).

field. Energy products $BH_{(max)}$ also follow this same trend with the isostatic losses approximately 25% higher at 100°C and 40% at 200°C than for the parallel pressed brand types, and 1 to 11% compared to the transverse pressed brand types. A comparison of induction coercive force losses observed are not quite as clear. Large differences in percent losses of $_{B}H_{C}$ at elevated temperatures were measured for those magnets produced by either isostatic or transverse pressing methods.

Since the reversible temperature coefficients are generally determined by composition rather than fabrication method, there may be chemical differences between three magnet types not revealed by the manufacturers.

For the 2-17 magnets of the same composition (C-2, C-3) by the same manufacturer, and differing only by parallel or transverse pressing the temperature coefficients are quite similar. This is as expected. The third 2-17 composition (B-3) exhibits coefficients of B_r similar in magnitude, but nearly linear over the entire temperature range. However, the coefficients for $_{B}H_{C}$ and $(BH)_{max}$ are significantly higher.

The 1-7 magnet material (F-1) generally exhibits better coefficients of $_{B}H_{C}$ and $(BH)_{max}$ than the other precipitation hardened 2-17 materials, but a much higher coefficient of B_r at elevated temperatures.

All four precipitation hardened magnet materials show smaller temperature variation of B_r than the seven 1-5 alloys, a consequence of their higher Curie points. The same is generally true for the intrinsic coercive force $_{M}H_{C}$ and loop squareness H_K, although their absolute change is much more than that of B_r. However, the variation of $_{B}H_{C}$ with temperature is less for 1-5 magnet specimens. It follows the remanent induction B_r variation in these high-coercivity magnets. For the lower intrinsic coercivity magnets (1-7 and 2-17), the induction coercive force is dtermined by the intrinsic coercivity.

C. Mechanical Property Characterization

a) Procedure and Instrumentation

During this phase of the study, only compression tests were performed on the sintered specimens from the 11 brand type magnet materials.

All of the compression tests were conducted on an Instron Universal Test Machine at a loading rate of 0.2 in. per min. using the test configuration shown in Figure 10.

A total of 166 permanent magnet specimens were tested in compression. Of the 11 different groups of magnets tested, eight were of the $SmCo_5$ type and three were modified Sm_2Co_{17}. During the manufacturing process, all but two of the eight $SmCo_5$ groups were uniaxially cold pressed prior to sintering. The two remaining $SmCo_5$ groups were isostatically cold pressed prior to sintering. Of the six uniaxially cold pressed $SmCo_5$ groups, four were die pressed perpendicular to the direction of magnetization and two were die pressed parallel to the direction of magnetization. All three groups of the Sm_2Co_{17} magnets were uniaxially cold pressed prior to sintering; two gropus perpendicular and one group parallel to the direction of magnetization.

The test specimens were cubes with a nominal dimension of 8 mm on a side. Each of the 11 groups of magnets was divided into three subgroups so that compressive strength tests could be conducted at different directions in relationship to the direction of magnetization. With the exception of one subgroup (A-1), each subgroup contained five test specimens. One subgroup of magnets from each of the 11 different magnet designations was tested with the compressive load applied parallel to the direction of magnetization (F_1). The other two subgroups were tested with the compressive load applied along the two directions perpendicular to the direction of magnetization (F_2 and F_3). Figure 11 shows the relationship between the direction of magnetization and compressive load direction.

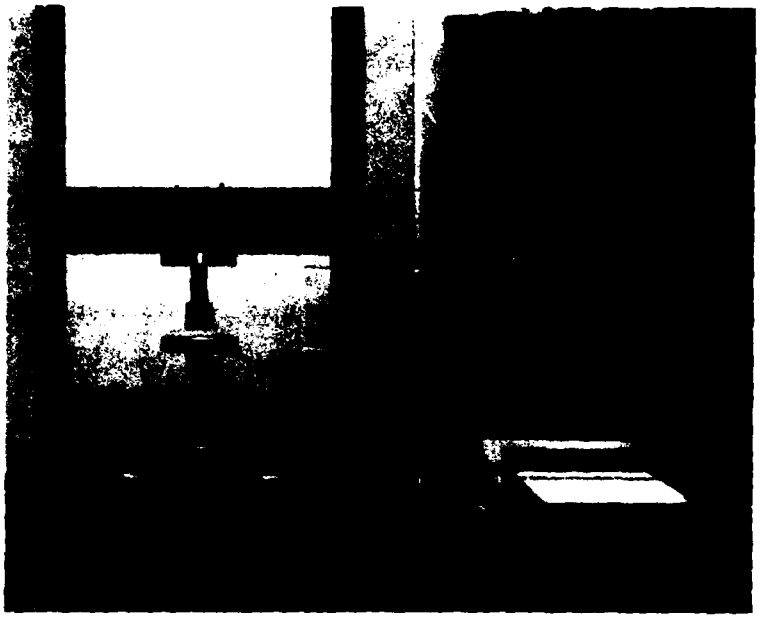

Figure 10. Compression Test Equipment.

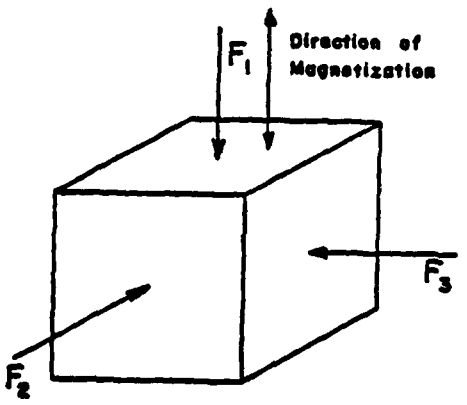

Figure 11. Compression Test Orientation with Respect to Magnetization Direction.

The results of the mechanical screening tests are given in Table 10.

All of the magnets tested had generally acceptable compressive strength (>100,000 psi), but the pure $SmCo_5$ material had consistantly higher strengths overall. In addition it was noted that the F_1 test orientation produced the lowest average strength magnets with the exception of two of the three brand types that were prepared by pressing in the direction uniaxial to the direction of magnetization.

Figure 12 shows the relative comparison of the different brand types in bar graph form, the width of the bars being two standard deviations.

TABLE 10

SUMMARY OF COMPRESSION TESTS ON SAMARIUM-COBALT PERMANENT MAGNETS

Material Designation/Type	Test Orientation	Number of Specimens	Average Compressive Strength ksi (S.D.)	MPa (S.D.)
A. Magnets Uniaxially Pressed Perpendicular to Magnetization Direction				
B-2	F_1	5	142.3(9.4)	981.0(64.7)
(SmPr) Co_5	F_2	5	142.6(12.0)	983.2(82.9)
	F_3	5	134.3(6.1)	926.3(42.2)
D-1	F_1	5	142.9(19.1)	985.5(131.6)
($SmCo_5$)	F_2	5	114.1(11.0)	786.7(75.7)
	F_3	5	145.8(6.4)	1005.2(43.9)
C-1	F_1	5	147.3(21.8)	1015.7(150.5)
($SmCo_5$)	F_2	5	157.2(7.6)	1083.9(52.6)
	F_3	5	158.6(17.7)	1093.8(122.3)
F-1	F_1	5	70.1(18.6)	438.1(128.5)
$Sm(CoCuFe)_7$	F_2	5	117.4(16.8)	809.8(115.9)
	F_3	5	119.1(7.6)	821.4(52.4)
B-3	F_1	5	92.1(8.6)	635.1(58.9)
$Sm_2(CoTM)_{17}$[a]	F_2	5	121.0(22.7)	834.4(156.3)
	F_3	5	124.1(15.7)	855.4(108.0)
C-3	F_1	5	99.6(4.9)	686.5(33.7)
$Sm_2(CoTM)_{17}$[a]	F_2	5	124.6(12.0)	859.3(83.0)
	F_3	5	112.0(7.3)	772.0(50.1)
B. Magnets Uniaxially Pressed Parallel to Magnetization Direction				
A-1	F_1	5	170.7(10.5)	1176.6(72.7)
($SmCo_5$)	F_2	5	152.8(15.3)	1053.8(105.7)
	F_3	5	152.3(11.7)	1049.9(80.8)
E-1	F_1	5	161.2(16.9)	1111.2(116.2)
($SmCo_5$)	F_2	5	154.4(8.0)	1064.7(55.5)
	F_3	5	145.8(15.6)	1005.2(107.7)
C-2	F_1	5	110.5(4.7)	762.1(32.2)
$Sm_2(CoTM)_{17}$[a]	F_2	5	119.7(9.9)	825.6(68.5)
	F_3	5	118.6(6.9)	817.7(47.6)
C. Magnets Isostatically Pressed				
B-1	F_1	5	139.1(9.3)	958.8(64.4)
($SmCo_5$)	F_2	5	147.9(13.6)	1019.8(93.9)
	F_3	5	137.7(10.9)	949.5(75.0)
A-2	F_1	5	142.6(13.6)	983.0(94.0)
($SmCo_5$)	F_2	5	163.1(5.6)	1124.5(38.4)
	F_3	5	159.7(11.2)	1100.8(77.20

[a] TM is one of several transition metals (Fe,Cu,Zr,Hf).

Brand Type	Alloy Composition	Fabrication Method
A-1	$SmCo_5$	P||M
A-2	$SmCo_5$	I
B-1	$SmCo_5$	I
C-1	$SmCo_5$	P⊥M
D-1	$SmCo_5$	P⊥M
E-1	$SmCo_5$	P||M
B-2	$(SmPr)Co_5$	P⊥M
F-1	$Sm(CoCuFe)_7$	P⊥M
B-3	$Sm_2(CoTM)_{17}$	P⊥M
C-2	$Sm_2(CoTM)_{17}$	P||M
C-3	$Sm_2(CoTM)_{17}$	P⊥M

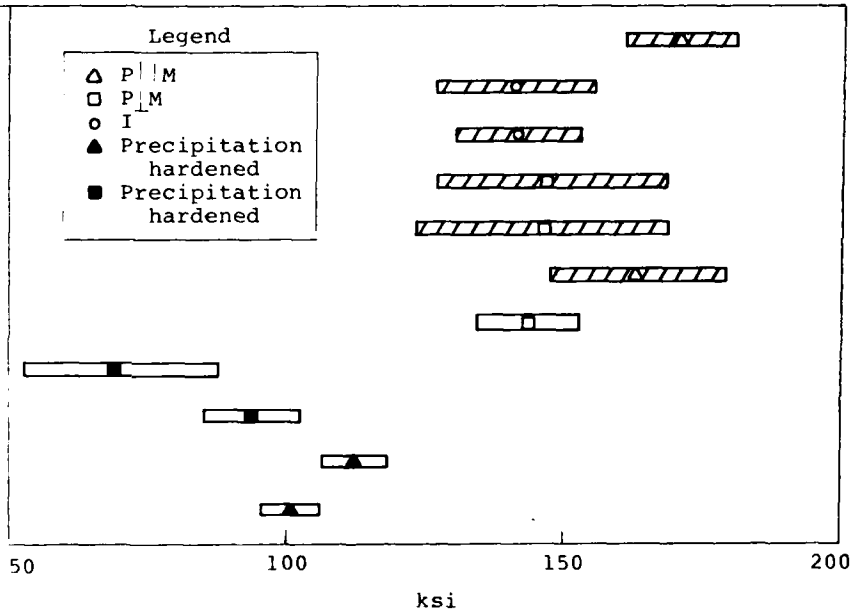

Figure 12. Phase I. Average Compressive Strength and Standard Deviation. F||M Only.

SECTION 3
PHASE II

A. Evaluation of Test Data, Phase I

Upon completion of the initial magnetic and mechanical characterization of the 11 brand types tested, the raw data were compiled for further analysis as shown in the various tables and figures presented in the previous section. General comparative comments were also made to illustrate the trends observed relative to what may be expected for the high-performance magnet materials tested.

To further add to these observations it can be generally concluded that the room temperature magnetic data indicates:

- only two of the six $SmCo_5$ material brand types measured, B-1 and E-1, had average remanence and energy product values comparable to or exceeding minimum specifications,
- two of the $SmCo_5$ compositions, C-1 and D-1, had loop squareness values H_K lower than the induction coercive force,
- all of the modified rare earth-transition metal materials modified on the rare earth or cobalt side had average remanence and energy product values in excess of the minimum specifications,
- all of the compositions except type B-3 had induction coercivities greater than the minimum specification, and
- only three of the compositions, B-1, B-2, and F-1, had B_d/H_d values equal to or greater than the minimum specification. The next closest types meeting this specification are C-3 (66%) and E-1 (60%).

The above comments are summarized on a percentage basis in Table 11, for comparison of each brand type examined. In each case, the percentage of specimens (out of a total of 18) whose salient properties meet or exceed the minimum specifications is tabulated.

TABLE 11

PERCENTAGE OF MAGNET SPECIMENS EQUAL TO OR GREATER THAN MINIMUM MAGNETIC PROPERTY SPECIFICATIONS[a]

Brand Type	Alloy Composition	Fabrication Method	B_r	BH_c	$(BH)_{max}$	Knee Position[b]
A-1	$SmCo_5$	P||M	0	100	0	0
A-2	$SmCo_5$	I	5	100	0	0
B-1	$SmCo_5$	I	100	100	100	100
C-1	$SmCo_5$	P⊥M	39	100	0	0
D-1	$SmCo_5$	P⊥M	28	100	0	0
E-1	$SmCo_5$	P||M	39	100	33	60
B-2	$(SmPr)Co_5$	P⊥M	100	100	100	100
F-1	$Sm(CoCuFe)_7$	P⊥M	100	100	100	100
B-3	$Sm_2(CoTM)_{17}$	P⊥M	100	0	100	0
C-2	$Sm_2(CoTM)_{17}$	P||M	100	100	100	0
C-3	$Sm_2(CoTM)_{17}$	P⊥M	100	100	100	66

[a]Based on room temperature data, test specimen quantity - 18.

[b]$B_d \geq 3.5$ kG at $H_d = 5.5$ kOe. See Figure 1.

As a function of temperature, the magnetic data indicates that:

- in spite of the typical loss in loop squareness H_K, at the highest elevated temperatures only the $SmCo_5$ material type E-1 maintained a value greater than ${}_BH_C$ at 200°C
- at elevated temperatures type C-1 possessed "unity" recoil permeability only for permeance values of $B/H \gtrsim -5$
- the same can be said for all the precipitation hardened 2-17 materials
- for the precipitation hardened 1-7 material, unity recoil would be exhibited only at permeance values of $B/H \gtrsim -2.5$
- the praseodymium substituted 1-5 material also had these same limitations at high temperatures. What is equally important is the effect the anomaly, indicated by the small perturbation in the intrinsic and induction demagnetization curves, had in conjunction with the limited unity recoil operation point, i.e., an operating permeance range of $-2.5 \gtrsim B/H \lesssim -5$ at the highest temperatures
- the salient property losses and temperature coefficients for each brand type generally follow what one would expect
- as previously noted, however, distinct differences in thermal losses and coefficients, especially at the higher temperatures, may be due to slight chemical differences in composition.

With regard to the mechanical compressive strength property data measured at room temperature, it can be concluded that:

- all of the brand types had acceptable compressive strengths, but the pure $SmCo_5$ magnets produced the high compressive strength magnets
- the lowest strength values were obtained in the F_1 test orientation with the exception of two of those

magnets produced by pressing uniaxial to the direction of magnetization (A-1 and E-1).

Based on the data observed, an objective analysis was prepared and presented at a project review requested by the Air Force Project Engineer. At the completion of this review the conclusion was reached to select two $SmCo_5$ alloy composition materials instead of one $SmCo_5$ and one $Sm_2(CoTM)_{17}$ type. The $SmCo_5$ compositions selected were type B-1 and E-1. The former offers potentially higher remanence values and energy product and the latter approaches the commercially produced "optimum" 20 MGOe permanent magnet materials. Both have compressive strength properties in excess of 137 ksi in any orthogonal direction. One type selected is of domestic manufacture and the other from a foreign source.

B. Test Plan and Magnet Procurement for Comprehensive Evaluation

Concurrent with the objective review of the testing evaluation, a general test plan and procedure specification was also prepared and submitted to the Air Force Project Engineer for approval. This instrument, in effect, finalized the approved test plans for the second and third phases of the program. The simplified block diagrams shown in Figure 13 (and in Figure 18, Phase III), serve to illustrate the general sequence and scope of the comprehensive evaluation to be performed.

To accomplish the comprehensive magnetic, mechanical, thermal, and electrical property evaluation of the two $SmCo_5$ brand types selected, approximately 400 test magnets having specific geometries were required for allocation in the general test program shown in a simplified diagram in Figure 13. Test magnets purchased were ordered with the same stipulations pertaining to magnetic properties, surface conditions, identifications, etc., as specified in the first purchase.

C. Magnetic Characterization at Room Temperature, Phase II

Upon receipt of the $SmCo_5$ test magnets, all specimens were identified and inventoried for future reference as before. Prior

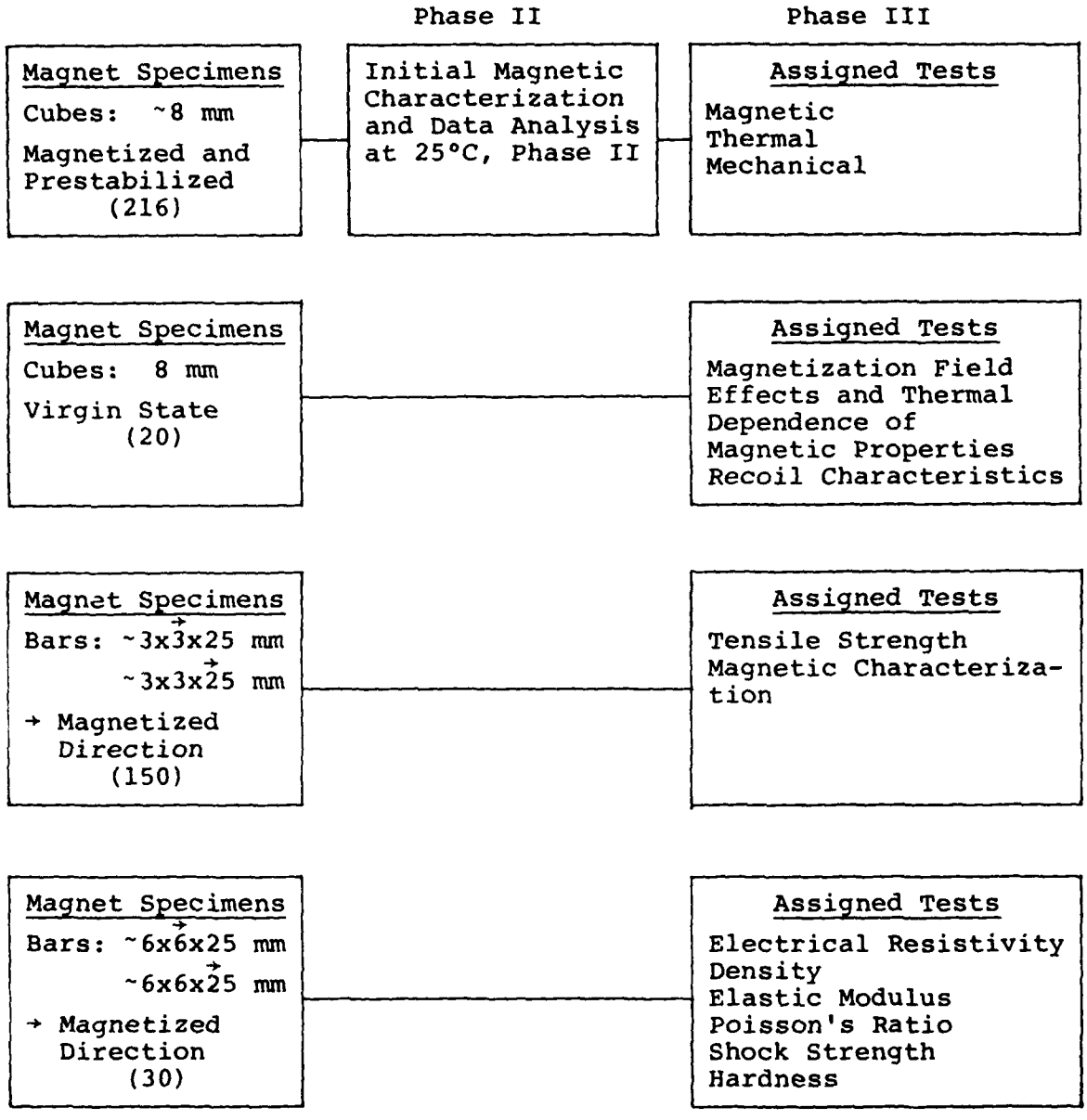

Figure 13. Phase II Initial Characterization and Test Specimen Allocation of $SmCo_5$ Magnet Specimens for Phase III.

to assignments for specific tests in Phase III, an initial magnetic property characterization was performed on 108 cubic-shaped test magnets from each manufacturer, in the as-received condition. Second-quadrant intrinsic demagnetization curves were plotted at room temperature using the same hysteresigraph-electromagnet system described in Section 2. Composite plots illustrating the range of intrinsic and induction demagnetization curves are illustrated in Figures 14 and 15, for the respective brand types B-1 and E-1. In Figures 15a and 15b we again observe a distinct difference in characteristic intrinsic curves (for $4\pi M$ -10 kOe) within the E-1 group lot. Approximately 84% of the magnets had intrinsic coercivity values in the range of ∿20-30 kOe, and 16% were much greater than 30 kOe.

Pertinent room-temperature properties of the specimens are shown in Table 11. A comparison of the magnetic property data obtained in Phase I (Table 2) for brand types B-1 and E-1, with the data obtained in this phase (six times greater data base), indicates the average values of remanence B_r, induction coercive force $_BH_C$, and energy product $(BH)_{max}$ are lower than previously measured for both brand types.

All three values of these salient properties for type B-1 are significantly lower, ranging from approximately 5 to 12% less. Although the average intrinsic coercive force $_MH_C$ increased approximately 8%, the average loop squareness H_K, decreased by about 0.6%.

For type E-1, the corresponding average values for the same three properties were only slightly lower than measured before. Average values ranged from 0.1 to 2.2% less, as shown in the table. A substantial improvement was observed in the average value of intrinsic coercive force and loop squareness of approximately 17% and 55%, respectively.

The data also indicates that with decreasing properties, the standard deviation (σ) for the B-1 type improved, i.e., the range within which 68% of the specimen property occur is narrower (95% in 2σ). There is also substantial improvement in the standard deviation of the coercivities and energy product of type E-1, but greater deivation in the remanence.

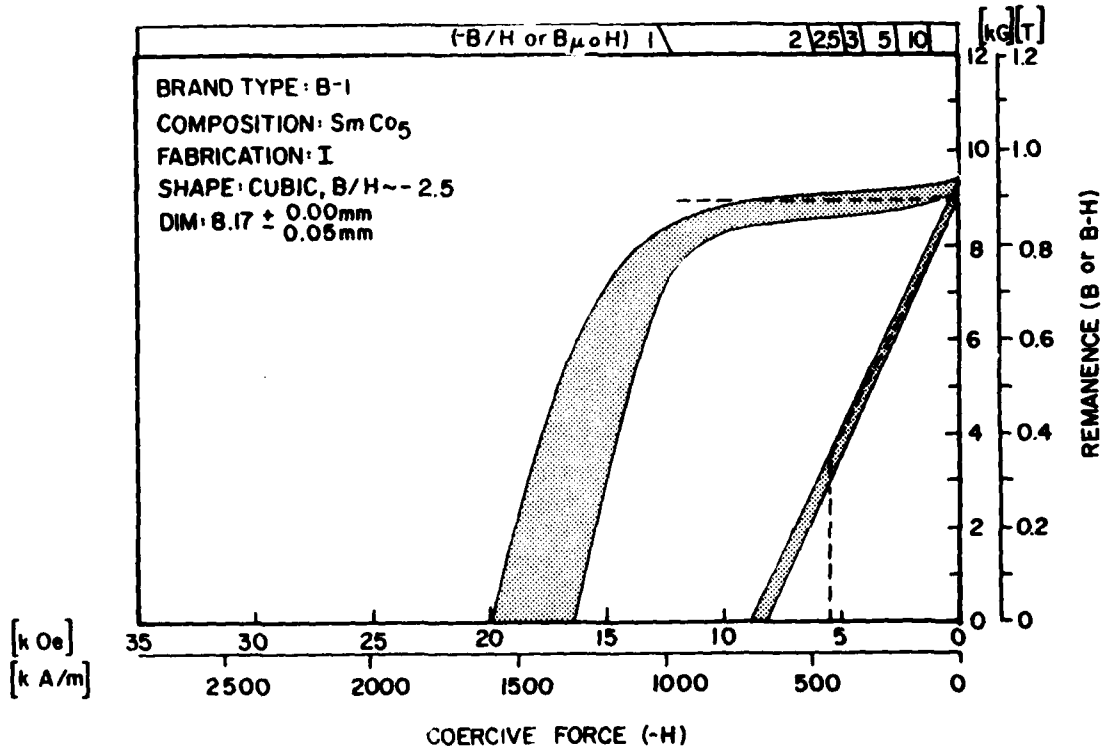

Figure 14. Phase II. Range of Demagnetization Curves for Sintered $SmCo_5$ Magnets. Brand Type B-1. Produced February 1980, 108 Test Magnets Measured As-Received.

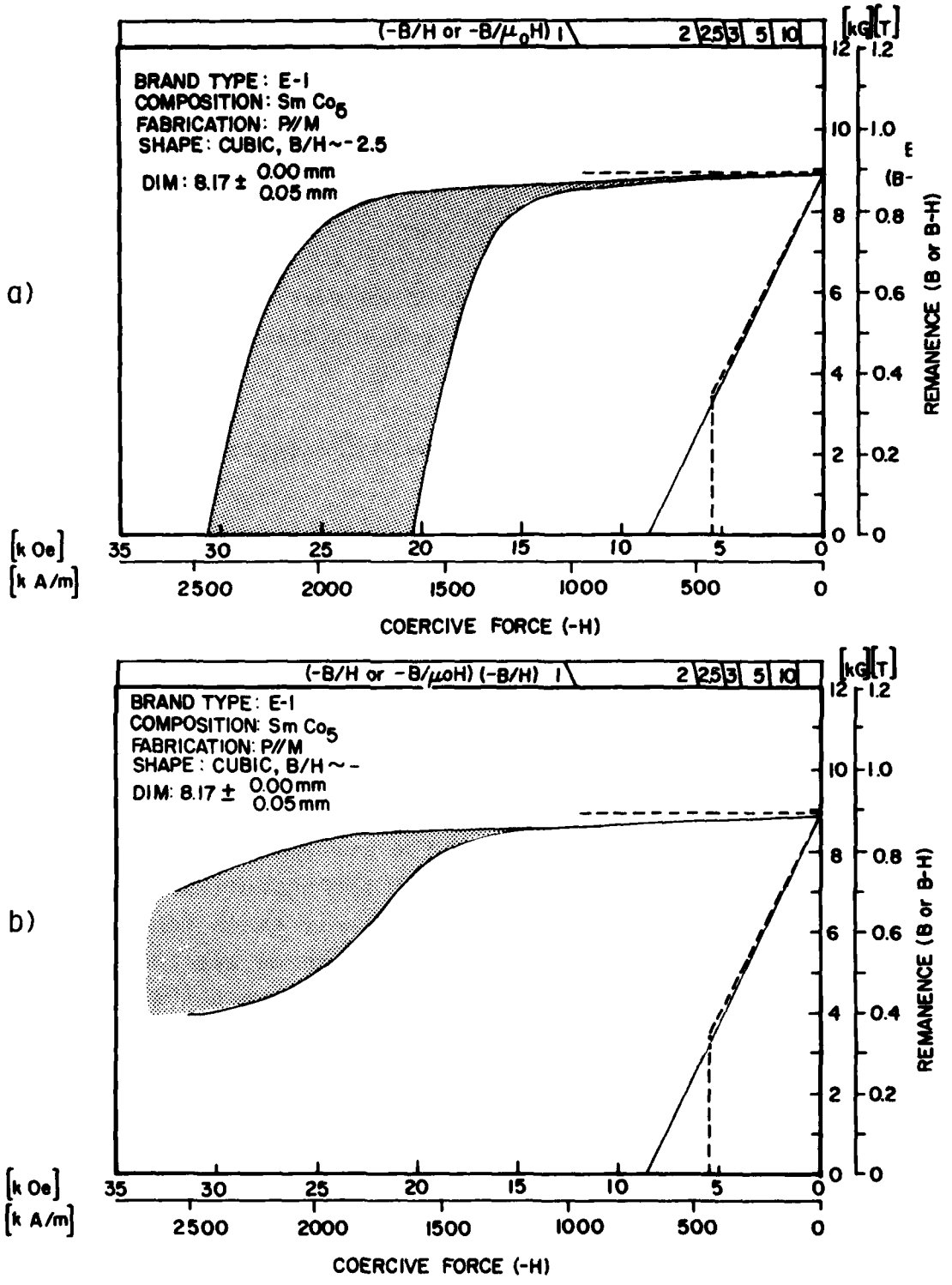

Figure 15a,b Phase II. Range of Demagnetization Curves for Sintered $SmCo_5$ Magnets. Brand Type E-1. Produced February 1980, 18 Test Magnets Measured As-Received.

An additional magnetic property check was performed by sampling approximately 15% of the test lot from each manufacturer and remeasuring after pulse magnetizing in a 100 kOe field in the original forward direction of magnetization. The resulting data curves showed that the test magnet curves initially plotted in the as-received condition were technically fully magnetized.

At this point, the initial characterization effort of the test magnet specimens were completed and the magnets stored for further allocation in Phase III.

D. Fixture Design, Construction, Modification, and Testing

a) Resistivity Fixture

To determine the electrical resistivity of the magnet materials, a four wire point contact specimen fixture was required that would satisfactorily operate over a test temperature range of -60° to +200°C. Typical specimen fixture designs follow the construction details outlined in ASTM-B-63.[12] These fixtures are used to measure the resistance of long specimen bars of known cross-sectional area and are generally used only at or near room temperature. For extremely low values of resistance a precision Kelvin bridge is used to provide the current to the test specimen during the measurement and to detect the potential drop measured between knife edge contacts at a precisely known separation distance. In practice the potential contacts are located away from the specimen ends to ensure a uniform current density in the region of resistance measurement.

For our purpose the fixture had to operate over a broad temperature span; therefore, lead and specimen contact surfaces had to be protected from corrosion or oxidation due to moisture condensation after low temperature tests and exposure at elevated temperatures. The fixture design also had to accommodate specimens much smaller in length than would normally be preferred. This limitation is imposed by both economics and practical manufacturing limitations in producing uniform specimens comparable in length to normal test bars.

With these considerations in mind, a fixture pictorially illustrated in Figure 16 was designed and constructed to accommodate specimens ∿6 mm square by 25 mm in length. The base and point contact insulator were cut from a machinable ceramic (MACOR)[a] material.

Current contacts were machined from copper and gold plated over a nickel base. One current contact was free moving to provide self alignment when uniform contact with the specimen was made. Consistent contact pressure was maintained during each measurement by applying the same torque to the clamping screw every time a specimen was placed in the fixture. The knife edges are ground hardened steel blades rigidly fastened to the spring loaded ceramic insulator to ensure parallel and uniform potential contact with the specimen surface at a precise separation distance. In practice, at temperatures above and below room temperature, the fixture was placed in an insulating enclosure and the specimen temperature monitored with a direct contact copper-constantan thermocouple.

The complete instrumentation required is shown in Figure 17. After the fixture was constructed, systematic tests were performed on test bars to define a standard procedure for preparing the specimen, loading it in the fixture, stabilizing the temperature, etc., until consistent results were obtained by the operator. As a routine measurement, all that was required was to determine the individual specimen height and width (to the nearest 3×10^{-3} mm) and calculate the cross-sectional area. Knowing the potential contact spacing (1.613 cm) and measured specimen resistance at a given temperature, the electrical resistivity was then calculated using Equation (3).

---

[a]Trademark Corning Glass Works, Corning, New York.

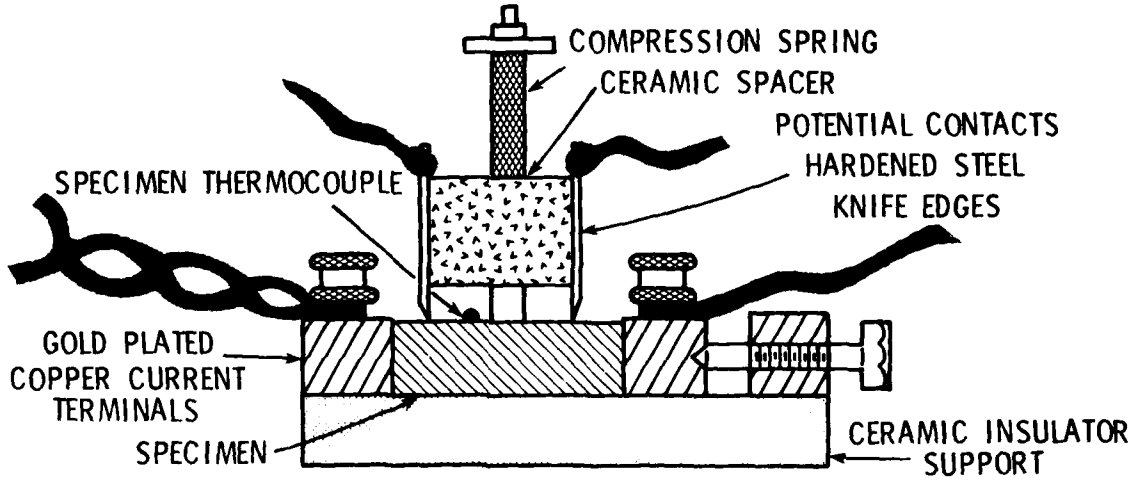

Figure 16. Sectional View, Four Wire Point Contact Resistance Fixture.

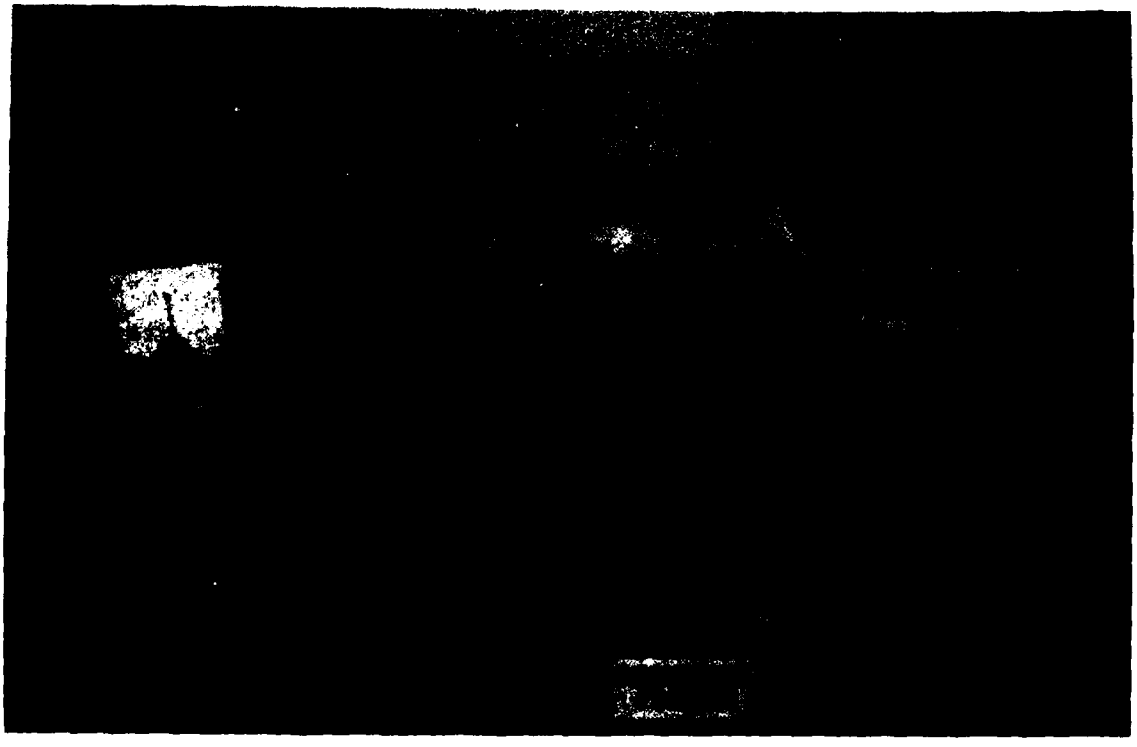

Figure 17. Instrumentation for Electrical Resistivity Measurements.

$$\rho = \frac{R.\ A_s}{\ell_p}\ (\Omega\text{-cm}) \qquad (3)$$

where: R is the measured d.c. resistance in ohms
A_s is the specimen area in cm^2
ℓ_p is the potential contact spacing in cm.

SECTION 4
PHASE III

A. Comprehensive Property Evaluation of Sintered $SmCo_5$ Permanent Magnets

Having completed the initial magnet property characterization at room temperature in Phase II and preparatory plans for full property characterization of the two designated high-performance $SmCo_5$ permanent magnet brand types, all of the test specimens were distributed according to the simplified program sequence outline shown in Figure 18. The order of testing and the number of brand type specimens allocated for each test is also indicated in the outline.

For simplicity, all aspects of the additional magnetic evaluations will be presented and discussed first followed by the mechanical, thermal, and electrical evaluations.

B. Magnetic Property Characterization, Phase III

a) Measurements at Temperatures of -60°, +100°, and +200°C

From the room temperature data plotted and recorded in Phase II, eight test specimens of each brand type were selected for further characterization at temperatures above (100°, 200°C) and below (-60°C) room temperature. Specimens selected were magnetically identical to the respective average values listed in Table 12 for each brand type.

Using the temperature controlled fixture and hysteresigraph probe, second-quadrant intrinsic demagnetization curves were measured and plotted at each specific temperature, starting at -60°C. Each of the magnet specimens were pulse field magnetized at 100 kOe in the original direction, prior to remeasurement at another temperature. Figures 19a and 19b illustrate the temperature dependent intrinsic and normal demagnetization curves for the two $SmCo_5$ type materials measured, relative to the characteristic curve at 25°C.

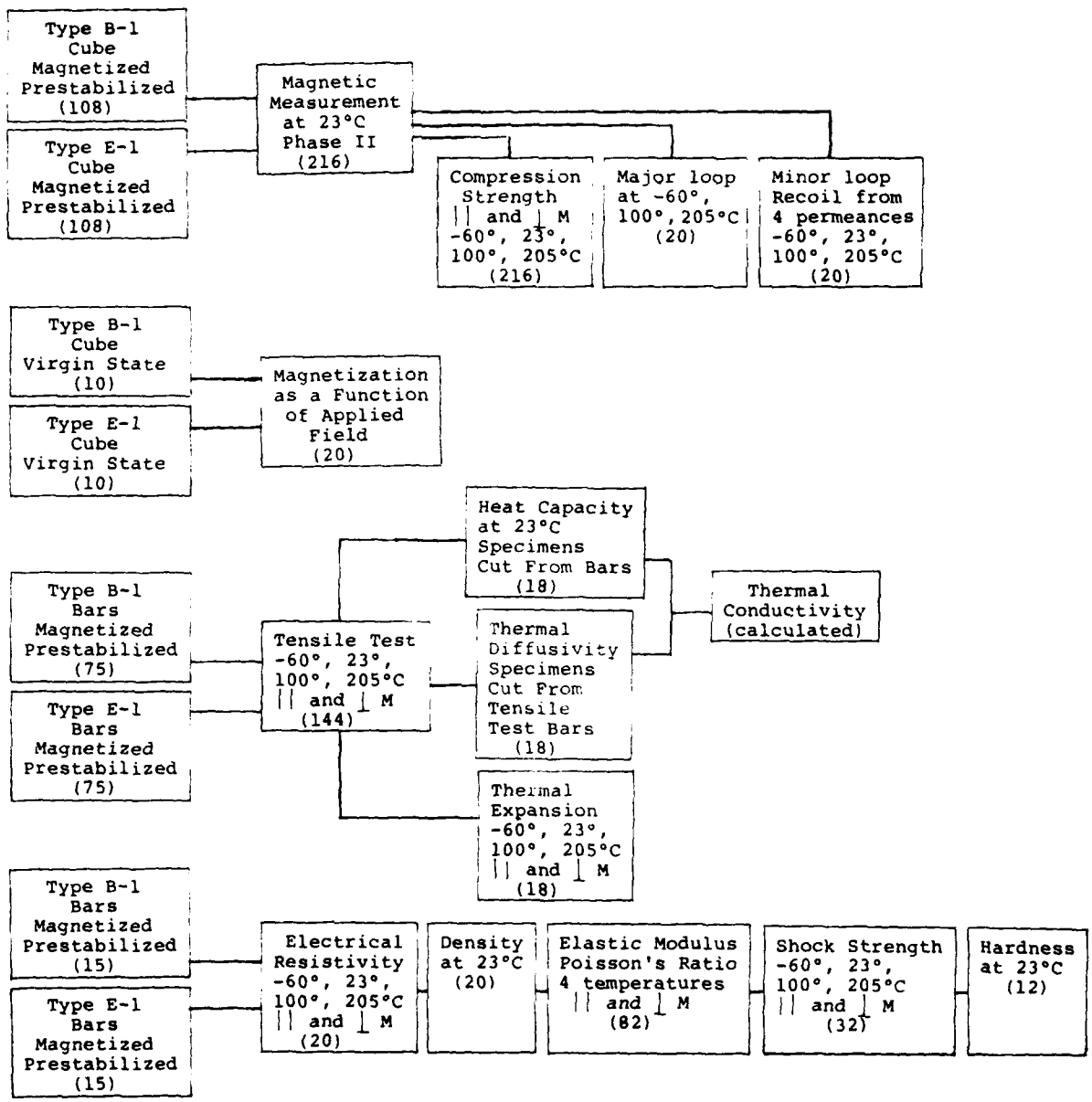

Figure 18. Phase III. Test Specimen Allocation of Two Brand Type Sintered $SmCo_5$ Magnets, B-1, E-1.

a)

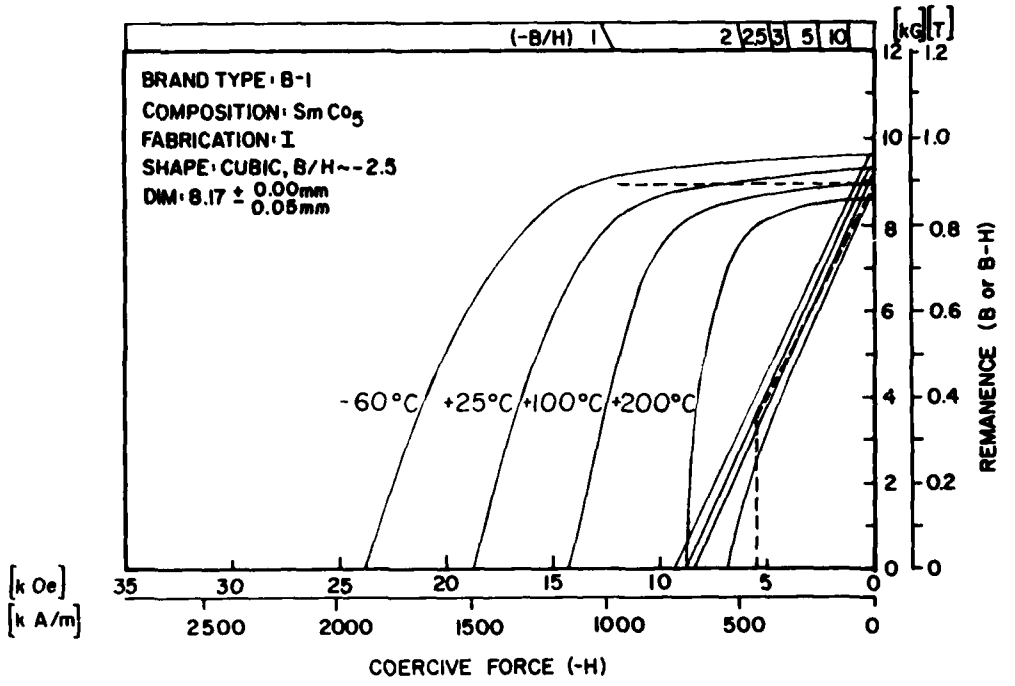

b)

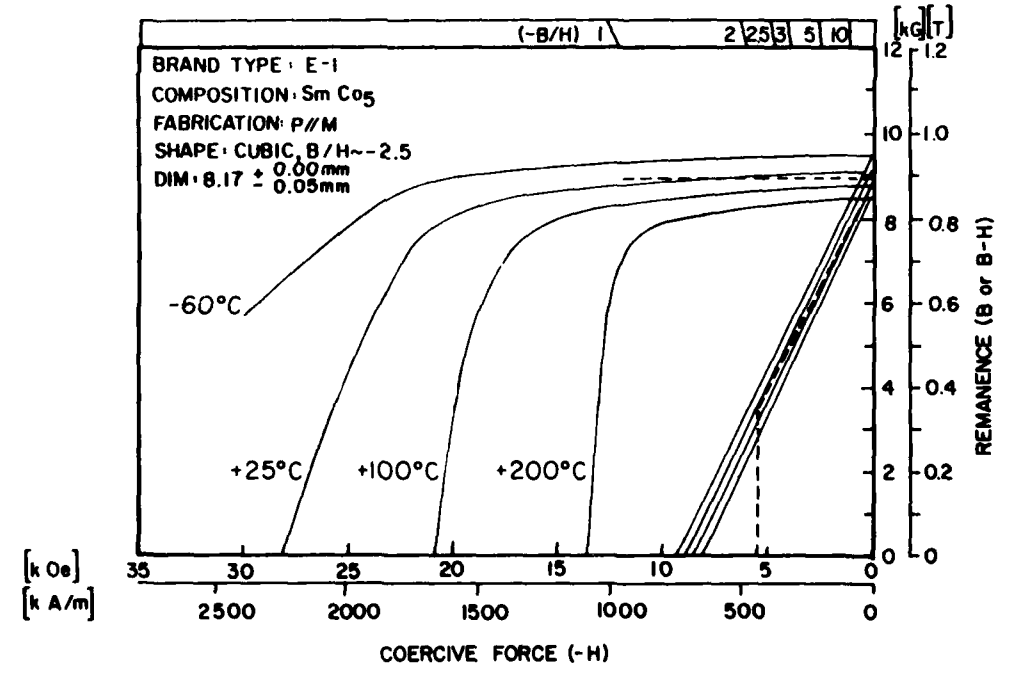

Figure 19a,b Phase III. Typical Demagnetization Curves for Sintered $SmCo_5$ Magnets Evaluated at Four Temperatures from -60° to +200°C. Brand Types B-1 and E-1.

TABLE 12

MAGNETIC PROPERTIES OF SINTERED $SmCo_5$ TEST MAGNETS AT 25°C

Permanent Magnet Property	Units	Brand Type B-1				Brand Type E-1			
		Avg.[a] Value	St. Dev.	Δ%[b] Avg.	Δ%[b] St. Dev.	Avg.[a] Value	St. Dev.	Δ%[b] Avg.	Δ%[b] St. Dev.
Residual Induction (B_r)	T	0.93	0.006	-6.68	+18.9	0.886	0.001	-0.44	-3.8
	kG	9.35	0.06			8.86	0.11		
Coercive Force ($_BH_c$)	kA/m	694	8	-5.42	+50.2	691	6	-0.11	+46.3
	kOe	8.72	0.10			8.68	0.08		
Coercive Force ($_MH_c$)	kA/m	1452	99	+8.63	-16.8	2217	230	+17.2	+46.2
	kOe	18.25	1.25			27.86	2.90		
Loop Squareness[c] (H_K)	kA/m	844	55	-0.65	+50.2	1628	189	+55.0	-24.2
	kOe	10.61	0.70			20.46	2.38		
Energy Product $(BH)_{max}$	kJ/m^3	163	3	-12.8	+22.4	153	2.6	-2.18	+31.2
	MGOe	20.49	0.38			19.27	0.33		

[a] Average value based on 108 specimens

[b] Δ% referred to values measured in Phase I (Table 2). Minus sign indicates lower average or larger standard deviation.

[c] Field value at 0.9 B_r.

The average numerical values of the salient magnetic properties as a function of temperature are presented in Table 13 for comparison of each brand type. The percent change in property values as a function of temperature, relative to room temperature values, are summarized in Table 14 for comparison. As in Phase I, these data were also used to plot the three thermally dependent salient magnetic properties shown in Figures 20a and 20b, for both brand types. Each data point represents an average of the measurements observed for eight representative specimens. From these curves, temperature coefficients of remanence, induction coercive force, and energy product were determined for these specimens. The coefficients at specific temperature levels and over practical operating spans are presented in Table 15. A comparison with the respective data (see Figures 8c and 8f, and Tables 8 and 9) previously measured in Phase I indicates that both brand type $SmCo_5$ magnets exhibit some improvement in magnetic property loss as a function of temperature. This can be attributed to both increased intrinsic coercivity and loop squareness of the specimens in the second lot of each brand type received. This improvement is reflected in the more linear graphical plots of temperature dependent property data illustrated in Figures 20a and 20b, and the nominally improved temperature coefficient data is presented in Table 15.

b) Magnetization Characteristics of $SmCo_5$ Permanent Magnets

It is generally well known that for high coercivity RE-TM permanent magnets, the shape of the magnetic hysteresis loop, particularly the intrinsic coercivity, remanence, and loop squareness, depend on the strength of the maximum field applied in charging the magnet. Sintered $SmCo_5$ type magnets exhibit a steeply rising initial magnetization curve from the virgin state. That is, the condition following all sintering and heat treatment steps, prior to the magnet experiencing an external magnetizing

TABLE 13

TEMPERATURE DEPENDENCE OF SINTERED $SmCo_5$ MAGNETIC PROPERTIES[a]

Magnet Property	Temp. of Measurement (°C)	Brand Type			
		B-1 I[b]		E-1 P||M	
		Average	St. Dev.	Average	St. Dev.
B_r (kG)	-60	9.60	0.025	9.40	0.018
	+25	9.24	0.042	9.01	0.025
	+100	9.00	0.033	8.72	0.013
	+200	8.58	0.037	8.41	0.045
$_BH_c$ (kOe)	-60	9.32	0.029	9.35	0.024
	+25	8.80	0.044	8.87	0.043
	+100	8.21	0.090	8.49	0.013
	+200	6.52	0.587	8.09	0.050
$(BH)_{max}$ (MGOe)	-60	22.42	0.08	22.04	0.09
	+25	20.48	0.30	20.24	0.17
	+100	18.98	0.16	18.82	0.07
	+200	17.17	0.17	17.08	0.09
H_k (kOe)	-60	14.68	0.65	22.73	0.63
	+25	11.39	0.52	20.36	1.56
	+100	8.85	0.44	16.23	1.33
	+200	5.62	0.43	11.75	1.41
$_MH_c$ (kOe)	-60	23.74	1.30	34.97[c]	--
	+25	18.46	1.17	28.14	2.17
	+100	13.70	1.00	21.26	2.04
	+200	8.55	0.71	13.76	1.35

[a]Average value based on eight specimens.

[b]Fabrication Methods: [I] Isostatically pressed. [P||M] Die pressed with force and field parallel.

[c]Estimated average.

TABLE 14

TEMPERATURE DEPENDENCE OF SINTERED $SmCo_5$ MAGNET PROPERTIES[a]
PERCENT CHANGE FROM VALUES AT 25°C

Permanent Magnet Property	Temp. of Measurement (°C)	Brand Type	
		B-1 [I][b]	E-1 [P||M][b]
		Δ[%]	Δ[%]
B_r	-60	+3.9	+4.3
	+100	-3.7	-3.3
	+200	-7.1	-6.7
B^{H_c}	-60	+5.9	+5.5
	+100	-6.7	-4.3
	+200	-25.9	-8.7
$(BH)_{max}$	-60	+9.5	+8.9
	+100	-7.3	-7.0
	+200	-16.2	-15.6
H_K	-60	+28.9	+11.7
	+100	-22.3	-20.3
	+200	-50.6	-42.3
M^{H_c}	-60	+28.6	+6.2
	+100	-25.8	-25.5
	+200	-53.7	-51.1

[a]Average value based on eight specimens.

[b]Fabrication Methods: [I] Isostatically pressed. [P||M] Die pressed with force and field parallel.

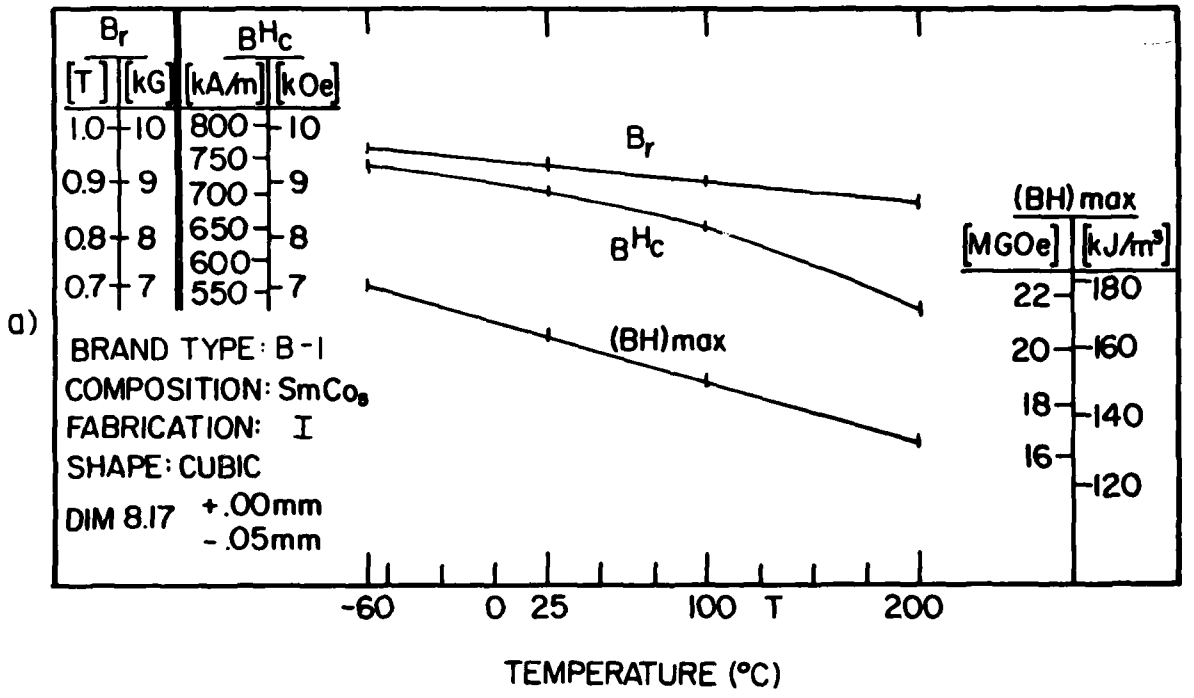

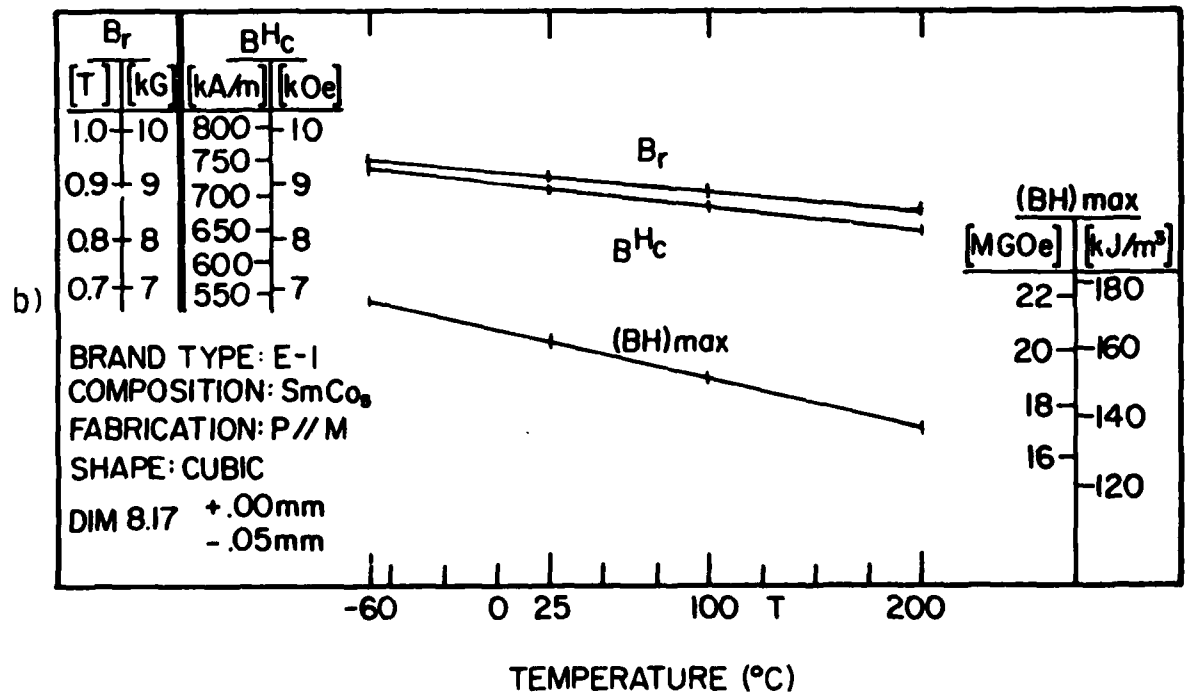

Figure 20a,b Phase III. Temperature Dependence of Selected Second-Quadrant Magnetic Properties of Sintered $SmCo_5$ Magnets, Over a Temperature Range of -60° to +200°C. Brand Types B-1 and E-1.

TABLE 15

AVERAGE TEMPERATURE COEFFICIENTS OF REMANENCE, COERCIVITY, AND ENERGY PRODUCT OF SINTERED $SmCo_5$ MAGNETS MEASURED[a]

Brand Type and Fabrication[b]	Magnetic Property	Temperature Coefficients (-% per °C)						
		At Temperature Level				Over Temperature Span		
		-60°	+25°	+100°	+200°	-60 — 100°	0° — 100°	0° — 200°
B-1 [I]	B_r	0.040	0.044	0.054	0.068	0.046	0.048	0.050
	$_BH_c$	0.071	0.104	0.164	0.308	0.074	0.188	0.138
	$(BH)_{max}$	0.118	0.120	0.184	0.292	0.096	0.121	0.110
E-1 [P||M]	B_r	0.038	0.040	0.046	0.058	0.043	0.044	0.046
	$_BH_c$	0.055	0.060	0.060	0.060	0.057	0.057	0.057
	$(BH)_{max}$	0.090	0.097	0.102	0.104	0.098	0.098	0.098

[a]Average value based on eight specimens.

[b]Fabrication methods: [I] Isostatically pressed. [P||M] Die pressed with force and field parallel.

field. In this state, the degree of dependency on the magnitude of charging field necessary to effect domain wall pining, and therefore achieve optimum magnet performance, is somewhat reduced. Magnets previously magnetized for quality control inspection by the manufacturer or user and then demagnetized for assembly generally require much higher remagnetization fields to achieve the same properties.

The degree of magnetization produced by specific charging field levels in either state was examined next for both brand type $SmCo_5$ magnets.

Initial d.c. magnetization curves were recorded using virgin magnets as illustrated in Figure 21. To accomplish this task each magnet specimen is placed in the zero field closed-circuit electromagnet yoke of the hysteresigraph system and a first-quadrant magnetization curve recorded as the field is increased to a specific charging field level as shown in Table 16. At this point the field was reduced to zero polarity, reversed, and increased again until the second-quadrant intrinsic demagnetization curve was complete. For each magnet specimen, the properties developed were compared to the maximum properties achieved after pulse magnetizing in the forward direction with a 100 kOe pulse field, applied in the original direction of magnetization. All comparative data were normalized relative to the average room temperature properties observed for the second lot of magnets for each brand type.

The data presented in Table 16 illustrates that nominal d.c. charging field levels of at least 1-1/2 to 2 times the coercive force are required to develop optimum magnetic properties. Owing to the fact that these two $SmCo_5$ magnet types have distinctly different characteristic intrinsic demagnetization curves, there is a considerable variation in the data for the two types with each incremental low-field step up to 25 kOe. Examining the data further, one can also visualize the potential problem of uniformly magnetizing large magnets assembled in a multipole configuration. Failure to provide sufficiently high-uniform magnetizing fields

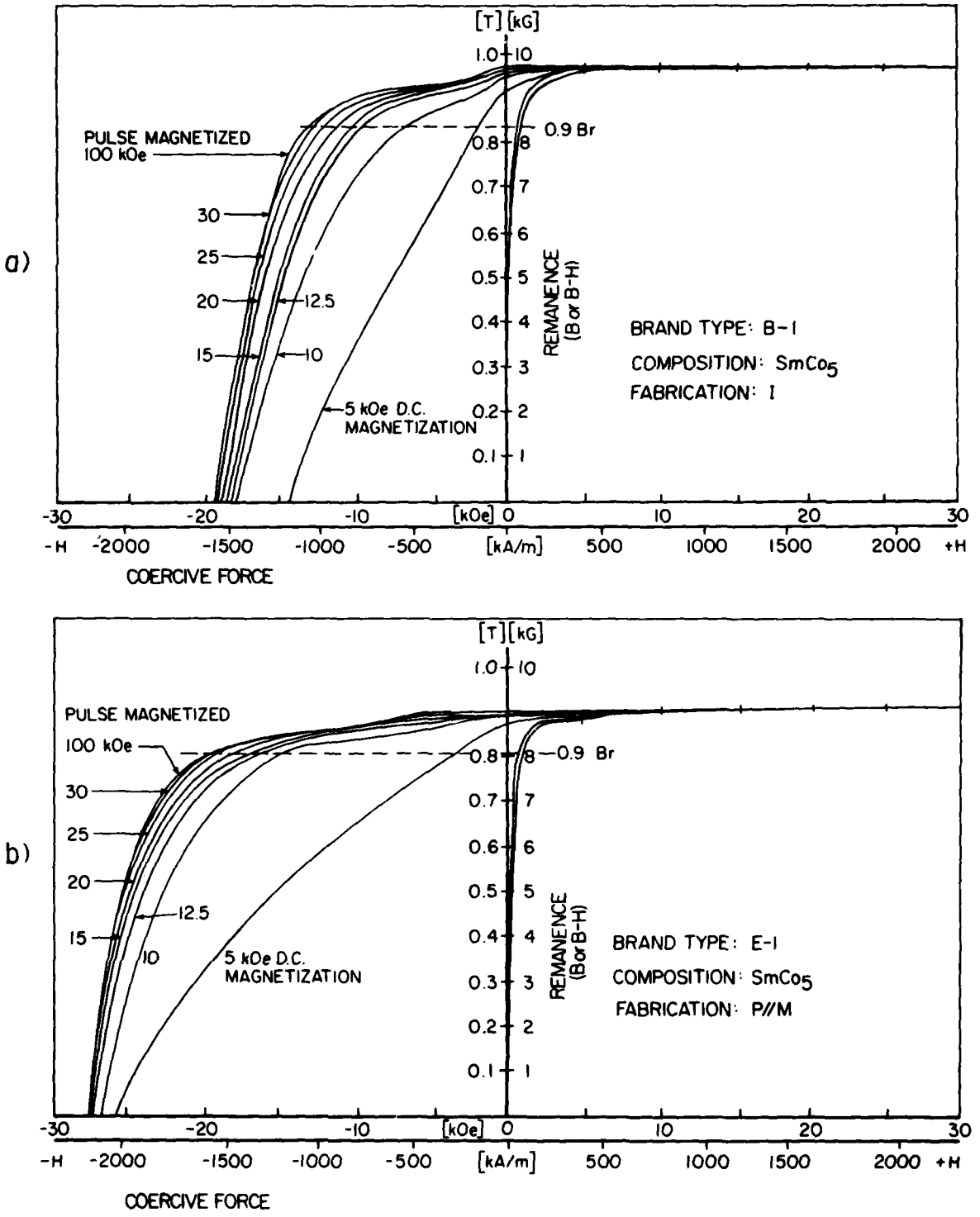

Figure 21a,b Characteristic Virgin State d.c. Magnetization and Demagnetization Hysteresis Curves of Sintered $SmCo_5$ Permanent Magnets. Brand Types B-1 and E-1.

TABLE 16

PERCENTAGE OF MAXIMUM MAGNETIC PROPERTIES OF VIRGIN SINTERED $SmCo_5$ MAGNETS AT SPECIFIC D.C. MAGNETIZATION FIELD LEVELS

Magnetizing Field	Brand Type B-1 [% of Maximum][a]			Brand Type E-1 [% of Maximum][a]		
[kOe]	B_r	$_MH_c$	H_K	B_r	$_MH_c$	H_K
5	96.0	81.3	14.2	98.6	94.2	29.0
10	98.9	95.0	60.1	99.0	98.0	75.1
12.5	99.5	96.1	84.1	99.0	98.4	77.0
15	100	97.7	85.9	99.7	99.0	86.0
20	100	99.1	92.0	100	99.2	88.2
25	100	99.5	95.3	100	99.5	90.5
30	100	100	98.1	100	100	99.1

[a] Compared to maximum values after pulse magnetization in 100 kOe field.

will adversely affect the loop squareness, first, and secondly the general homogeneity of the magnets properties. Recognizing that the temperature stability of RE-TM permanent magnets is related to effective domain wall pining, as evidenced by the intrinsic hysteresis loop squareness, the lower H_k becomes relative to the induction coercive force ${}_BH_C$, the higher the initial irreversible, and long term reversible, thermal aging losses will be at temperatures greater than 100°C. As a consequence, high performance machine stability at elevated temperatures could be degraded, even with the best potential magnet materials, if adequate magnetization procedures are not carefully applied.

For magnets previously magnetized and then reduced to zero remanent (∿50-100 Gauss) flux density, the overall optimum property values, shown in Figure 22, do not develop until the d.c. magnetization fields are in excess of 25 kOe for each brand type. If lower magnetizing fields are utilized, both the coercive force and loop squareness will rapidly diminish in comparison to the optimum values possible, as indicated by the data presented in Table 17.

The effective magnetic properties developed by pulse field magnetization from a d.c. knock down remanent state were also measured for comparison. The charging solenoid used develops a pulse field 10 milliseconds in duration, measured at 90 percent of pulse height. The data presented in Table 18 and Figure 23 clearly indicates pulse fields on the order of 40-50 kOe are necessary to achieve magnetic properties comparable to those produced by d.c. closed-circuit charging fields. This can be attributed to initial eddy current shielding developed by fast rise time pulse magnetization.

It should be noted that the effective percentage magnetization achieved, compared to the optimum possible, will be greatly influenced by: (1) the magnitude of the near zero knock down remanent flux density and (2) whether the remanent flux is aiding or opposing the direction of applied external magnetizing field.

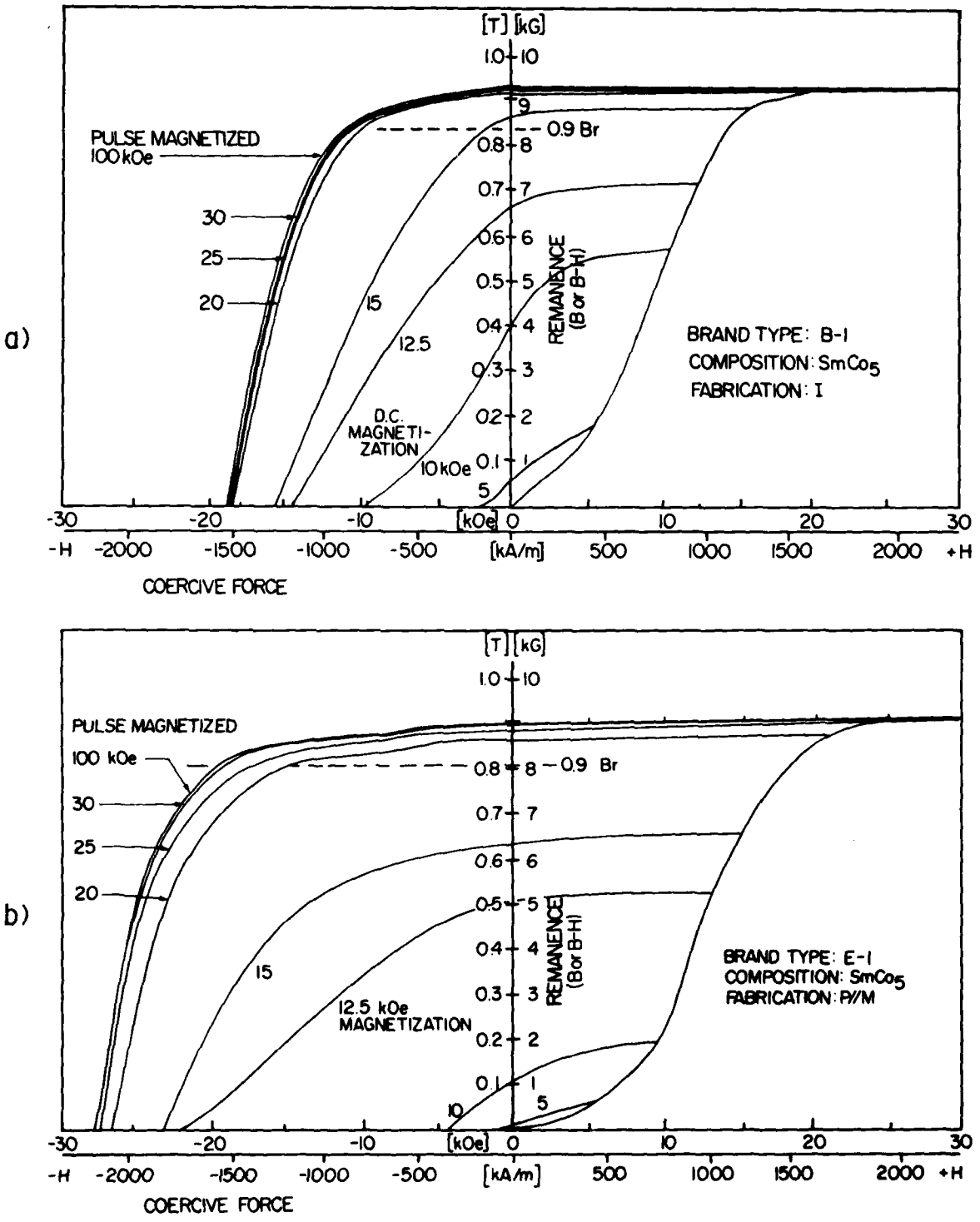

Figure 22a,b Characteristic d.c. Magnetization and Demagnetization Hysteresis Curves of Sintered $SmCo_5$ Permanent Magnets from a Zero Remanence d.c. Knock Down State. Brand Types B-1 and E-1.

TABLE 17

PERCENTAGE OF MAXIMUM MAGNETIC PROPERTIES OF SINTERED $SmCo_5$ MAGNETS AT SPECIFIC D.C. MAGNETIZATION FIELD LEVELS[a]

Magnetizing Field	Brand Type B-1 [% of Maximum][b]			Brand Type E-1 [% of Maximum][b]		
[kOe]	B_r	$_MH_c$	H_K	B_r	$_MH_c$	H_K
5	8.0	8.7	--	1.2	0.5	--
10	42.6	53.5	--	13.3	19.4	--
12.5	72.3	79.2	--	58.4	78.7	--
15	92.3	84.1	19.0	70.0	83.3	--
20	98.9	96.2	93.7	95.9	97.7	77.9
25	99.0	98.4	98.2	98.5	99.0	90.9
30	100	99.6	99.1	99.9	100	97.4

[a]Magnets were previously magnetized and knocked down to zero.

[b]Compared to maximum values after pulse magnetization in 100 kOe field.

TABLE 18

PERCENTAGE OF MAXIMUM MAGNETIC PROPERTIES OF SINTERED $SmCo_5$ MAGNETS AT SPECIFIC PULSE MAGNETIZATION FIELD LEVELS[a]

Magnetizing Field	Brand Type B-1 [% of Maximum][b]			Brand Type E-1 [% of Maximum][b]		
[kOe]	B_r	$_MH_c$	H_K	B_r	$_MH_c$	H_K
15	60.0	69.5	46.4	96.8	96.5	91.5
20	87.5	90.5	82.7	98.0	98.3	94.9
25	99.0	97.8	96.2	99.4	99.1	98.0
30	99.5	99.9	98.7	99.8	100	99.6
40	99.9	100	99.5	100	100	99.8
50	100	100	99.9	100	100	100

[a]Pulse magnetized from a d.c. knock down state.

[b]Compared to maximum values after pulse magnetization in 100 kOe field.

a)

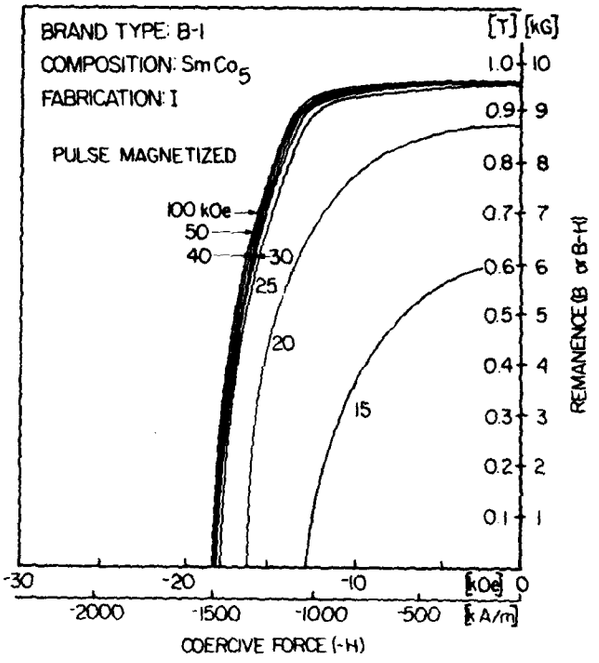

b)

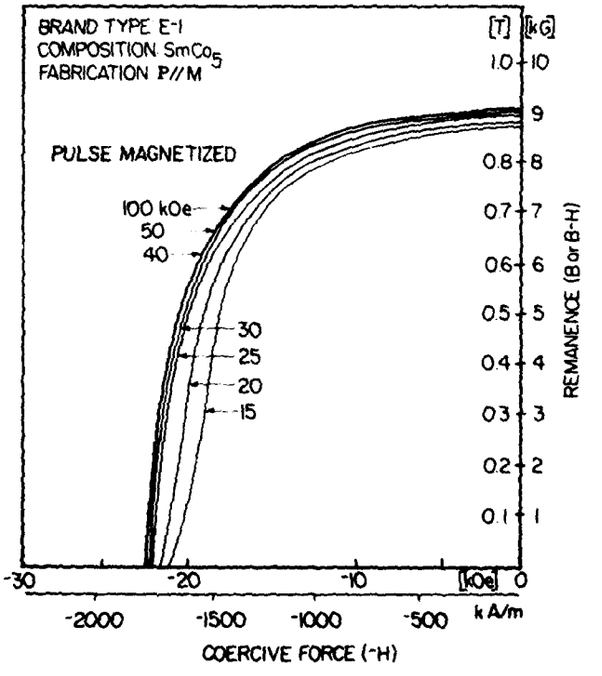

Figure 23a,b Characteristic Demagnetization Hysteresis Curves of Sintered $SmCo_5$ Permanent Magnets Pulse Magnetized from a Zero Remanence d.c. Knock Down State. Brand Types B-1 and E-1.

c) Minor Loop Recoil Characteristics

Examination of commercial manufacturing brochures relating to RE-TM permanent magnet materials reveal that it is generally assumed that most of these alloy compositions exhibit unity recoil permeability in the second-quadrant of the demagnetization curves. In practice this is not always the case even for the same general type material composition as shown in Figures 24a and 24b. In these figures, for illustration, the average value of the minor loop recoil lancets, at room temperature (solid curves) and 200°C (dotted curves), are plotted from four low permeance levels on the intrinsic demagnetization curves.

As an aid in optimizing heavy duty high performance machine design calculations, minor loop recoil loops from four permeance levels, in the range of B/H = -4 to -1/4, were recorded at temperatures from -60°C to +200°C. Eight magnet specimens of each brand type were pulse magnetized in a 100 kOe field prior to recoil measurements at a given temperature. The average recoil data are graphically illustrated in Figures 25 and 26 and presented in Table 19.

The data presented in Table 19 illustrates the degree of variation in permeability as a function of one or both variables for each brand type. The range of recoil permeability data values for each brand type tested are $1.00 \geq \mu r \leq 1.17$. The permeability data changes observed are inversely proportional to temperature and directly proportional to increasing permeance. That is, the recoil permeability approaches unity as the temperature approaches -60°C and/or the permeance approaches -4.

Over the range investigated, the data indicates that for type E-1, the percent change in recoil permeability values are approximately one-half the percent change measured for B-1 magnets. This applies to both recoil from various permeance levels at constant temperature or a change in temperature at constant permeance levels.

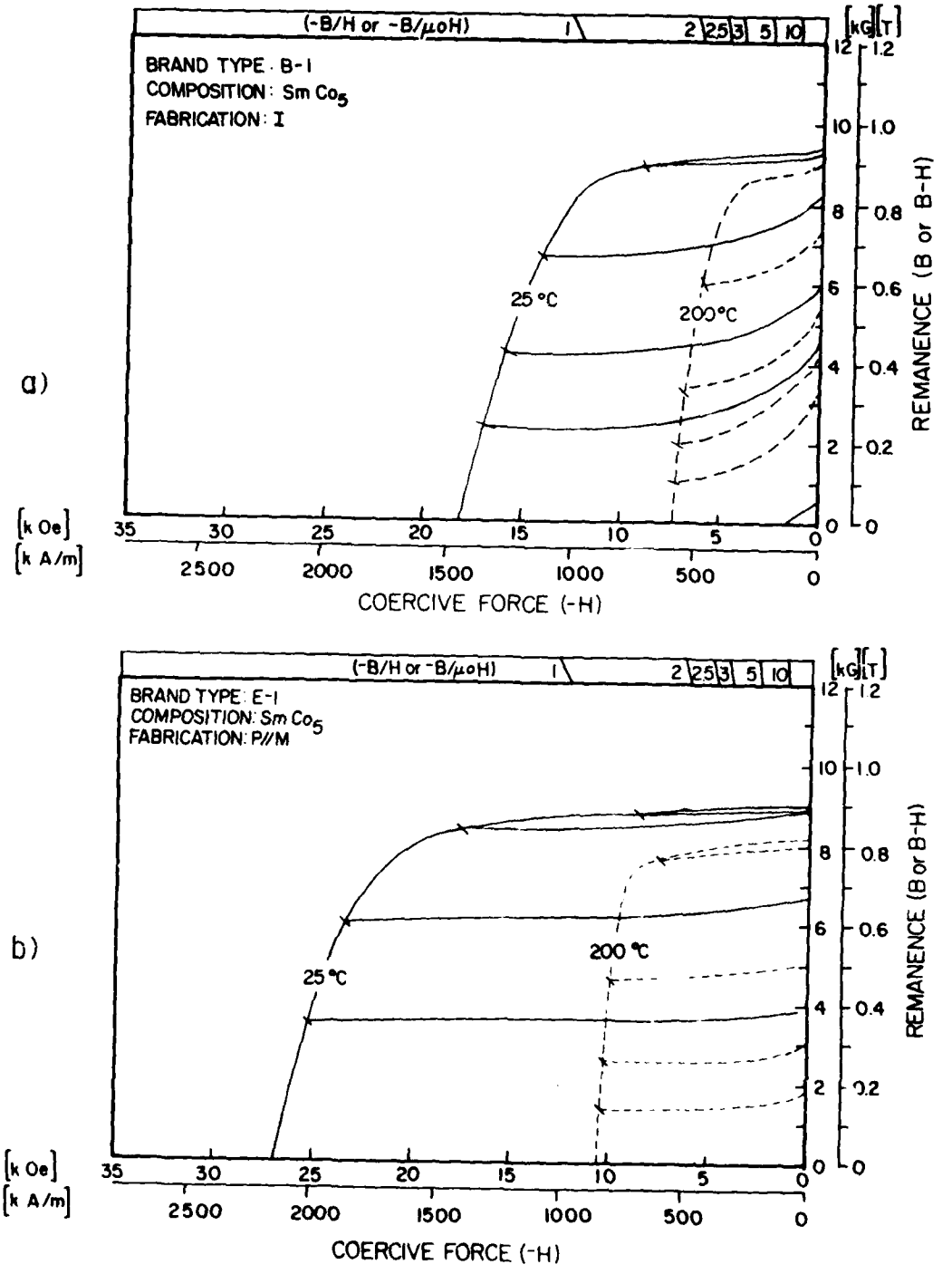

Figure 24. Typical Minor Loop Recoil Characteristics of Sintered $SmCo_5$ Permanent Magnets from Low Permeance Intercepts on the Intrinsic Demagnetization Curve. Brand Types B-1 and E-1.

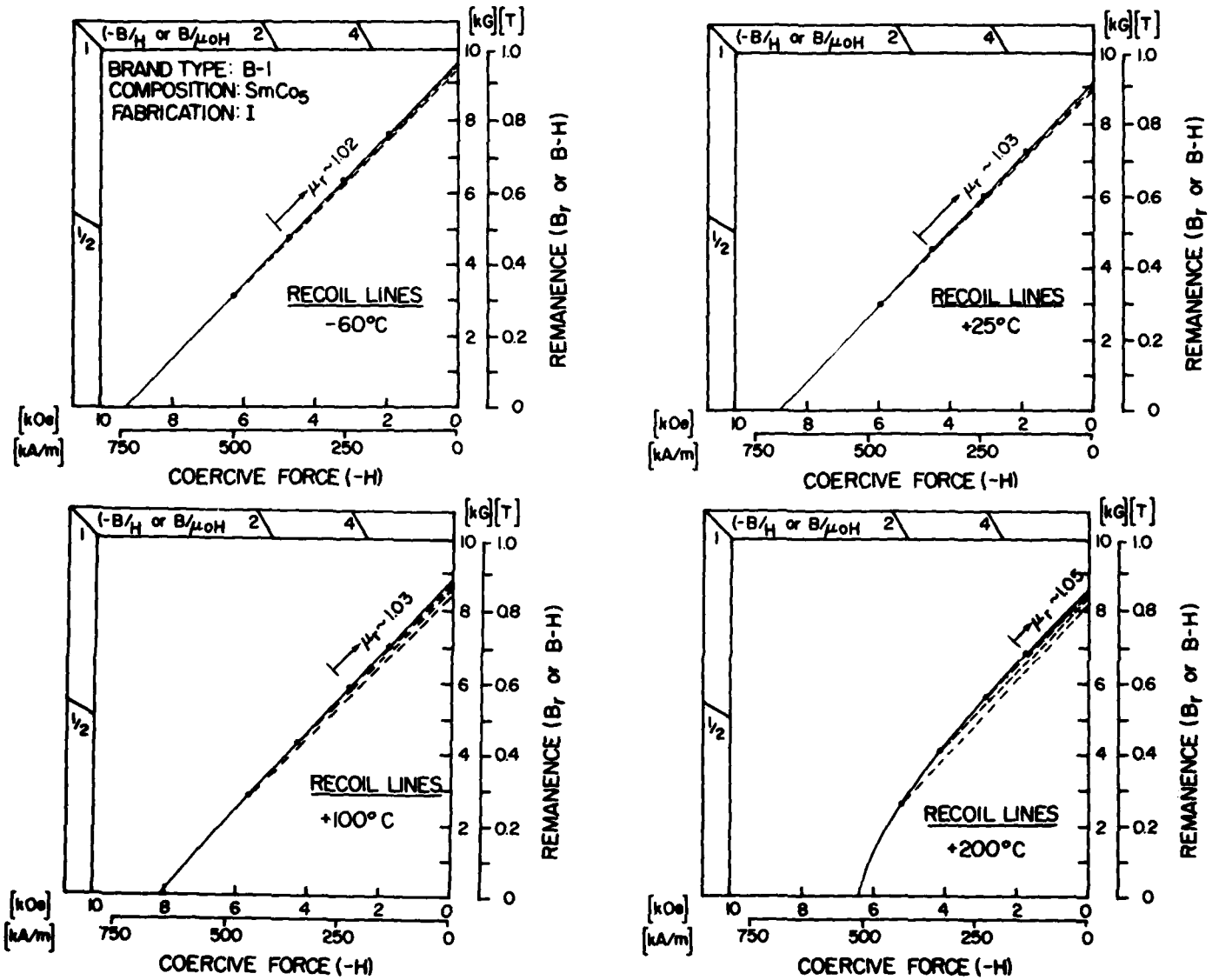

Figure 25. Average Minor Loop Recoil Lines from the Normal Induction Curve (B vs. H) at Four Permeance Intercepts from -1/2 to -4 and Temperatures of -60° to +200°C. Brand Type B-1.

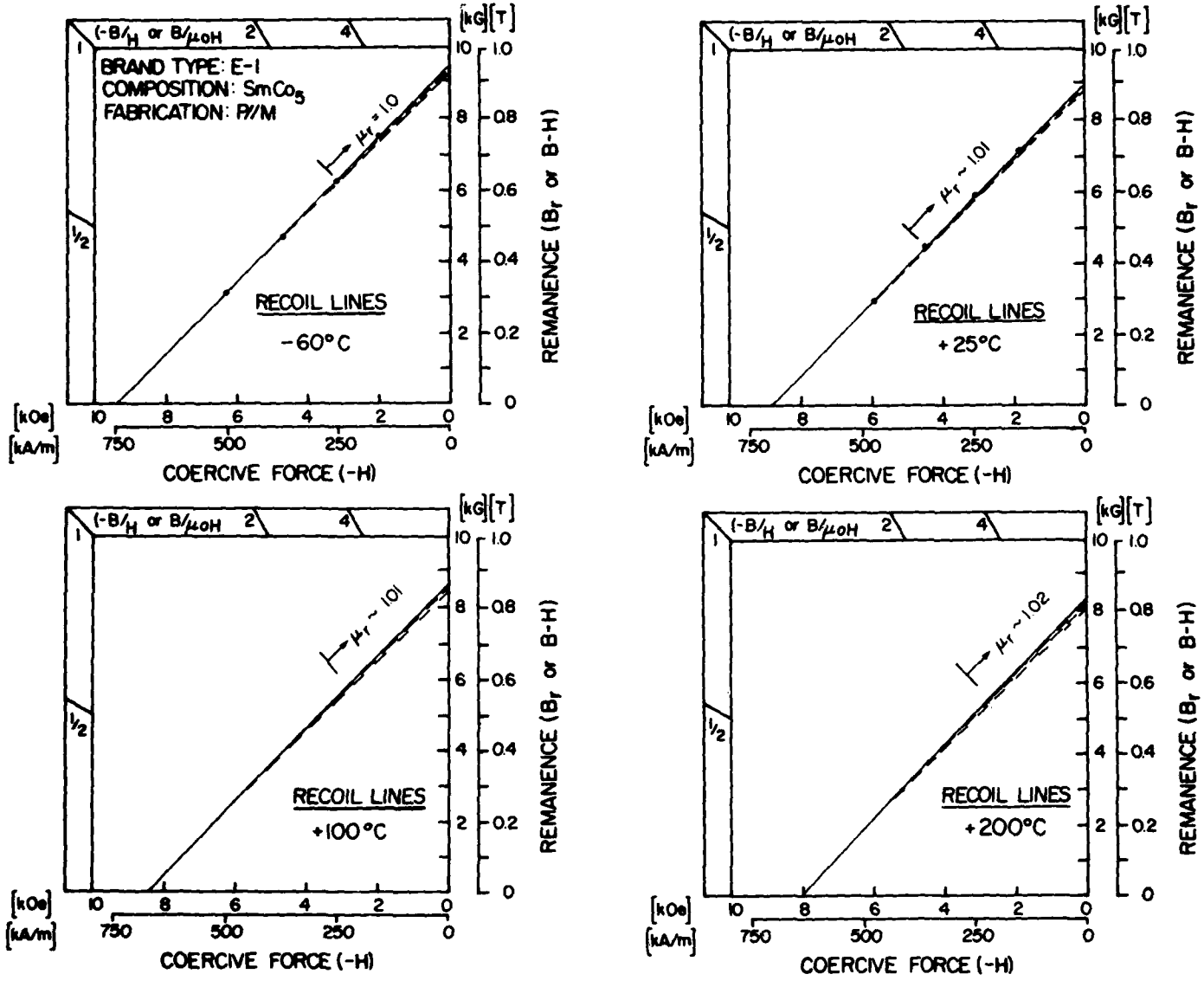

Figure 26. Average Minor Loop Recoil Lines from the Normal Induction Curve (B vs. H) at Four Permeance Intercepts from -1/2 to -4 and Temperatures of -60° to +200°C. Brand Type E-1.

TABLE 19

AVERAGE RECOIL PERMEABILITY OF SINTERED $SmCo_5$ PERMANENT MAGNETS[a]

Specimen Temp./°C	Brand Type B-1 [I][b] From Permeance Level, B/H				Brand Type E-1 P||M[b] From Permeance Level, B/H			
	-1/2	-1	-2	-4	-1/2	-1	-2	-4
-60°	1.06	1.02	1.02	1.02	1.02	1.01	1.00	1.00
+25°	1.10	1.03	1.03	1.03	1.02	1.01	1.01	1.01
+100°	1.15	1.06	1.03	1.03	1.05	1.02	1.01	1.01
+200°	1.17	1.15	1.06	1.05	1.08	1.04	1.02	1.02

[a]Average value based on eight specimens.

[b]Fabrication Methods: [I] Isostatically pressed. [P||M] Die pressed with force and field parallel.

d) Magnetic Property Evaluation in Test Bars

To verify the magnetic quality of test specimen bars received for flexural strength and elastic modulus evaluations, intrinsic demagnetization curves were measured and the data compared with the average magnet property values previously measured in Phase II. After the physical property tests were concluded, three cubic specimens (~3 mm on edge) were sliced by electric spark discharge machining from test bar pieces salvaged from each lot.

All measurements were done with a vibrating specimen magnetometer (Princeton Applied Research-VSM Model 155). A shape demagnetization factor was determined for the geometric shape of the specimen for use in shearing the original magnetometer curves plotted. The density of the sintered magnets used was 8.30 g/cm^3 for type B-1, and 8.47 g/cm^3 for type E-1 (see Section 4, C, Paragraph a,5).

Each specimen was pulse magnetized in a 100 kOe field and then inserted in the magnetometer specimen holder and aligned in the protection tube assembly. A continuous plot of $4\pi M$ versus H was produced and the VSM electromagnet field swepth at 0.5 kOe/min from 0 to -15 kOe, which was sufficient to decrease the remanence to zero.

Using the previously determined shape demagnetizing factor, a sheared second-quadrant demagnetization curve on a Gauss/Oersted scale was drawn. A summary of the data measured from the sheared curve is presented in Table 20 and should be compared with the data in Table 12. The average data value of both specimen lots are comparable, with the exception of the E-1 specimens, where the field was parallel to one of the short dimensions for both size test bars.

TABLE 20

MAGNETIC PROPERTIES OF SPECIMEN BARS USED IN MECHANICAL TEST EVALUATIONS

Magnetic Property	Units	Brand Type B-1				Brand Type E-1			
		~3x3x25 mm[a]		~6x6x25 mm		~3x3x25 mm		~6x6x25 mm	
		⊥[b]	∥[c]	⊥	∥	⊥	∥	⊥	∥
B_r	kG	9.4	9.35	9.25	9.37	8.65	9.60	8.90	9.45
$_BH_c$	kOe	8.80	8.70	8.71	8.84	8.13	8.47	8.42	8.81
$(BH)_{max}$	MGOe	18.5	20.5	19.9	21.1	18.0	20.4	19.1	20.1

[a]Original test specimen bar dimensions.

[b]Specimen bar fabricated with magnetization oriented in short dimension.

[c]Specimen bar fabricated with magnetization oriented in long dimension.

C. Measuring Techniques and Instruments Used in Task III Thermal and Mechanical Property Determinations

a) Thermal Properties

1. Thermal Diffusivity

As an indirect approach to the measurement of thermal conductivity the thermal diffusivity was measured and the thermal conductivity calculated from it. [13] Measurements were made at -55°, 23°, 100°, and 205°C. For the diffusivity measurements a flash technique was employed using a Xenon flash lamp as the heat source. Sample response temperatures were sensed with an InSb detector (Figure 27). The transit time of a heat pulse to pass through a thin specimen was measured. The flash technique is much less sensitive to specimen geometry and heat source characteristics and does not require elaborate instrumentation. Materials for this technique were cut from elastic modulus test bars to obtain 2 mm thick specimens.

The flash technique required the initial deposition of energy to be confined to the near-surface region of the specimen. Therefore, magnet samples having relatively different surface finishes, either because of composition differences or as a result of grinding, sintering, and post-sintering heat treatments, were polished and coated with an opaque, energy absorbing layer of uniform emissivity. For measurements over the temperature range studied, a vapor-deposited layer of silver, chemically treated to produce a silver sulfite surface, was found satisfactory for this purpose. Specimens were cut from the rectangular bars used in the elastic modulus determinations.

2. Heat Capacity (Specific Heat)

The heat capacity was determined at 70°C using a Perkin-Elmer, DSC-2, differential scanning calorimeter (DSC). The DSC employed uses a reference material of aluminum oxide and compares the temperature rise in the unknown versus the reference material as the furnace, containing the two materials, undergoes a temperature change at a preprogrammed and precisely controlled rate. Very simplified and straightforward calculations were then employed to determine the specific heat (C_p)

Figure 27. Thermal Diffusivity Measuring Apparatus.

(reported as J/kgm°C - specific heat). Very thin (<1 mm) specimens were required and they were cut from fractured flexural test specimens.

3. Thermal Conductivity

The thermal conductivity (k) was calculated from the experimentally determined values of thermal diffusivity (α), specific heat (C_p), and density (ρ) using the expression:

$$k = \alpha \rho C_p \qquad (4)$$

where: k = thermal conductivity
α = thermal diffusivity
ρ = density
C_p = specific heat.

4. Coefficient of Thermal Expansion

A precise quartz-tube dilatometer was employed for thermal expansion measurements over the temperature range from -60° to 205°C. A bar-shaped specimen rested in a quartz tray with quartz push rods lightly spring loaded against its ends (Figure 28). Thermal expansion of the specimen was translated through the push rods and detected by a linear voltage displacement transducer. The specimen and its support fixture were enclosed in a tube furnace programmed to heat the assembly at a controlled rate. Furnace temperature and the specimen displacement were simultaneoulsy plotted on an x-y recorder. By using a standard sample, accuracies better than ±1 percent were routinely obtained. Specimens were prepared from a rectangular fractured flexural test specimen.

5. Density Measurements

Specimens of both brand types (10 each) were determined using the Archimedes method. Each specimen was weighed in air and distilled water five times. No wetting agent was used

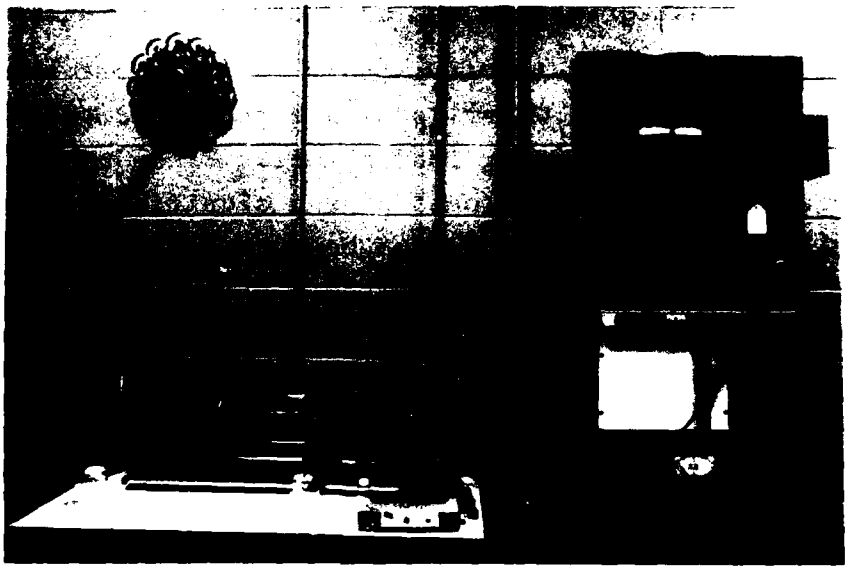

Figure 28. Thermal Expansion Measuring Apparatus.

and the density of the water was corrected for temperature variations. The average density of the E-1 brand type magnets was determined to be 8.47 ± 0.02 gm/cm^3, and the B-1 brand type was 8.30 ± 0.02 gm/cm^3.

b) Mechanical Properties

1. Flexural Strength

Four-point flexure testing was selected for this program in preference to a uniaxial tension test for several

reasons. Uniform-stress uniaxial tensile tests using the familiar "dogbone" shaped specimens, or the more complex theta-ring and trussed-beam specimens, are simply too wasteful of material. Moreover, direct tension tests are very susceptible to parasitic stresses resulting from eccentric loading, and to cracking of specimens in the test grips, in the case of brittle materials.

In contrast, the four-point flexure test uses a very simple specimen geometry. Under load, a constant moment is developed between the two inner load points. Consequently, a uniform surface stress is developed over a significant portion of the sample and valid test data can be obtained for failures which occur anywhere in that region. To minimize errors from fixture misalignment, friction effects, and contact point wedging, a kinematically designed bend fixture was employed (Figure 29). This fixture incorporates the basic design features recommended by the NATO Advisory Group for Aerospace Research and Development.[14] This fixture was evaluated using glass, ceramic and acrylic specimens, shown to perform properly, providing uniform loading.[15] An Instron Universal Testing Machine, Model 1123 (Figure 30), was employed to load the specimens to failure.

The specimens were prepared in three groups with the direction of magnetization parallel to the longitudinal axis of the bar (F_1) and the two directions perpendicular to the longitudinal axis (F_2 and F_3). Twenty-four specimens, six at each temperature, from each of the three groups were tested at -60°, 23°, 100°, and 205°C. All of the specimens were loaded to failure at a rate of 0.5 mm/min (0.02 in/min).

2. Young's Modulus and Poisson's Ratio

Young's modulus (E) and Poisson's ratio (ν) were measured nondestructively in four-point bending. "T-type" strain gages were placed on the tensile surface and their output monitored with a Vishay P-350A strain indicator through a Vishay Switch Balance Unit, which allowed for both longitudinal and transverse strain to be recorded at the same time. The measurements were taken at

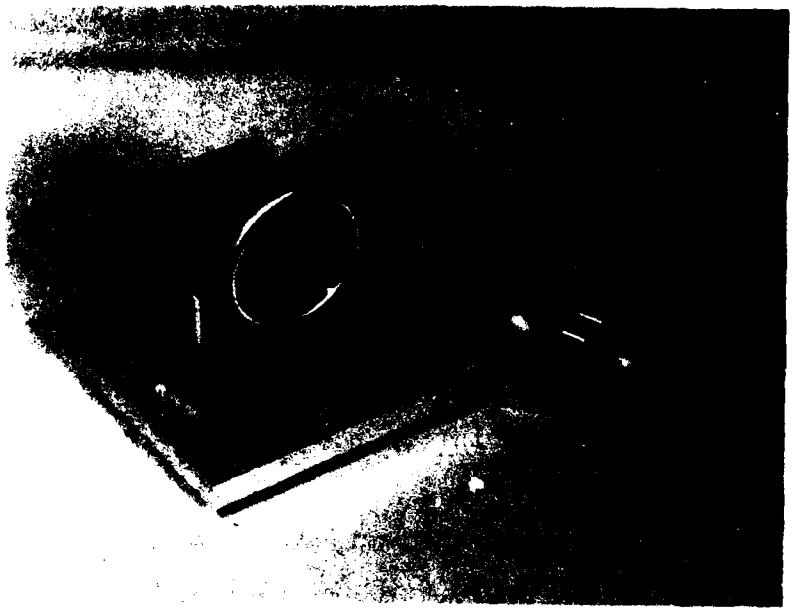

Figure 29. NATO Four-Point Bend Fixture.

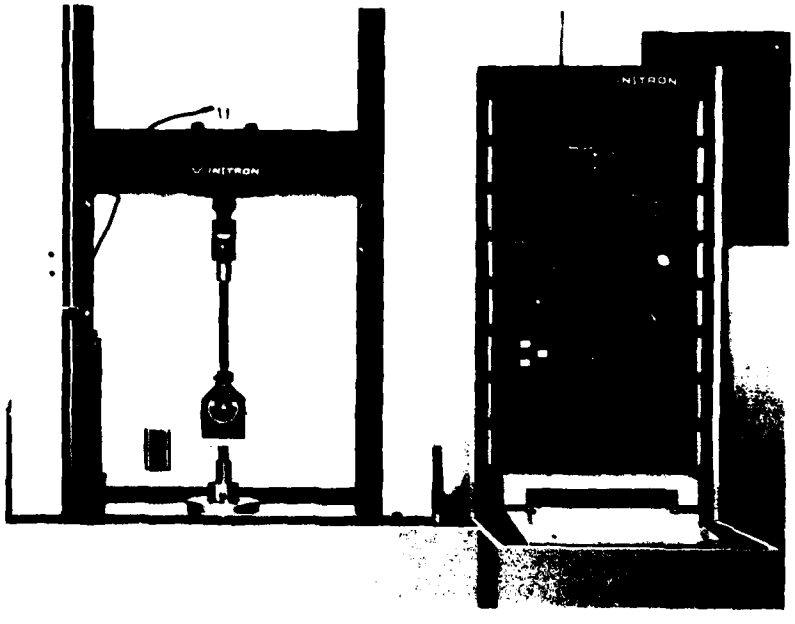

Figure 30. Instron Universal Testing Machine.

-60°, 23°, 100°, and 205°C on specimens with the direction of magnetization along the longitudinal axis of the bar (F_1) transverse to the axis (F_2) and 90° to the transverse and longitudinal axis (F_3).

3. Compressive Strength

Compressive strength measurements will be performed as described in Phase I, Section 2, with the exception that the tests were also carried out at temperatures of -60°, 100°, and 200°C. An Instron Universal Tester with self-alignment fixture and load pacer was used in these compressive strength tests. Cubic specimens, 8 mm (0.32 in) on a side, were employed for both phases of the program.

4. Shock Strength (Impact Strength)

A standard Charpy impact test apparatus was used to determine the energy to fracture of the same test specimens used to determine elastic modulus and Poisson's ratio.

D. Discussion of Experimental Plan and Results of Mechanical and Thermal Property Determinations

a) Mechanical Properties

1. Mechanical Strength and Elasticity, General Comments

Experience has shown that sintered Sm-Co magnets contain many small voids, microcracks, and often even relatively large processing imperfections hidden beneath the magnet surface. This is particularly true for the die-pressed variety. Magnets made by isopressing before sintering are structurally more sound and have more uniform properties. However, because of its lower cost, die-pressing is quickly becoming the sole process used in mass production.

The mechanical fracture strength of brittle materials under any kind of loading, but particularly in the presence of tensile stresses, is determined by structural defects and not by the intrinsic strength properties of the polycrystalline, textured magnet material, per se. This also implies that the fracture strength

under tension, bending, compression, and shear will depend on the size and shape of the magnet. Different sizes and shapes mean variations in detail of compaction and heat treatment, which in turn cause differences in the density and the distribution of flaws responsible for brittle failure. We chose, therefore, to perform compressive and flexural strength tests on a sufficient number of magnets to provide a statistically significant value for compressive and flexural strengths with confidence limits narrow enough to provide the design engineer with a reasonable degree of reliability.

In contrast, one could expect the elastic constants to be relatively independent of the defect structure. But since they are different for different directions in the RCo_5 crystal lattice, the elastic tensor for a magnet must reflect the degree of grain alignment and, in an indirect way, depends on magnet geometry and other production variables. A study of the effects of these variables on the elastic properties was deemed outside the scope of the program. However, the anisotropy of Young's modulus and Poisson's ratio was determined.

The use of brittle material in structural applications must take into account that the load response behavior of these materials is distinctly different from that of metals. Brittle materials are extremely sensitive to tensile stresses and characteristically exhibit a large statistical variability of strength when loaded in tension.

Microscopic flaws are present in all real materials. The tips of these flaws are stress concentrations sites which, in ductile metals, can be reconfigured under load to a more benign geometry (rounded crack tip) via the mechanism of plastic deformation. Brittle structural materials cannot deform plastically and as loads increase, flaw tip stresses eventually reach levels where the material ruptures and the flaw is lengthened. This process of flaw extension amounts to a conversion of stored plastic energy in the immediate vicinity of the flaw tip to surface energy which is then dissipated by an increase in the surface area of the flaw. If the elastic energy

dissipation is sufficient to reduce stresses at the newly formed flaw tip below critical levels, no further cracking will occur. However, if the rate of strain energy release exceeds the rate of dissipation by new surface formation (at the crack tip), the flaw will propagate through the material and fail the structural member catastrophically.

According to the Griffith criterion for brittle fracture, the critical value of stress required to propagate a flaw is given by

$$\sigma_c = \left(\frac{2E\gamma_s}{\pi C}\right)^{1/2} \qquad (5)$$

where: σ_c is the critical stress
E is the Young's modulus
γ_s is the surface energy, and
C is the radius of a cricular crack.

Thus, the strength of a brittle material depends both upon intrinsic materials properties (E and γ_s) and upon an extrinsic factor (flaw size) which is related to the method and quality of fabrication.

In real materials, process-related microstructural factors such as grain size, dislocations, pores, inclusions, and cracks and the residual stress state of the material will affect its structural behavior.

Ordinarily, the flaws which influence strength are statistically distributed with respect to severity and orientation. It, therefore, follows that the strength of a brittle material will be a statistical quantity.

Past experience with compression tests on 6.5 mm cylinders of $SmCo_5$ was that they fracture at stresses over a wide range (large standard deviation).[1] Fracture-strength tests therefore had to be conducted on a relatively large number of specimens of any given type and size to allow for a statistical analysis.

2. Statistical Method for Selecting Magnet Types for Phase III Testing

Phase I experimentation involved determining magnetic and mechanical strength properties of materials from 11 magnet types. The primary objective of these tests was to identify two types from which additional test specimens will be obtained for further characterization of the properties during Phase III. A secondary objective (which was a natural product of the tests) was to provide a preliminary data base for ease in planning the Phase III experiment. Two sets of criteria had to be established to meet the primary objectives of the Phase I experiment.

First, it was expected that the measurements of any one of the physical properties would display some degree of variability among the specimens of any one manufacturer. If this variability was large in comparison with the differences between magnet types, then statistical methods would have been required to ascertain the significance of apparent differences. For the sample sizes that were available, tests of hypotheses would be possible only for comparison among the average values and degrees of scatter (standard deviations) in specimens from each magnet type. However, only two brand-types tested in Phase I had the magnetic properties required and their compressive strengths were among the highest among the 11 groups making a statistical analysis unnecessary for the selection of magnets for Phase III.

In Phase III, specimens were obtained from the magnets selected, and the mechanical strength properties were characterized using statistical methods. To resolve the question of the required number of specimens (sample size), it was assumed that property characterization would be expressed in terms of the average response among specimens of a single manufacturer. It was further assumed that the ratio of the standard deviation to the average that was observed in the Phase I tests represented the true coefficient of variation. Figure 31 presents the

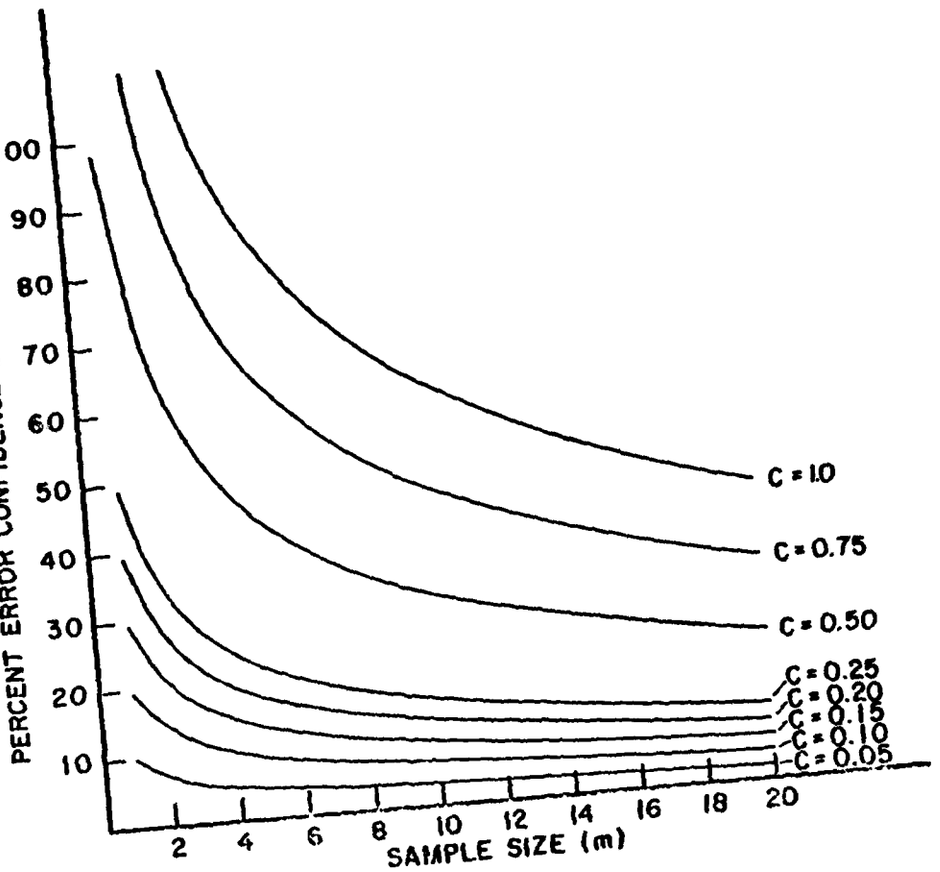

Figure 31. Confidence Limits for Various Sample Sizes.

half-width of a 95 percent confidence interval expressed as a percentage of the mean as a function of sample size for representative values of the coefficient of variation.

By taking this approach one can hope to achieve two things: (1) detect any drastic differences, if they exist, in the average strength (mean value of distribution) and the standard deviation between groups of magnets manufactured by different methods or producers; (2) find an upper bound for the fracture strength which constitutes a lower limit for the strength of structurally sound material and demonstrates what properties may be approached consistently in production if proper processing techniques and quality control measures are applied.

3. Mechanical Strength

In view of the necessity for statistical treatment, we flexurally tested 72 specimens from each of the two vendors selected from Phase I of the program. Twenty-four specimens were magnetized along one axis of the rectangle and along each of the two mutually perpendicular directions. Six specimens from each brand type group of 24 were tested at -60°, 23°, 100°, or 205°C.

With the exception of the B-1 transverse and 90° transverse specimen groups tested at 205°C, the E-1 specimens had higher flexural strengths (Table 21) and the standard deviations for the E-1 material was consistently lower. Tables 22 and 23 give the individual strength values for each specimen tested. This is more dramatically illustrated in Table 24 showing the range of flexural strength values. With the exception of two E-1 90° transverse tests (at 205°C) the values for all of the specimens tested for this brand type were above 10 ksi. The large scatter in the B-1 brand type material was attributed to the inhomogeneity in the materials microstructure as shown in Figure 32. The photomicrographs were obtained from flexural strength specimens with low, medium, and high strength values for the overall B-1 magnet group. Figure 33 is a similar

TABLE 21

AVERAGE FLEXURAL STRENGTH VERSUS TEMPERATURE

Brand Type	Test Temp. (°C)	Magnetization Direction					
		Longitudinal (F_1)		Transverse (F_2)		90° Transverse (F_3)	
		MPa (std.dev.)	ksi (std.dev.)	MPa (std.dev.)	ksi (std.dev.)	MPa (std.dev.)	ksi (std.dev.)
E-1	-60	105.6 (17.7)	15.3 (2.6)	106.5 (10.4)	15.5 (1.5)	93.1 (7.7)	13.5 (1.1)
	23	102.4 (20.5)	14.9 (3.0)	100.0 (6.6)	14.5 (1.0)	96.6 (13.4)	14.0 (1.9)
	100	108.5 (11.4)	15.7 (1.6)	100.3 (12.8)	14.6 (1.9)	85.6 (8.4)	12.4 (1.2)
	205	113.6 (10.9)	16.5 (1.6)	98.3 (3.2)	14.3 (0.5)	73.3 (12.0)	10.6 (1.8)
B-1	-60	83.1 (7.2)	12.0 (1.1)	61.0 (25.0)	8.8 (3.6)	68.4 (27.2)	9.9 (3.6)
	23	82.4 (11.8)	12.0 (1.7)	82.5 (26.6)	12.0 (3.9)	79.7 (28.2)	11.6 (4.1)
	100	92.3 (2.7)	13.4 (0.4)	106.6 (31.8)	15.5 (4.6)	80.5 (34.9)	11.7 (5.1)
	205	72.0 (24.8)	10.4 (3.6)	117.5 (8.2)	17.0 (1.2)	81.4 (23.7)	11.8 (3.4)

All values are averages of data obtained from six specimens.
Nominal specimen size: 25 x 3.2 x 3.2 mm.

TABLE 22

PHASE III FLEXURE TEST RESULTS FOR BRAND TYPE B-1 MAGNETS

Test Temperature	Test Orientation: Longitudinal 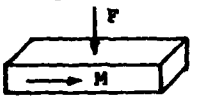		Transverse 		90° Transverse 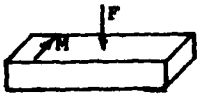	
	MPa	ksi	MPa	ksi	MPa	ksi
-60°C	90.3	13.1	40.7	5.9	64.1	9.3
	86.9	12.6	35.2	5.1	93.8	13.6
	71.0	10.3	93.1	13.5	44.1	6.4
	80.0	11.6	60.7	8.8	40.7	5.9
	88.9	12.9	46.9	6.8	108.3	15.7
	81.4	11.8	89.6	13.0	59.3	8.6
25°C	77.4	11.2	42.3	6.1	47.2	6.8
	77.5	11.2	85.0	12.3	51.2	7.4
	83.9	12.2	103.1	15.0	72.4	10.5
	102.0	14.8	103.3	15.0	109.4	15.9
	71.3	10.4	103.7	15.0	113.4	16.5
			57.9	8.4	84.6	12.3
100°C	91.5	13.3	113.1	16.4	110.8	16.1
	93.2	13.5	128.2	18.6	42.7	6.2
	89.0	12.9	114.5	16.6	115.7	16.8
	96.4	14.0	130.3	18.9	87.5	12.7
	91.4	13.2	44.1	6.4	45.6	6.6
			109.6	15.9		
205°C	75.4	10.9	110.9	16.1	62.2	9.0
	99.2	14.4	117.7	17.1	54.3	7.9
	34.9	5.1	116.0	16.8	102.1	14.8
	86.0	12.5	129.1	18.7	108.0	15.7
	49.2	7.1	124.3	18.0	80.5	11.7
	87.2	12.6	107.1	15.5		

TABLE 23

PHASE III FLEXURE TEST RESULTS FOR BRAND TYPE E-1 MAGNETS

Test Temperature	Test Orientation: Longitudinal 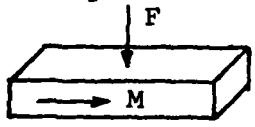		Transverse 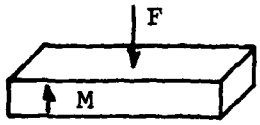		90° Transverse 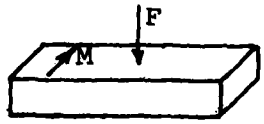	
	MPa	ksi	MPa	ksi	MPa	ksi
-60°C	101.8	14.8	116.7	16.9	90.3	13.1
	110.0	16.0	112.7	16.4	86.9	12.6
	128.6	18.9	97.1	14.1	84.8	12.3
	82.7	12.0	93.7	13.6	105.5	15.3
	89.6	13.0	112.5	16.3	92.4	13.4
	120.7	17.5			98.6	14.3
25°C	112.1	16.3	93.0	13.5	86.4	12.5
	134.1	19.5	111.6	16.2	91.1	13.2
	89.4	13.0	94.6	13.7	115.1	16.7
	86.4	12.5	99.1	14.4	103.7	15.0
	90.1	13.1	100.2	14.5	79.1	11.5
			101.4	14.7	104.4	15.1
100°C	128.2	18.6	95.2	13.8	72.4	10.5
	97.2	14.1	113.1	16.4	80.7	11.7
	111.0	16.1	96.5	14.0	85.5	12.4
	109.6	15.9	81.4	11.8	91.7	13.3
	97.2	14.1	99.3	14.4	96.5	14.0
	107.6	15.6	116.5	16.9	86.9	12.6
205°C	108.1	15.7	97.9	14.2	90.1	13.1
	114.7	16.6	97.9	14.2	65.7	9.5
	110.4	16.0	100.4	14.6	77.8	11.3
	119.8	17.4	101.3	14.7	58.7	8.5
	130.4	18.9	92.3	13.4	74.0	10.7
	98.3	14.3	99.8	14.5		

TABLE 24

RANGE OF FLEXURE STRENGTH VALUES FOR PHASE III MAGNETS

Test Temp. (°C)	Brand Type	Flexure Strength Rank	Test Orientation 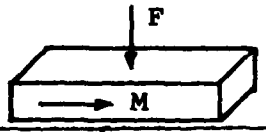		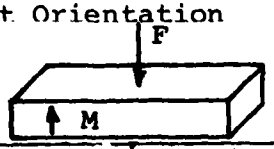		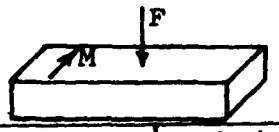	
			MPa	ksi	MPa	ksi	MPa	ksi
-60	B-1	Highest	90.3	13.1	93.1	13.5	108.3	15.7
		Lowest	80.0	11.6	35.2	5.1	40.7	5.9
	E-1	Highest	128.6	18.7	112.7	16.4	105.5	15.3
		Lowest	82.7	12.0	93.7	13.6	84.8	12.3
25	B-1	Highest	102.0	14.8	103.7	15.0	113.4	16.5
		Lowest	71.3	10.4	42.3	6.1	47.2	6.8
	E-1	Highest	134.1	19.5	111.6	16.2	115.1	16.7
		Lowest	86.4	12.5	93.0	13.5	79.1	11.5
100	B-1	Highest	96.4	14.0	130.3	18.9	115.7	16.8
		Lowest	89.0	12.9	44.1	6.4	42.7	6.2
	E-1	Highest	128.2	18.6	116.5	16.9	96.5	14.0
		Lowest	97.2	14.1	81.4	11.8	72.4	10.5
205	B-1	Highest	99.2	14.4	129.1	18.7	108.0	15.7
		Lowest	34.9	5.1	107.1	15.5	54.3	7.9
	E-1	Highest	130.4	18.9	101.3	14.7	90.1	13.1
		Lowest	98.3	14.3	92.3	13.4	58.7	8.5

High Strength
(16.5 ksi)

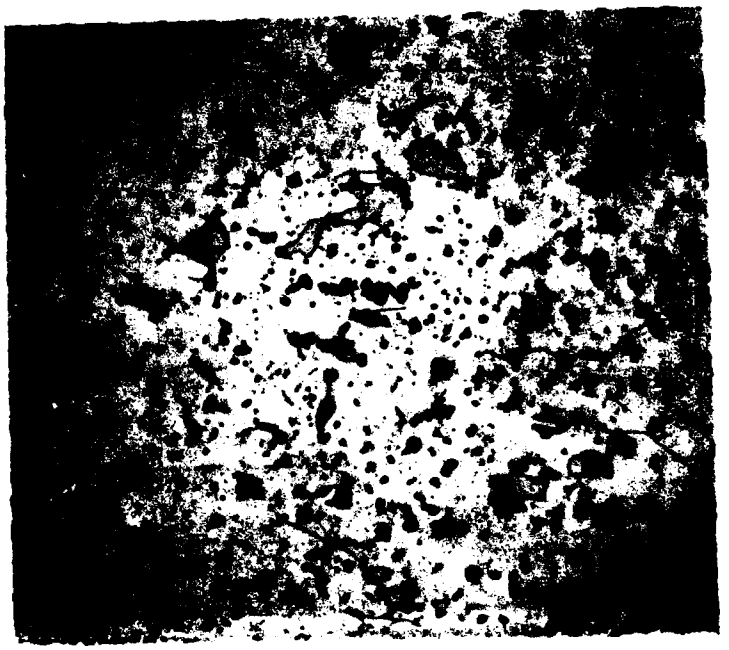

Low Strength
(6.3 ksi)

Figure 32. Representative Photomicrographs of the Microstructure of B-1 Type Magnets at Three Flexural Strength Levels (300X).

High Strength
(16.7 ksi)

Low Strength
(11.5 ksi)

Figure 33. Representative Photomicrographs of the Microstructure of E-1 Type Magnets at Three Flexural Strength Levels (300X).

representation of the E-1 magnet group. The differences are apparent. The E-1 brand type has a smaller overall grain size and smaller voids than its counterpart in the B-1 brand type group. The inconsistency in the microstructure also manifested itself in the compressive strength results (Table 25). Again, the strength values varied over a wide range. In this case, however, both brand types were highly variable from specimen to specimen (Table 26).

4. Elastic Modulus and Poisson's Ratio

The results of the elastic modulus and Poisson's ratio determinations are summarized in Table 27. The values given are the averages obtained from two specimens for each temperature. The variation in values between the two brand types is attributed to the large differences in microstructure between groups and from specimen to specimen within groups, as mentioned previously. Due to the variation in microstructure, no attempt was made to correlate differences in elastic modulus or Poisson's ratio with differences in magnetization direction.

5. Impact Strength

Some difficulty was encountered in the testing of the 1 inch long impact specimens in the Charpy impact tester. The width of the 2 foot-pound impact head required that the span of the load points be 0.875 inch. Therefore, the ends of the specimen did not overlap enough to allow for them to be held firmly in place. This resulted in the magnets becoming jammed between the hammer and the specimen holder and causing some tests to be invalid. However, enough valid tests were completed to allow for a range of results that were judged representative of the materials. Due to the large variation in microstructure for both materials, a range of 0.5 to 1.5 ft./lbs is reported for both brand types.

TABLE 25

PHASE III - AVERAGE COMPRESSIVE STRENGTH AND STANDARD DEVIATION

Brand Type	Test Orientation	-51°C		25°C		100°C		200°C	
		$\bar{x}$ (s) MPa	$\bar{x}$ (s) ksi	$\bar{x}$ (s) MPa	$\bar{x}$ (s) ksi	$\bar{x}$ (s) MPa	$\bar{x}$ (s) ksi	$\bar{x}$ (s) MPa	$\bar{x}$ (s) ksi
B-1	F_1	395.0 (161.2)	57.3 (23.4)	371.0 (207.1)	53.8 (30.0)	436.5 (234.1)	63.3 (34.0)	554.8 (235.7)	80.5 (34.2)
E-1	F_1	729.2 (308.7)	105.8 (44.8)	475.1 (256.2)	68.9 (37.2)	236.0 (96.2)	34.2 (14.0)	237.1 (116.3)	34.4 (16.9)
B-1	F_2	701.1 (217.9)	101.7 (31.6)	764.5 (208.1)	110.9 (30.2)	187.4 (165.8)	27.2 (24.0)	662.9 (236.5)	99.1 (34.3)
E-1	F_2	695.8 (352.2)	100.9 (51.1)	741.8 (185.0)	107.6 (26.8)	415.8 (328.0)	60.3 (47.6)	324.0 (257.0)	47.0 (37.3)
B-1	F_3	666.2 (307.5)	97.2 (45.2)	577.3 (289.1)	83.7 (41.9)	331.9 (199.9)	48.2 (29.0)	657.2 (240.1)	95.4 (34.8)
E-1	F_3	706.4 (389.4)	102.5 (56.5)	645.5 (135.4)	93.6 (19.6)	317.7 (162.0)	46.1 (23.5)	404.7 (213.1)	58.7 (31.0)

Average and Standard deviations obtained from nine test specimens.

TABLE 26

PHASE III - COMPRESSIVE STRENGTH OF BRAND TYPE B-1 MAGNETS

Test Temperature: -51°C

Specimen Number	Test Orientation		Compressive Strength MPa	Compressive Strength ksi
71	F_1		246.5	35.7
75	F_1		485.3	70.4
76	F_1		196.0	28.4
80	F_1		270.4	39.2
84	F_1		419.1	60.8
85	F_1		628.0	91.1
89	F_1		520.0	75.4
		$\bar{x}$	395.0	57.3
		s	161.2	23.4
104	F_2		719.9	104.4
105	F_2		925.2	134.2
106	F_2		671.3	97.4
108	F_2		445.7	64.6
110	F_2		327.9	47.5
111	F_2		913.5	132.5
115	F_2		823.9	119.5
118	F_2		567.3	82.3
120	F_2		915.1	132.7
		$\bar{x}$	701.1	101.7
		s	217.9	31.6
91	F_3		91.3	13.2
92	F_3		307.0	44.5
93	F_3		715.8	103.8
98	F_3		915.3	138.0
99	F_3		868.6	126.0
100	F_3		446.1	64.7
101	F_3		901.5	130.8
102	F_3		861.0	124.9
103	F_3		888.9	128.9
		$\bar{x}$	666.2	97.2
		s	307.5	45.2

TABLE 26 (Continued)

PHASE III - COMPRESSIVE STRENGTH OF BRAND TYPE B-1 MAGNETS

Test Temperature: 25°C (Room Temperature)

Specimen Number	Test Orientation		Compressive Strength MPa	ksi
22	F_1		182.5	26.5
23	F_1		165.3	24.0
26	F_1		439.4	63.7
29	F_1		736.1	106.8
31	F_1		185.9	27.0
32	F_1		375.2	54.4
33	F_1		310.6	45.1
34	F_1		554.3	80.4
36	F_1		231.1	33.5
67	F_1		216.3	31.4
69	F_1		684.4	99.3
		$\bar{x}$	371.0	53.8
		s	207.1	30.0
52	F_2		972.5	141.0
53	F_2		822.2	119.2
56	F_2		953.9	138.3
58	F_2		464.3	67.3
62	F_2		662.9	96.1
63	F_2		753.0	109.2
64	F_2		459.2	66.6
65	F_2		763.1	110.7
66	F_2		1029.2	149.3
		$\bar{x}$	764.5	110.9
		s	208.1	30.2
37	F_3		977.5	141.8
38	F_3		840.8	121.9
39	F_3		786.7	114.1
40	F_3		168.8	24.5
42	F_3		562.2	81.5
43	F_3		791.8	114.8
45	F_3		493.5	71.6
48	F_3		229.8	33.3
49	F_3		344.4	50.0
		$\bar{x}$	577.3	83.7
		s	289.1	41.9

TABLE 26 (Continued)

PHASE III - COMPRESSIVE STRENGTH OF BRAND TYPE B-1 MAGNETS

Test Temperature: 100°C

Specimen Number	Test Orientation		Compressive Strength MPa	Compressive Strength ksi
119	F_1		368.0	53.4
121	F_1		309.6	44.9
122	F_1		912.6	132.4
123	F_1		563.1	81.7
124	F_1		584.0	84.7
125	F_1		528.8	76.7
126	F_1		188.2	27.3
127	F_1		278.2	40.4
128	F_1		196.0	28.4
		$\bar{x}$	436.5	63.3
		s	234.1	34.0
21	F_2		INVALID TEST	
24	F_2		55.8	8.1
41	F_2		562.2	81.5
46	F_2		114.8	16.7
54	F_2		97.8	14.2
57	F_2		57.4	8.3
73	F_2		222.9	32.3
83	F_2		155.2	22.5
96	F_2		233.0	33.8
		$\bar{x}$	187.4	27.2
		s	165.8	24.0
30	F_3		299.8	43.5
50	F_3		182.5	26.5
51	F_3		322.5	46.8
55	F_3		186.4	27.0
68	F_3		721.9	104.7
72	F_3		187.9	27.3
78	F_3		518.5	75.2
113	F_3		106.7	15.5
114	F_3		461.0	66.9
		$\bar{x}$	331.9	48.2
		s	199.9	29.0

TABLE 26 (Continued)

PHASE III - COMPRESSIVE STRENGTH OF BRAND TYPE B-1 MAGNETS

Test Temperature: 200°C

Specimen Number	Test Orientation	Compressive Strength MPa	Compressive Strength ksi
27	F_1	447.5	64.9
35	F_1	574.0	83.3
44	F_1	326.9	47.4
47	F_1	810.4	117.5
59	F_1	290.4	42.1
61	F_1	405.6	58.8
90	F_1	709.1	102.8
107	F_1	442.3	64.2
112	F_1	986.9	143.1
	$\bar{x}$	554.8	80.5
	s	235.7	34.2
28	F_2	336.3	48.8
60	F_2	324.2	47.0
70	F_2	813.8	118.0
74	F_2	635.4	92.2
77	F_2	759.7	110.2
79	F_2	892.3	129.4
82	F_2	554.3	80.4
116	F_2	864.4	125.4
117	F_2	965.7	140.1
	$\bar{x}$	682.9	99.1
	s	236.5	34.3
25	F_3	648.3	94.0
81	F_3	845.0	122.5
86	F_3	618.5	89.7
87	F_3	688.8	99.9
88	F_3	476.6	69.1
94	F_3	678.7	98.4
95	F_3	759.7	110.2
97	F_3	169.0	24.5
109	F_3	1033.2	149.9
	$\bar{x}$	657.2	95.4
	s	240.1	34.8

TABLE 26 (Continued)

PHASE III - COMPRESSIVE STRENGTH OF BRAND TYPE E-1 MAGNETS

Test Temperature: -51°C

Specimen Number	Test Orientation		Compressive Strength MPa	Compressive Strength ksi
75	F_1		1207.3	175.1
77	F_1		288.7	41.9
78	F_1		680.8	98.7
80	F_1		936.6	135.8
81	F_1		677.4	98.2
82	F_1		1140.2	165.4
83	F_1		428.8	62.2
84	F_1		610.4	88.5
85	F_1		593.0	86.0
		$\bar{x}$	729.2	105.8
		s	308.7	44.8
102	F_2		335.0	48.6
104	F_2		461.0	66.9
107	F_2		1113.6	161.5
108	F_2		1069.8	155.2
109	F_2		224.3	32.5
111	F_2		350.4	50.8
114	F_2		845.1	122.6
116	F_2		1025.6	148.7
117	F_2		837.6	121.5
		$\bar{x}$	695.8	100.9
		s	352.2	51.1
87	F_3		317.0	46.0
88	F_3		609.8	88.4
89	F_3		797.6	115.7
91	F_3		992.2	143.9
93	F_3		1113.4	161.5
98	F_3		160.0	23.2
99	F_3		1324.9	192.2
100	F_3		674.1	97.8
101	F_3		368.5	53.4
		$\bar{x}$	706.4	102.5
		s	389.4	56.5

TABLE 26 (Continued)

PHASE III - COMPRESSIVE STRENGTH OF BRAND TYPE E-1 MAGNETS

Test Temperature: 25°C (Room Temperature)

Specimen Number	Test Orientation		Compressive Strength MPa	ksi
21	F_1		674.1	97.8
23	F_1		487.9	70.8
25	F_1		1031.9	149.7
29	F_1		397.8	57.7
32	F_1		204.6	29.7
33	F_1		275.4	39.9
35	F_1		275.6	40.0
36	F_1		373.8	54.2
37	F_1		555.0	80.5
		$\bar{x}$	475.1	68.9
		s	256.2	37.2
51	F_2		872.8	126.6
54	F_2		763.9	110.8
58	F_2		766.3	111.1
60	F_2		893.7	129.6
62	F_2		1039.6	150.8
63	F_2		524.0	76.0
66	F_2		448.9	65.1
73	F_2		726.1	105.3
74	F_2		640.5	92.9
		$\bar{x}$	741.8	107.6
		s	185.0	26.8
38	F_3		750.5	108.8
40	F_3		711.9	103.3
41	F_3		459.0	66.6
42	F_3		429.3	62.3
43	F_3		599.7	87.0
44	F_3		630.8	91.5
45	F_3		804.9	116.7
46	F_3		793.1	115.0
49	F_3		630.5	91.4
		$\bar{x}$	645.5	93.6
		s	135.4	19.6

TABLE 26 (Continued)

PHASE III - COMPRESSIVE STRENGTH OF BRAND TYPE E-1 MAGNETS

Test Temperature: 100°C

Specimen Number	Test Orientation		Compressive Strength MPa	Compressive Strength ksi
118	F_1		235.2	34.1
121	F_1		220.0	31.9
122	F_1		226.7	32.9
123	F_1		209.1	30.3
124	F_1		189.0	27.4
125	F_1		143.5	20.8
126	F_1		206.4	29.9
127	F_1		482.4	70.0
128	F_1		211.9	30.7
		$\bar{x}$	236.0	34.2
		s	96.2	14.0
26	F_2		136.3	19.8
53	F_2		465.5	67.5
64	F_2		134.1	19.5
76	F_2		141.1	20.5
86	F_2		185.1	26.8
90	F_2		226.1	32.8
112	F_2		906.4	131.5
115	F_2		633.4	91.9
120	F_2		913.9	132.5
		$\bar{x}$	415.8	60.3
		s	328.0	47.6
22	F_3		300.9	43.6
52	F_3		133.6	19.4
68	F_3		80.5	11.7
79	F_3		227.2	32.9
92	F_3		334.1	48.4
97	F_3		503.0	73.0
106	F_3		283.6	41.1
110	F_3		426.6	61.9
119	F_3		570.1	82.7
		$\bar{x}$	317.7	46.1
		s	162.0	23.5

TABLE 26 (Concluded)

PHASE III - COMPRESSIVE STRENGTH OF BRAND TYPE E-1 MAGNETS

Test Temperature: 200°C

Specimen Number	Test Orientation		Compressive Strength MPa	Compressive Strength ksi
24	F_1		205.6	29.8
28	F_1		133.8	19.4
30	F_1		123.7	17.9
31	F_1		307.0	44.5
47	F_1		226.7	32.9
57	F_1		360.8	52.3
67	F_1		92.0	13.3
96	F_1		241.2	35.0
113	F_1		442.7	64.2
		$\bar{x}$	237.1	34.4
		s	116.3	16.9
27	F_2		137.2	19.9
34	F_2		117.6	17.1
39	F_2		INVALID TEST	
50	F_2		292.0	42.4
59	F_2		622.0	90.2
65	F_2		119.8	17.4
72	F_2		701.5	101.7
94	F_2		66.5	9.6
105	F_2		535.3	77.6
		$\bar{x}$	324.0	47.0
		s	257.0	37.3
48	F_3		570.7	82.8
55	F_3		264.4	38.3
56	F_3		260.3	37.3
61	F_3		440.3	63.9
69	F_3		614.0	89.1
70	F_3		608.5	88.3
71	F_3		13.1	1.9
95	F_3		272.0	39.5
103	F_3		599.0	86.9
		$\bar{x}$	404.7	58.7
		s	213.1	31.0

TABLE 27

YOUNG'S MODULUS AND POISSON'S RATIO VERSUS TEMPERATURE

Brand Type	Test Temp. (°C)	Magnetization Direction								
		Longitudinal			Transverse			90° Transverse		
		E GPa	(ksi)	ν	E GPa	(ksi)	ν	E GPa	(ksi)	ν
E-1	-60	90	(13)	0.35	138	(20)	0.35	127	(19)	0.28
	23	96	(14)	0.36	126	(18)	0.35	134	(20)	0.30
	100	91	(13)	0.34	119	(17)	0.31	132	(19)	0.30
	205	121	(17)	0.31	124	(18)	0.34	147	(21)	0.28
B-1	-60	141	(21)	0.27	112	(16)	0.34	121	(18)	0.22
	23	154	(22)	0.34	126	(18)	0.33	125	(18)	0.28
	100	153	(22)	0.30	126	(18)	0.32	125	(18)	0.25
	205	157	(23)	0.34	163	(24)	0.28	136	(20)	0.23

6. Knoop Hardness

Hardness measurements were made using a standard Knoop hardness apparatus with a 100 gm load. Twelve specimens were selected and tested at random. The individual results for each brand type and their averages and standard deviations are given in Table 28.

7. Thermal Property Results

The thermal property data for the two brand types were nearly identical and fall within a range of values predicted for this type of material. A summary of the results is given in Table 29. The most notable result is the dependence of thermal expansion on the direction of magnetization.

E. Electrical Properties

a) Electrical Resistivity

In heavy duty high performance electrical machines it is important to know the resistance of the individual material components of the magnetic circuit and the total effect they have on the dynamic performance under extreme operating conditions. The resistances can be determined from each materials resistivity and the dimensions of the component part. Almost as important as the value of the resistivity itself is the amount of variation in properties which may be obtained through small composition alloy content or changes that may result from physical working and heat treatments.

The electrical resistivity of each brand type $SmCo_5$ permanent magnets tested in this phase were determined from two sets of 10 test magnet bars ($\sim$6.4 x 6.4 x 25.4 mm). These bars were carefully machined by the manufacturers. The direction of magnetization for each set was either parallel or perpendicular to the direction of magnetization. Resistance measurements were performed from -60° to +200°C using the test fixture and apparatus described and illustrated in Section 3, D-1, Figures 16 and 17.

TABLE 28

HARDNESS VALUES OBTAINED FROM B-1 AND E-1
FLEXURAL TEST SPECIMENS

Brand Type	Knoop Hardness at 23°C kg/mm^2 (100 gm load)
B-1	598 610 610 654 630 556 616 628 622 576 592 647
	$\bar{x}$ 612
	s 28
E-1	674 681 647 647 648 661 727 667 621 634 710 682
	$\bar{x}$ 667
	s 31

TABLE 29

THERMAL PROPERTIES OF SINTERED $SmCo_5$

Property	Brand Type	
	B-1	E-1
Coefficient of Thermal Expansion $°C^{-1}$		
$\perp$ direct. of mag.	13×10^{-6}	12×10^{-6}
$\parallel$ direct. of mag.	7×10^{-6}	6×10^{-6}
Thermal Diffusivity cm^2/s	0.045	0.041
Specific Heat $J/(kg \cdot °C)$	5.2×10^{-4}	5.4×10^{-4}
Thermal Conductivity $W/(m \cdot °C)$	1.9×10^{-3}	1.9×10^{-3}

Calculated value of resistivity and temperature coefficients were determined from precise measurements of test length, cross-sectional areas, and resistance as a function of temperature. Values determined for both types are given in Table 30 and plotted in Figure 34.

The similarity in the slope of the graphs over the temperature range is apparent after comparing the respective temperature coefficient for both materials. This is as expected for similar alloys. The small difference in magnitude of the resistivity can ordinarily be expected as a result of changes in heat treatment of small changes in the Sm-Co alloy content used by the respective manufacturers.

TABLE 30

AVERAGE ELECTRICAL RESISTIVITY AND
TEMPERATURE COEFFICIENT
(-60° to +200°C)

Brand Type	Direction of Measurement	Resistivity ρ [μΩ-cm][a]					Coefficient [μΩ-cm/°C]
		-60°	0°	+25°	+100°	+200°	
B-1	Perpendicular to Magnetization	43	51	55	67	83	0.154
	Parallel to Magnetization	35	42	46	56	71	0.138
E-1	Perpendicular to Magnetization	44	53	57	69	85	0.157
	Parallel to Magnetization	40	47	51	61	76	0.138

[a] Based on test lot of 10 samples. Standard deviation: 1 μΩ-cm.

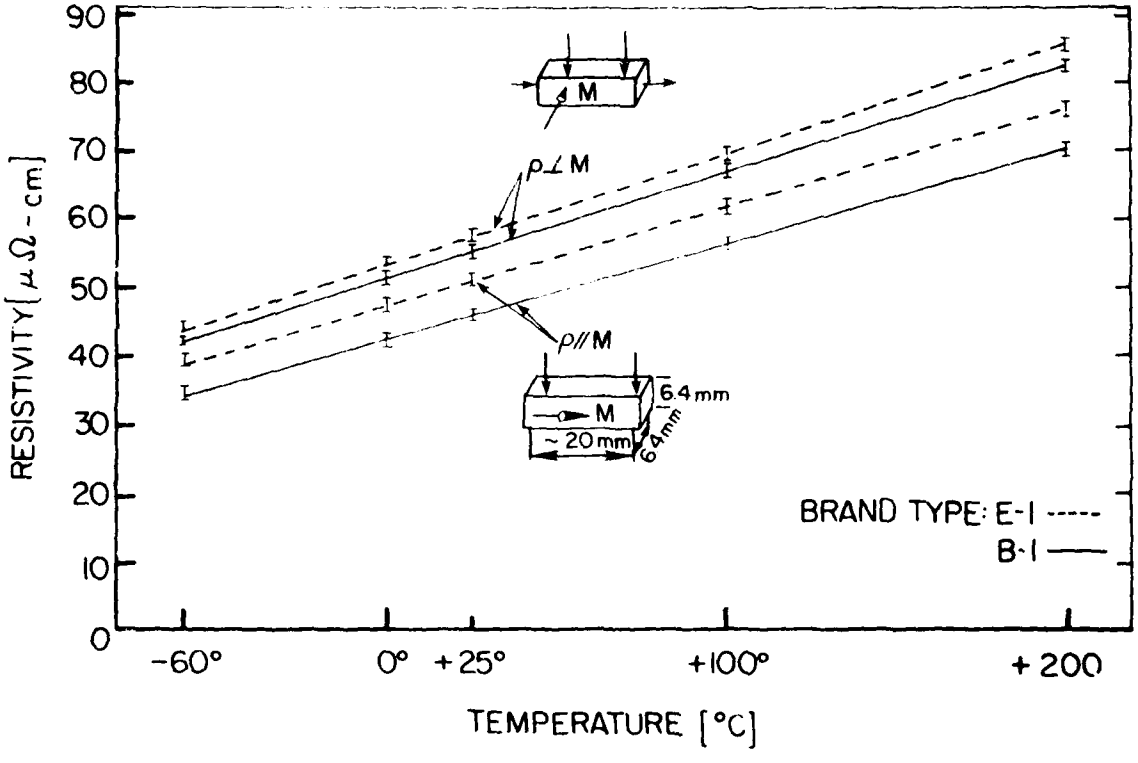

Figure 34. Resistivity Versus Temperature for Brand Types B-1 and E-1.

SECTION 5
CONCLUSION AND RECOMMENDATION

To conclude, the authors wish to suggest that the engineering data presented in all phases of this report serve as an indication of the optimum magnetic, mechanical, and thermal properties for high energy product rare-earth transition metal permanent magnets in production circa 1979-1980.

The basis for this statement is that all of the magnet specimens used in the study were carefully machined and surface finished ($\leq$ 16 μ inch) chip free, right prisms. Understandably, production economics and process variables can cause a significant change in the properties of standard production magnets due to less well prepared surfaces.

From an engineering viewpoint, most of the test and data evaluations reported focus on identifying real parameter values and their statistical variation limits which must be considered in any critical design application. The remaining data presented illustrate the commercial magnet production variations of property values that are often attributed to specific alloy composition and heat treatment variations utilized by individual manufacturers.

As the results in this report indicate, one underlying problem which plagues both magnet manufacturers and users alike is quality control of production magnets. Particularly for critical applications that require large multiple magnet pieces that are often assembled in a virgin state. As indicated in the discussion of mechanical properties, the flexural and compressive strengths of these materials is highly dependent on their microstructure. For this reason we would suggest that a routine micrographic analysis inspection of large magnet specimens would identify possible inhomogeneities . . the microstructure that could result in low strength. Thus, at minimal cost, in comparison to total magnet assembly investment, optimum optimization and/or control of

grain size, minimized inclusions and voids, and chemical composition homogeneity would inevitably lead to higher average magnetic and mechanical property strengths and lower standard deviations.

REFERENCES

1. H. F. Mildrum and D. J. Iden, Magnetic and Physical Properties of Commercially Available Rare Earth-Cobalt Permanent Magnets, Goldschmidt informiert, 4/75, N.35, Th. Goldschmidt A.G., Essen, West Germany (1975), p. 54.

2. K. J. Strnat, Rare-Earth Magnets in Present Production and Development, Journal of Magnetism and Magnetic Materials 7, (1978), p. 351.

3. K. J. Strnat, Review of Devices Using Rare Earth-Cobalt Magnets, Proc. 4th International Workshop on Rare Earth-Cobalt Permanent Magnets and Their Applications, Society of Nontraditional Technology, Tokyo, Japan (1979), p. 8.

4. K. J. Strnat, Rare Earth Permanent Magnets: Materials and Application Development Trends and Their Implications for Industry, Proc. 14th Rare Earth Research Conference (G. J. McCarthy and J. J. Rhyne, Editors), Plenum Press, New York (1980), p. 505.

5. H. Nagel, Rare Earth-Transition Metal Permanent Magnets: Physics and Manufacturing Technology (in German), Thyssen Edelstahl, Technische Berichte, Vol. 6-1, Thyssen Edelstahlworke A.G., Krefeld, W. Germany (1980), p. 5.

6. W. U. Borger, Rare Earth Magnets and 400 Hz Aircraft Power Systems, Proc. 3rd International Workshop on Rare Earth-Cobalt Permanent Magnets and Their Applications, San Diego, California (1978), p. 88.

7. L. J. Bailey and E. Richter, Development Report on a High-Speed Permanent Magnet Generator of the 200 kVA Rating Class Utilizing Rare Earth-Cobalt Magnets, Proc. 2nd International Workshop on Rare Earth-Cobalt Permanent Magnets and Their Applications, Dayton, Ohio (1976), p. 251.

8. R. L. Fisher, Magnet Requirements for High Performance DC Motors, Proc. 4th International Workshop on Rare Earth-Cobalt Perm. Magnets and Their Applications, Hakone, Japan (1979), p. 19.

9. R. W. Kubach, A Hysteresigraph for Plotting Magnetization Curves, Master's Thesis, University of Dayton, December 1966, Air Force Materials Laboratory Technical Report AFML-TR-67-216 (December 1966).

10. H. F. Mildrum and K. J. Strnat, Research to Investigate the Aging Effects of Samarium-Cobalt Magnets, AFML-TR-73-46 (March 1973); AFML-TR-73-249 (October 1973); AFML-TR-74-50 (March 1974).

11. H. F. Mildrum and K. J. Strnat, Physical Properties of Rare Earth-Cobalt Magnets, (Alternator Service Aging Study), AFML-TR-75-190 (December 1975).

12. ASTM-B-63, Standard Method of Test for Resistivity of Metallically Conductive Resistance and Contact Metals, Vol. 44.

13. W. J. Parker, et al., Flash Method of Determining Thermal Diffusivity, Heat Capacity, and Thermal Conductivity, J. Appl. Phys., 32(9), pp. 1679-1687 (1961).

14. W. H. Dukes, Handbook of Brittle Material Design Technology, Advisory Group for Aerospace Research and Development, North Atlantic Treaty Organization, Paris, France, AGARD-AG-152-71, AD-719712 (February 1971).

15. G. A. Graves, D. L. McCullum, and J. M. Wimmer, Final Report, Air Force Contract No. F33615-75-C-5011, AFML-TR-77-23 (1977).

*U.S.Government Printing Office: 1981 — 559-003/2006